



**REDUCING BUILDING THERMAL LOADS BY ADDING WASTE  
TO CONSTRUCTION MATERIALS**

**A THESIS**

**SUBMITTED TO THE DEPARTMENT OF MECHANICAL ENGINEERING  
TECHNIQUES OF POWER**

**IN PARTIAL FULFILLMENT OF THE REQUIREMENTS FOR THE  
DEGREE OF MASTER THERMAL TECHNOLOGIES IN MECHANICAL  
ENGINEERING TECHNIQUES OF POWER (M.TECH.)**

**BY**

**SHAHAD HASAN HAMEED**

**Supervised by**

**Asst. Prof. KAREEM JAFAR ALWAN**

**November/2023**

## Declaration

I hereby declare that the work in this thesis is my own and has not been submitted to other organizations or for acquiring any other degree.

Signature:

Name: Shahad Hasan Hameed

Date: / / 2023

## SUPERVISOR CERTIFICATION

I certify that the thesis entitled “**REDUCING BUILDING THERMAL LOADS BY ADDING WASTE TO CONSTRUCTION MATERIALS**” which is submitted by **SHAHAD HASAN HAMEED** was prepared under supervision at the Department of Mechanical Engineering Techniques of Power, the College of Technical Engineering-Najaf, AL-Furat Al-Awsat Technical University, as partial fulfillment of the requirements for the degree of Master in Techniques in Thermal Engineering.

In view of the available recommendations, forward this thesis for debate by the examining committee.

Signature:

Name: Asst. Prof. Kareem Jafar Alwan

Supervisor

Date:     /     / 2023

Signature:

Name: Asst. Prof. Dr. Adel A. Eidan

Head of the Department of Mechanical Engineering Techniques  
of Power

Date:     /     / 2023

## EXAMING COMMITTEE CERTIFICATE

We certify that we have read this thesis entitled “**REDUCING BUILDING THERMAL LOADS BY ADDING WASTE TO CONSTRUCTION MATERIALS**” which is being submitted by **Shahad Hasan Hameed** and, as Examining Committee, examined the student in its contents. In our opinion, the thesis is adequate for the award of the degree of Master of Techniques in Thermal Engineering.

**Signature:**

**Prof. Dr. Ali Shakir Baqir**  
(Chairman)

Date:     /     / 2023

**Signature:**

**Asst. Prof. Dr. Zaid M. AL-Dulaimi**  
(member)

Date:     /     / 2023

**Signature:**

**Asst. Prof. Dr. Aimen R. N. Zeiny**  
(member)

Date:     /     / 2023

**Signature:**

**Asst. Prof. Kareem Jafar Alwan**  
(Supervisor and Member)

Date:     /     / 2023

Approval of the Engineering Technical College- Najaf

**Signature:**

**Name: Asst. Prof. Dr. Hassanain Ghani Hameed**  
Dean of Engineering Technical College- Najaf

Date:     /     / 2023

## CERTIFICATE OF THE LINGUISTIC EXPERT

I certify that I have read the thesis entitled “**REDUCING BUILDING THERMAL LOADS BY ADDING WASTE TO CONSTRUCTION MATERIALS**” and have linguistically proofread it; therefore, it has become qualified for debate by the examining committee.

Signature:

Lect. Dr. Ekhlās Alī Mohsin Al-Shammari

Ph.D. Linguistics and English Language / Newcastle University, UK

Address: the Department of English Language / Faculty of Arts

Date:     /     / 2023

## ACKNOWLEDGMENTS

I would like to express my profound respect and gratitude to my supervisor Asst. Prof. Kareem Jafar Alwan for his unwavering support and guidance while conducting the research, which was instrumental in completing this study.

I extend my sincere thanks to (Asst. Prof. Dr. Hassanain Ghani Hameed, the Dean )of the College of Technical Engineering-Najaf, and the esteemed Chief Mechanic, M. Technique from the Department of Energy Ass. Prof. Dr. Adel A. Eidan)for providing invaluable assistance to facilitate the study process. Special thanks go to the staff at the department for their assistance and collaboration.

I am also deeply grateful to my mother, my husband, and my dear brothers for their patience, continuous support, and encouragement throughout my life.

SHAHAD HASAN HAMEED

2023

## ABSTRACT

The construction sector is moving towards building energy-efficient constructions, and the development of sustainable thermal insulation materials contributes to this trend. The use of these materials significantly reduces energy consumption, reducing the need for non-renewable materials and reducing waste. In this study, three groups of insulating construction materials were produced. The first group relied on cement and sand with waste. Five different samples were produced. The second group, based on gypsum and waste, produced five samples, and the third group, based on waste and wood glue, produced four different samples.

Thermal and physical tests were conducted on the samples, including tests for thermal conductivity, compressive strength, dry density, and water absorption. The results revealed that the values of the first group of thermal conductivity, compressive strength, dry density, and water absorption ranges from 0.118 W/m K to 0.362 W/m K, 2.64 MPa to 5.92 MPa, 1272 kg/m<sup>3</sup> to 1664 kg/m<sup>3</sup>, 15% to 20%, respectively. While for the second group, the values ranged from 0.116 W/m<sup>3</sup> to 0.291 W/m<sup>3</sup>, 1.12 MPa to 4.08 MPa, 320 kg/m<sup>3</sup> to 1224 kg/m<sup>3</sup> and 19% to 33%, respectively. Finally, the values of the third group ranged from 0.043 W/mK to 0.054 W/MK, 1.43 MPa to 1.7 MPa, 438 kg/m<sup>3</sup> to 528 kg/m<sup>3</sup>, and 31% to 37%, respectively.

After that, two samples were chosen for practical application and the rate of heat transfer through them was calculated and their ability to reduce heat transfer in the rooms designated for testing. Sample (G3) was applied to the inner wall of the insulated test room, and sample (WG1) was applied to the outer wall of the insulated test room. The insulated room showed a decrease in heat transfer rate of about 83% compared to the non-insulated room.

## NOMENCLATURE

Letter	Description	Units
A	Surface area	$m^2$
K	Thermal conductivity	$W/m.k$
$U$	Overall Heat Transfer Coefficient	$W/m^2.k$
$\Delta x$	Thickness of wall	m
$h_i$	Convection heat transfer coefficient for membrane layer inner wall	$W/m^2.k$
$h_o$	$h_o$ Convection heat transfer coefficient for membrane layer outer wall	$W/m^2.k$
$\sigma$	compressive strength	MPa
$P$	maximum applied load	N
$W_f$	weight of the sample after immersion in water	kg
$W_i$	weight of the dry sample before immersion	kg
$\rho$	density of water	$kg/m^3$
CLTD	Cooling Load Temperature Difference	0C
Q	The amount of heat transfer across the conductor	W
DR	Average daylight hours during the day	
f	Correction factor for the presence of ventilation between the secondary roof and the inclined roof	
LM	correction factor for latitude and longitude and backward value by wall direction	
TR	Correction for Indoor Air Temperature	
$T_o$	Correction for Outdoor Air Temperature	
OPC	Ordinary Portland Cement	
$t_o$	External ambient temperature	



## SAMPLE LABELS

Sampls	Details
C1	Fine Rice Husk, Sand, Cement
C2	Polystyrene, Sand, Cement
C3	Fine Rice Husk, Cement
C4	Sawdust, Sand, Cement
C5	Polystyrene, Sawdust, Rice Husk, Sand, Cement
G1	Fine Rice Husk, Gypsum
G2	Rice Husk, Gypsum
G3	Polystyrene, Gypsum
G4	Sawdust, Gypsum
G5	Polystyrene, Sawdust, Rice Husk, Gypsum
WG1	Rice Husk, Wood glue
WG2	Fine Rice Husk, Rice Husk, Sawdust, Wood glue
WG3	Sawdust, Wood glue
WG4	Fine Rice Husk, Sawdust, Wood glue

## LIST OF CONTENTS

Declaration.....	II
------------------	----

SUPERVISOR CERTIFICATION .....	III
EXAMING COMMITTEE CERTIFICATE .....	IV
CERTIFICATE OF THE LINGUISTIC EXPERT .....	V
ACKNOWLEDGMENTS .....	VI
ABSTRACT .....	VII
LIST OF CONTENTS .....	IX
TABLE OF FIGURES.....	XIV
LIST OF TABEL .....	XVII
CHAPTER ONE .....	1
INTRODUCTION .....	1
1.1 General eview .....	2
1.2 Thermal insulation .....	4
1.3 Benefits of using thermal insulation.....	5
1.4 Insulation Material Classification .....	6
1.4.1 Classification according to the heat exchange characteristics .....	6
1.4.1.1 Mass insulation .....	7
1.4.1.2 Reflective insulation . .....	7
1.4.2 Classification according to form .....	7
1.4.3 Classification according to composition.....	8
1.5 Bio-Based Insulation Material Properties .....	8
1.6 Study Objectives .....	10
CHAPTER TWO .....	12
LITERATURE REVIEW .....	12
2.1 Introduction. ....	12

2.2 Literature Review.....	12
2.2.1 Studies that used waste with cement.....	12
2.2.2 Studies that used waste with gypsum.....	17
2.2.3 Studies that used waste with different binder .....	21
<b>2.3 Summary of Literature Review .....</b>	<b>24</b>
<b>3. CHAPTER THREE .....</b>	<b>39</b>
<b>EXPERIMENTAL WORK .....</b>	<b>39</b>
<b>CHAPTER THREE .....</b>	<b>40</b>
3.2 Experimental Materials.....	40
3.2.1 Cement .....	40
3.2.2 Sand.....	42
3.2.3 Calcined gypsum.....	42
3.2.4 Polystyrene Beads (EPS) .....	44
3.2.5 Rice husk.....	45
3.2.6 Wood chips .....	47
3.2.7 Wood glue .....	48
3.2.8 Water .....	49
3.3 Samples' preparation.....	49
3.4 Samples failure .....	51
3.5 Mixing Procedure.....	53
3.6 Casting and Curing.....	53
3.7 Tests procedures .....	56
3.7.1 Thermal Conductivity Test .....	56
3.7.2 Compressive Strength Test .....	57

3.7.3 Water Absorption Test .....	59
3.7.4 Bulk Dry Density Test .....	60
3.8 Practical application .....	61
3.9 Measurement of Temperature .....	62
3.9.1 Thermocouples .....	62
3.9.2 Data logger .....	64
3.7 Solar Radiation.....	64
3.9.3 Reflectivity .....	65
CHAPTER FOUR .....	68
RESULTS AND DISCUSSION.....	68
4.2 Tests Results.....	68
4.2.1 Thermal conductivity .....	68
4.2.1.1 Cement_base products.....	68
4.2.1.2 Gypsum_base products .....	70
4.2.1.3 Wood glue_base products .....	73
4.2.2 Compressive Strength .....	72
4.2.2.1 Compressive strength of Cement_base products.....	73
4.2.2.2 Compressive strength of gypsum_base products.....	73
4.2.2.3 Compressive strength of wood glue_base products.....	74
Figure 4-6 Compressive strength of wood glue_base products.....	75
4.2.1 Water absorption .....	75
4.2.1.1 Water absorption of cement_base products.....	76
4.2.1.2 Water absorption of gypsum_base products.....	76
Figure 4-8 Water absorption of gypsum_base products .....	77

4.2.1.3	Water absorption of wood glue_base products.....	77
4.2.2	Bulk Dry Density .....	78
4.2.2.1	Bulk dry density of cement_base products .....	78
4.2.2.2	Bulk density of gypsum_base products .....	79
	Figure 4-6 Bulk dry density of gypsum_base products .....	80
4.2.2.3	Bulk dry density of wood glue_base products.....	81
	Figure 4-12Bulk dry density of wood glue_base products .....	81
4.3	Practical application of thermal insulation materials .....	82
4.3.1	Material selection .....	82
4.3.2	Applying thermal insulation materials.....	82
4.4	Temperature measuring .....	84
4.4.1	Data analysis .....	88
4.4.2	Glossiness measurement .....	89
4.6	Heat transfer rate calculations.....	90
	CHAPTER FIVE .....	96
	CONCLUSIONS AND RECOMMENDATIONS.....	96
5.1	Conclusions .....	96
5.2	Recommendations.....	98
	Appendix-A .....	107
	Heat transfer reduction calculations .....	107
	الملخص.....	106

## Table of Figures

Figure 1-1 Aggregate Energy Consumption in Residential and Commercial Buildings Across Various Global Regions.....	2
Figure1- 2 Approximate Residential Energy Consumption in the Middle East.....	3
Figur1-3 Papadopoulos classification of insulating materials for building applications .....	9
Figure 3 -1 Polystyrene granules (EPS) .....	45
Figure 3 -2 (a) Rice husks (b) Fine rice husks.....	46
Figure 3 -3 Wood chips .....	50
Figure 3 -4 Submersion of the cementitious samples in water r .....	55
Figure 3 -5 (a) Thermal conductivity test model (b) Water absorption test mode (c) Compressive strength test model .....	55
Figure 3 -6 Samples prepared for testing .....	56
Figure 3 -7 Thermal conductivity test device.....	58
Figure 3 -8 Compressive strength test device.....	59
Figure 3 -9 the failure of the model.....	60
Figure 3 -10 (a) Test room that are covered with insulating materials (b) Test room without insulation.....	63
Figure 3 -11 Cross-section of the rooms wall .....	64
Figure 3 -12 Thermocouples.....	65
Figure 3 -13 Locations of thermocouples in each direction.....	66
Figure 3-14 Data logger.....	65
Figure 3-15 Solar power meter.....	66
Figure 3-16-Gloss meter .....	68
Figure 4-1 Thermal conductivity of cement_base products.....	70
Figure 4-2 Thermal conductivity of gypsum_base products .....	71
Figure 4-3 Thermal conductivity of Wood glue_base products.....	74

Figure 4-4 Compressive strength of Cement_base products.....	75
Figure 4-5 Compressive strength of gypsum_base products.....	75
Figure 4-6 Compressive strength of wood glue_base products .....	76
Figure 4-7 Water absorption of cement_base products.....	78
Figure 4-8 Water absorption of gypsum_base products.....	79
Figure 4-10 Bulk dry density of cement_base products.....	81
Figure 4-1 Bulk dry density of gypsum_base products.....	83
Figure 4-12 Bulk dry density of wood glue_base products .....	83
Figure 4-2 Casting and installation of the outer insulation layer .....	85
Figure 4-3 Casting and installation of the internal insulating layer .....	88
Figure 4-4 The solar radiation on May 17 <sup>th</sup> , 2023.....	89
Figure 4-5 Temperature differences between the outdoor and indoor surface temperatures of the ceilings . .....	78
Figure 4-17 Temperature difference between the outdoor and indoor surface temperatures of the northern walls. ....	88
Figure 4-18 Temperature difference between the outdoor and indoor surface temperatures of the eastern walls.....	88
Figure 4-19 Temperature difference between the outdoor and indoor surface temperatures of the southern walls. ....	89
Figure 4-20 Temperature difference between the outdoor and indoor surface temperatures of the western walls. ....	89
Figure 4-22 Glossiness of insulated and non-insulated rooms .....	92
Figure 4-23 Maximim heat transfer rates through the two test rooms based on Fourier’s law. ....	93
Figure 4-23 Heat transfer rates through the two testing rooms on May 17 <sup>th</sup> , 2023, based on CLTD method (before improving the reflectivity of the surfaces).....	94
Figures A5 Tables of CLTDc and LM values.....	135

Figure 4-24 Heat transfer rates through the two testing rooms on June 20<sup>th</sup>, 2023, based on CLTD method (after improving the reflectivity of the surfaces)..... .97



## List of Tables

Table 2- 1 Summary of studies that dealt with agricultural and industrial waste mixed with traditional building materials (cement) .....	26
Table 2- 2 Summary of studies that dealt with agricultural and industrial waste mixed with traditional building materials (gypsum) .....	31
Table 2- 3 Summary of studies dealing with agricultural and industrial waste mixed with different binders.....	34
Table3-1 Chemical analysis of Ordinary Portland Cement (OPC) .....	41
Table 3- 2 Physical analysis of Ordinary Portland Cement (OPC) .....	42
Table 3- 3 The chemical composition of Gypsum .....	43
Table 3- 4 1 Physical characteristics of Gypsum .....	44
Table 3- 5 Chemical properties of the Iraqi rice husk .....	45
Table 3- 6 sample names and components .....	50
Table 3- The components of the samples and the proportions of the materials used .....	50
Table 3-9 Failed mixtures that were excluded.....	53
Table 4-1 Heat transfer rates of Room-1 and Room-2 based on Fourier's law .....	93
Table A-1 Heat transfer rates of Room-1 and Room-2 based on Fourier's law.....	128
Table A2CLTD <sub>C</sub> values calculations for room2 on May 17.....	133
Table A3 CLTD <sub>C</sub> values calculations for room 1 on May 17.....	134.
Table A4 CLTD <sub>C</sub> values calculations for room2 on June 20 <sup>t</sup> .....	135
Table A5 CLTD <sub>C</sub> values calculations for room on June 20 <sup>th</sup> .....	136

**CHAPTER ONE**  
**INTRODUCTION**

## CHAPTER ONE

### Introduction

#### **1.1 General review**

The continuous increase in energy consumption patterns has captured widespread attention, mainly due to concerns about depleting energy resources and various environmental issues, such as CO<sub>2</sub> emissions, global warming, and climate change. The International Energy Agency (IEA) predicted that the buildings sector accounted for 132 EJ of energy consumption in 2021, or 30% of total global final energy consumption. The sector's 3 Gt CO<sub>2</sub> emissions accounted for 15% of total emissions from end-use sectors in 2021, but this share doubles if indirect emissions from electricity and heat production are included. Despite a gradual shift away from fossil fuels, direct emissions from the buildings sector have risen by 0.5% per year since 2010, driven by rising demand for energy services [1]. One of the most major future issues in the field of buildings is the need to reduce energy consumption at all stages of their existence, from construction through demolition. The construction industry today contributes 40% of global energy consumption, and nearly 30% of carbon dioxide emissions [2]. Most of the energy consumption in the building sector is for residential use, as shown in Figure 1-1. Energy consumption in the residential sector is approximately twice that of energy consumption in the commercial sector in various regions of the world [3].

The application of efficient insulation, in addition to the application of efficient insulation strategies, serves to diminish the utilization of valuable natural resources like petroleum and gas reserves, commonly employed in power generation [4].

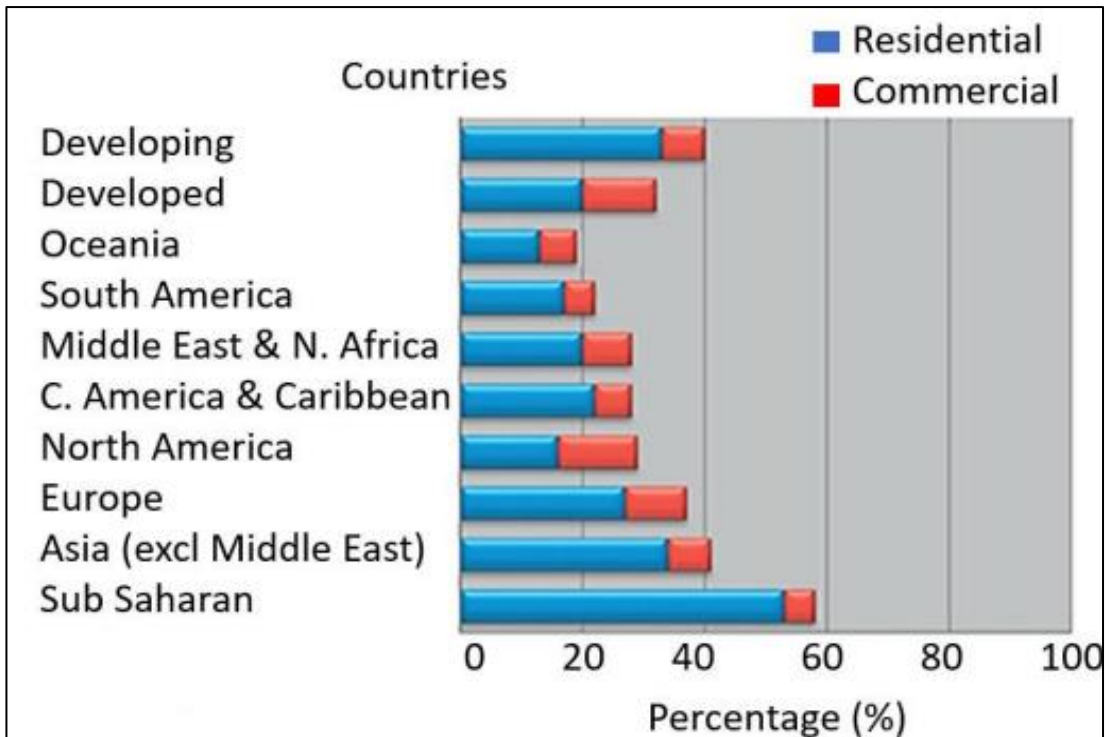


Figure 1-1 Percentage of Consumption in Residential and Commercial Buildings Across Various Global Regions [3]

In Iraq, the utilization of air conditioning systems plays a pivotal role in ensuring thermal comfort within buildings. These systems constitute a significant portion of energy consumption, exemplified by their substantial impact on energy usage in Middle Eastern nations. Notably, in the residential sector of these countries, space cooling alone contributes to approximately 50% of the overall energy consumption, as illustrated in Figure 1-2[5].

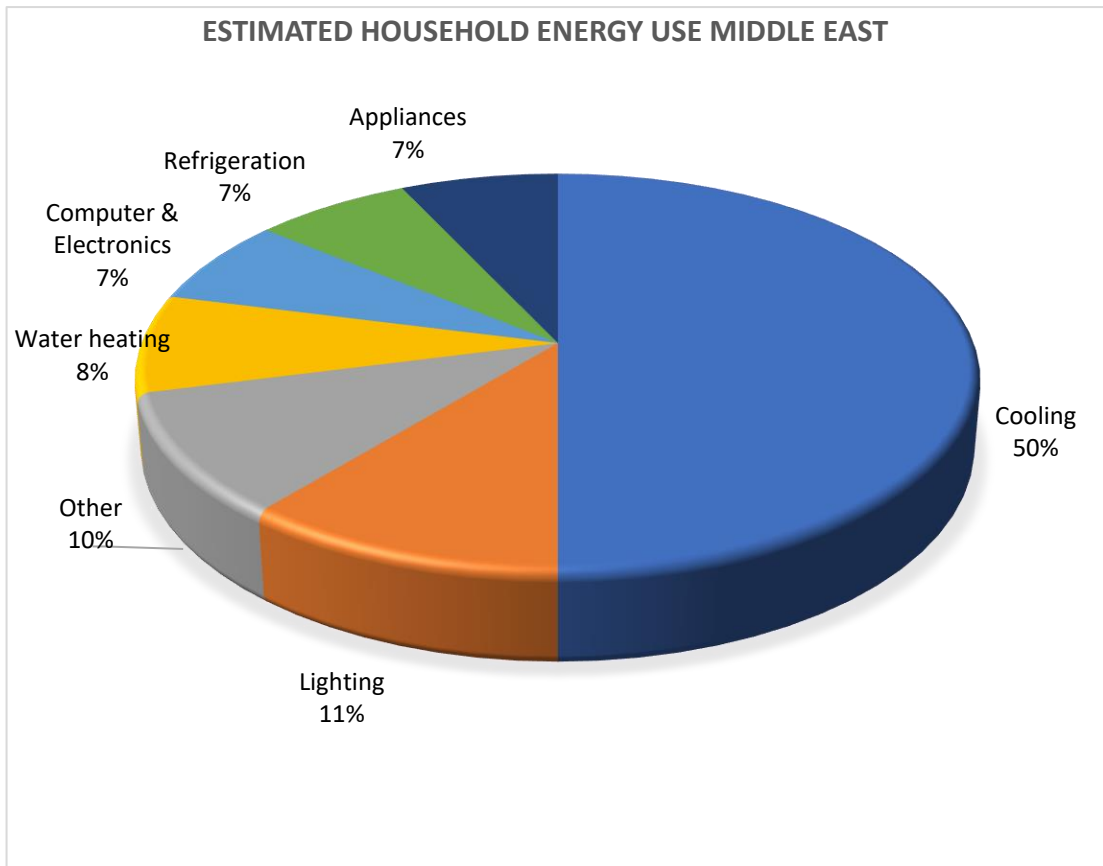


Figure 1-2 Approximate Residential Energy Consumption in the Middle East[5]

The construction sector, encompassing residential, industrial, and commercial buildings, is a significant energy consumer, particularly in the pursuit of thermal comfort. However, this sector has the potential to diminish its energy consumption by implementing effective insulation strategies. Efficient insulation minimizes energy usage, reducing the need for cooling during summer and heating during winter, thereby contributing to energy conservation[6].

## 1.2 Thermal insulation

Thermal insulation refers to a composite of materials or a synergistic combination thereof, which, when meticulously employed, effectively

inhibits the rate of heat transfer through mechanisms of conduction, convection, and radiation.

Its proficiency in retarding the flow of thermal energy into or out of a structural enclosure can be attributed to its elevated thermal resistance properties[7].

### **1.3 Benefits of using thermal insulation**

The utilization of thermal insulation in buildings offers a multitude of advantages that are succinctly listed as follows[8]:

- **Principled Energy Conservation:** The incorporation of thermal insulation in building design aligns with the fundamental principle of reducing dependence on mechanical and electrical systems for maintaining indoor comfort. This principled approach not only conserves energy but also safeguards valuable natural resources.
- **Economic Efficiency:** Energy costs constitute a significant portion of operational expenses. By incorporating thermal insulation, substantial energy savings can be achieved with a relatively modest upfront investment, typically amounting to approximately 5% of the total construction cost. This not only leads to ongoing cost reductions but also results in decreased initial expenses for heating, ventilation, and air conditioning (HVAC) equipment, as reduced equipment size is required.
- **Noise Abatement:** Utilizing thermal insulation effectively minimizes disruptive noise from neighboring areas or external sources, enhancing the acoustic comfort within insulated buildings.
- **Preservation of Building Structural Integrity:** Temperature fluctuations can lead to undesirable thermal movements that may compromise the structural integrity of buildings and their

contents. Employing proper thermal insulation helps maintain temperature stability, thus safeguarding both building structures and their longevity.

- **Prevention of Vapor Condensation:** Thoughtful design and meticulous installation of thermal insulation play a pivotal role in preventing vapor condensation on building surfaces. However, it is imperative to exercise caution to avert potential adverse effects on building structures, which may result from improper insulation material installation or subpar design. Typically, vapor barriers are deployed to shield low-temperature insulation from moisture penetration.

## **1.4 Insulation Material Classification**

Despite that all insulation materials share a common objective of limiting the speed at which heat enters or exits an enclosed area, certain materials fulfill specific roles that lead to their categorization based on their designated functions, forms, and compositions. These categories allow for the organized classification of insulation materials according to their unique properties and applications[9].

### **1.4.1 Classification according to the heat exchange characteristics**

Insulation materials can be broadly divided into two primary categories based on their role in influencing heat transfer: bulk insulation and reflective insulation. Bulk insulations are those that impede the movement of heat through conduction, whereas reflective insulations work by diminishing heat transfer through radiation[10].

### **1.4.1.1 Mass insulation**

High thermal mass objects store heat, moderating solar heat absorption and post-sun heat loss. Insulation prevents rapid re-radiation, balancing the indoor temperature.

Mass insulation retards heat through conduction, curbing direct heat gain to the exterior. In hot climates, low thermal mass exteriors enhance insulation efficacy. Widely used, mass insulation reduces heat flow via conduction. Its effectiveness hinges on material thickness, which correlates with performance. Material density and subdivision impact thermal performance[10].

### **1.4.1.2 Reflective insulation**

Reflective insulation counteracts radiation heat by reflecting it, aided by a low-emittance surface. This halts heat transfer across surfaces. Consequently, it curbs solar heat gain, enhancing interior conditions. Radiated energy relies on surface temperature and emissivity—a higher value emits more radiation. This insulation type employs low-emittance surfaces enclosing air gaps. Typically used in attics, roofing, and wall systems for homes[11], [12].

## **1.4.2 Classification according to form**

Building thermal insulation materials are manufactured in diverse forms, shaped by the materials' distinct physical and chemical attributes as well as the intended insulation site. The forms and physical characteristics of insulating materials differ due to the varying material compositions. The selection of each type is contingent upon the insulation's placement and its appropriateness for the specific location. As there exists a wide range of options, certain materials are naturally solid, while others adopt foam or granular configurations[8].



### **1.4.3 Classification according to composition**

The composition of insulation materials plays a significant role in determining their insulation characteristics, which are closely tied to their chemical and physical structure [13]. Papadopoulos[13] classified insulation materials based on their composition, mainly categorizing them as organic, inorganic, combined materials, and new technology materials. This classification, as displayed in Figure 1-3, offers a valuable framework for understanding the diverse types of insulation materials used in building applications.

### **1.5 Bio-Based Insulation Material Properties**

Bio-based insulation materials are produced from renewable biological resources such as lignocellulosic, agriculture plant waste, and animal materials 'fur and wool' [14]. The high internal porosity provides a low bulk density and low thermal conductivity [15]. These features enable bio-based insulation materials to fulfill the required needs and properties without the necessity of a massive transformation. The natural biological features of these materials reduce the landfill waste amount due to their high biodegradability.

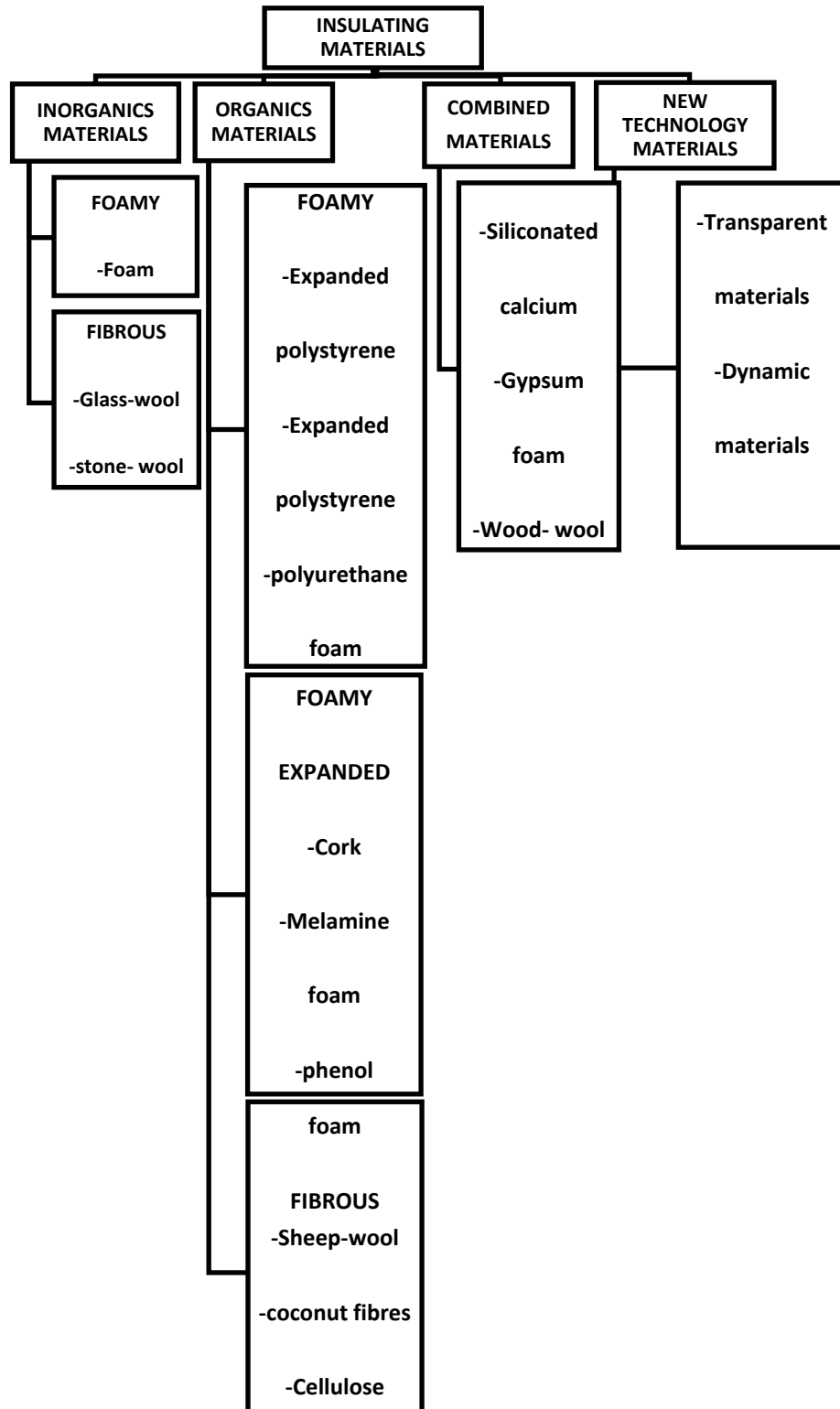


Figure 1-3 Classification of the commonly used insulating materials [13]

## 1.6 Study Objectives

This study focuses on the development and use of insulation materials based on sustainable resources, which are derived from agricultural and industrial waste. The scope of the study includes the production, characterization, and practical application of these materials in the field of construction. The study includes exploring different types of composite materials and their ability to transform into effective thermal insulators.

The main objectives of this study are as follows:

- 1- The production of insulation materials using a mixture of agricultural and industrial waste, such as rice husks, wood chips, and polystyrene beads. These materials will be incorporated into various types of composites, including cement-, gypsum- and wood glue-based compounds.
- 2- The evaluation of the thermal properties of the developed insulation materials, including heat conduction, heat resistance, and their ability to absorb solar radiation. Comparisons will be made with conventional insulation materials to evaluate their thermal efficiency.
- 3- The evaluation of the physical properties of insulation materials, such as compressive strength, density, and water absorption. It will be ensured that the materials meet the required standards for construction applications.
- 4- The practical application of the developed insulation materials in controlled test scenarios. The goal is to evaluate their effectiveness in reducing heat transfer and maintaining stable internal temperatures.

**CHAPTER TWO**  
**LITERATURE REVIEW**

## **CHAPTER TWO**

### **LITERATURE REVIEW**

#### **2.1 Introduction**

This chapter aims to review previous research and work related to the application of bio-based materials in the field of thermal insulation and how to integrate them with traditional building materials. This approach aims to achieve more sustainable and effective building structures in terms of thermal insulation. Bio-based materials include substances derived from organic sources, such as agricultural waste, plant fibers, and other organic materials. These materials are often renewable and biodegradable, making them a sustainable choice for use in various applications.

#### **2.2 Literature Review**

##### **2.2.1 Studies that used waste with cement**

**Wei et al.** 2023 [16] examined sawdust addition to Magnesium Oxysulfide Cement (MOSC) and Ordinary Portland Cement (OPC) for lightweight composites. Sawdust impacted mechanical, thermal, hydration, water absorption, and water resistance properties. SD-MOSC had lower density, higher compressive strength, and better thermal insulation than SD-OPC. MOSC showed compatibility as a bonding agent for sawdust, making it promising for eco-friendly thermal insulation boards.

**Charai et al.** 2022 [17] created concrete composites with Alfa fibers (AF) for both structural and insulation applications. They evaluated five formulations with varying AF ratios (0-10 wt%) for thermal insulation, mechanical strength, moisture sorption, and durability.

Increasing AF content improved thermal insulation and moisture sorption but reduced strength. Durability tests indicated that AF enhanced abrasion

resistance up to 5 wt% incorporation. Formulations with 5 wt% and 10 wt% AF exhibited compressive strengths of 3.78–0.6 MPa and thermal conductivity of 0.46–0.19 W/m·K, respectively.

**Marques et al.** 2021 [18] evaluated cement-based composites containing rice husk for use as acoustic barriers and heat insulating materials in multilayer systems. Laboratory tests assessed mechanical, durability, and acoustic properties, along with specific heat capacity and thermal conductivity for insulation. Life cycle assessment indicated their environmental viability. These composites offer a promising and eco-friendly solution for building applications.

**Selvaranjan et al.** 2021[19] created a sustainable rice husk ash (RHA) based mortar for wall plastering to enhance thermal insulation and energy efficiency in buildings. Sand was partially replaced with RHA to create RHA-based gypsum. The results showed that RHA effectively replaced up to 30% of sand, producing thermally enhanced grout with lower environmental impact, highlighting its potential for improved thermal insulation and energy efficiency in construction.

**Maaroufi et al.** 2021 [20] developed composite mortar using recycled expanded polystyrene, evaluating its hygienic, thermal, physical, and mechanical properties. Emphasis was on thermal performance for building materials. Results revealed favorable thermal conductivity, heat capacity, and water vapor permeability. Recycled expanded polystyrene mortar holds promise for construction due to its positive thermal attributes.

**Barbieri et al.** 2020 [21] developed degraded lime concrete using raw wheat husk as a lightweight aggregate.

Physical, chemical, and technological properties of particles and concrete were examined. Wheat husk concrete was compared to hemp concrete with similar thermal conductivities (0.09 W/(mK)).

Although wheat husk concrete had slightly lower compressive strength due to particle-binder interface weakness, it showcased potential for innovative and sustainable construction materials.

**Salem et al.** 2020 [22] evaluated industrial waste from vegetable synthetic sponges (VSS) as a sand substitute in cement slurries. Incorporating VSS with silica fume reduced porosity and boosted mechanical strength. Substituting natural sand with VSS enhanced thermal performance, indicating potential for construction with better insulation.

**Asim et al.** 2020 [23] explored the use of various natural fibers (jute, coconut, sugar cane, sisal, basalt) to develop environmentally friendly materials with improved thermal insulation properties. The research revealed that as the percentage of natural fibers in concrete increased, the thermal conductivity of the concrete also increased, leading to enhanced thermal insulation properties. However, this improvement in thermal insulation was accompanied by a decrease in compressive strength.

**Chen et al.** 2020 [24] investigated the use of Miscanthus biomass fibers as lightweight aggregates in concrete to improve sound absorption and thermal insulation properties. They tested two types of Miscanthus fibers for their insulation capabilities and characterized other mechanical properties like bulk and flexural density. The findings showed that Miscanthus concrete with 30% of 2-4 mm Miscanthus fibers achieved a remarkably low density of 554 kg/m<sup>3</sup>, a low thermal conductivity of 0.09 W/(m·K), and a high acoustic absorption coefficient of 0.9 at low frequencies.

This lightweight concrete is well-suited for use in interior ceiling panels and non-structural walls, providing a comfortable and energy-efficient indoor living environment.

**Berger et al.** 2020 [25] confirmed substituting waste wood into wood wool cement boards as viable. Comprehensive evaluation showcased wood waste's feasibility in fiber cement for eco-friendly construction.

**Binici et al.** 2020 [26] studied the effect of sunflower and wheat stalks, combined with vermiculite, creating effective, cost-efficient insulation. This eco-friendly approach offers an alternative to plastic-based synthetics. The proposed compressed material, including vermiculite, stalks, and gypsum, displays promising thermal conductivity (0.063 to 0.334 W/m·K), compressive strength (0.363 MPa), and density (0.166 to 0.302 g/cm<sup>3</sup>). This sustainable solution presents potential for efficient building insulation.

**Abbas et al.** 2019 [27] aimed to create an eco-friendly, lightweight, and thermally insulating cement material by incorporating rice husk-derived silica aerosol gel. Composite ratios were varied, and tests assessed porosity, density, strength, and thermal conductivity. Results showed promising thermal and light insulation properties, indicating potential for environmentally friendly construction applications.

**Dixit et al.** 2019 [28] developed a lightweight cementitious compound by adding polystyrene granules, enhancing its insulation capacity. They varied EPS bead proportions (3-5 mm diameter) from 0% to 45% and conducted tests. Results showed that improved concrete with polystyrene achieved 45 MPa compressive strength, 1677 kg/m<sup>3</sup> density, and 0.58 W/mK thermal conductivity, promising for insulation and lightweight applications.

**Wei et al.** 2019 [29] studied corn stalk (CS) bio-composites using magnesium phosphate cement (MPC) and ordinary Portland cement (OPC) binders. CS-MPC had lower porosity, reduced water absorption, and influenced thermal properties. CS-OPC composites exhibited different characteristics. The study suggested an MPC binder for aggregate concrete production.



**Ahmad et al.** 2018 [30] developed a bio-composite using magnesium phosphate cement (MPC), fly ash (FA), and corn stalk (CS) for thermal insulation and structural use. Evaluating properties like compressive strength, thermal conductivity, and water absorption, CS-MPC exhibited improved thermal properties with conductivity values of 0.0510 and 0.0986 W/m.K, indicating its potential for eco-friendly thermal insulation applications.

**Abdelkarim et al.** 2018 [31] produced insulation materials by blending palm tree roof fibers, cactus fibers, and Sodom apple fibers, bound with corn starch, gum, and white cement. Thermal conductivity tests across temperatures yielded values from 0.04234 to 0.05291 W/m.K. These hybrid samples consisted of safe natural materials and biodegradable substances, aligning with eco-friendly practices. The materials exhibit heat insulation and sound absorption qualities, holding promise for building applications.

**Zhou et al.** 2018 [32] conducted a study on fiber cement composites with positive mechanical and thermophysical traits. They compared concrete wall panels reinforced with traditional fiberglass and staple fibers. Results indicated staple fibers as effective substitutes for glass fibers in cement wall panels, providing similar structural and insulation performance. The use of staple fibers also exhibited promising environmental attributes, underscoring their potential as sustainable alternatives.

**Haba et al.** 2017 [33] innovated a construction bio-composite, blending cement, sand, water, and date palm fibers. Their study assessed water vapor permeability, isobaric absorption, moisture diffusion, and thermal conductivity. The inclusion of palm fibers improved performance, lowering resistance to vapor diffusion and enhancing moisture transfer. Performance was compared to other commonly used construction bio-composites.

**Boumhaout et al.** 2017 [34] carried out a study to create composite materials for building insulation by combining mortar with palm fiber (DPF). The researchers tested different fiber percentages ranging from 0% to 51% and assessed the thermal and mechanical properties of the resulting compounds. The findings indicated that incorporating DPF positively influenced the composite material, boosting its insulation capacity, enhancing the damping of heat diffusion, and reducing the overall weight of the mortar. Additionally, DPF improved the flexibility of the mortar, enabling it to be categorized as both a structural and insulating material based on RILEM functional classification.

### 2.2.2 Studies that used waste with gypsum

**Ding et al.** 2022 [35], utilized hydrogel granules from decomposed and purified leather waste. These were combined with gypsum, creating a lightweight composite. The composite featured porosity (22.64% - 55.37%) and low density (0.76 g/cm<sup>3</sup> - 1.47 g/cm<sup>3</sup>). Thermal conductivity ranged from 0.383 W/m·K to 0.190 W/m·K. The study underscores composite materials' role in innovative building materials, particularly for low-density and effective thermal insulation applications.

**Mehrez et al.** 2022 [36] investigated the application of plaster mixed with untreated plant fibers, wood fibers, and straw fibers for insulation purposes.

They varied the weight percentages of these fibers (ranging from 0% to 20% by volume) and observed that the combination of wood fibers and straw grain fibers with gypsum led to a reduction in thermal conductivity, heat capacity, efficiency, and weight of the composite materials. Consequently, these findings highlight the potential of these materials to compete favorably with traditional insulation materials.

**Bouzit et al.** 2021[37] investigated adding polystyrene balls to Moroccan gypsum. Analysis covered mechanical, thermal, acoustic aspects. Results showed polystyrene notably improved thermal insulation. A 3 cm layer effectively enhanced heat, acoustics, and environmental sustainability, presenting an attractive choice for construction.

**Boquera et al.** 2021[38] employed bio-waste-derived lignin to create construction-suited gypsum plasters. Combining lignin with distinct gypsum types, they aimed to balance increased lignin while maintaining mechanical and thermal attributes. Gypsum/lignin composites showed superior thermal insulation compared to cladding materials, though formulations with  $\geq 70\%$  gypsum met wall panel strength needs. Despite this, higher lignin composites improved overall insulation, showing promise for energy-efficient building uses.

**Ouhaibi et al.** 2021[39] investigated the incorporation of aerosols into plaster to enhance its insulating properties. They prepared gypsum samples with different aerosol percentages and measured their thermophysical properties, observing improved thermal conductivity. The gypsum composite with 10% aerosols showed excellent water absorption properties compared to the 15% sample. This indicates its potential as a competitive alternative to traditional building insulation materials, highlighting aerosol-infused gypsum as an effective and efficient insulation solution.

**Benallel et al.** 2021 [40] used four plant fiber types (reed, alpha, fig branches, olive leaves) were investigated individually and in combination with various cardboard waste ratios. The findings indicated higher fiber content slightly raised density, and thermal conductivity, but notably reduced water absorption rate. A composite with 0.072 W/m·K thermal conductivity and 176 kg/m<sup>3</sup> density showed the best insulation. Another composite with 40% alpha fiber and 60% cardboard had 262% water absorption. These composites displayed improved insulation properties

and environmental benefits, promising sustainable thermal insulation options.

**Capasso et al.** 2020[41] developed lightweight gypsum compounds by blending with plant-based protein foam. Two methods evaluated the thermal, acoustic properties, and porosity of composites for insulation assessment. Foam addition notably enhanced mechanical performance and porosity, impacting microstructure. Gypsum compounds exhibited improved insulation properties. Incorporating plant-based protein foam is a promising method to enhance gypsum compounds' insulation and overall construction material performance.

**Sair et al.** 2019 [42] developed an insulating material using natural fibers from cork and cardboard combined with gypsum. Five samples were created with varying ratios. Results showed decreased heat conduction, indicating insulation effectiveness. Mechanical properties were non-structural, with thermal conductivity ranging from 223.17 to 62.30 mW m<sup>(-1)</sup> K<sup>(-1)</sup>, and compressive strength from 0.17 to 0.30 MPa. The material is suitable for thermal insulation, not for structural use.

**Jiang et al.** 2019 [43] developed lightweight gypsum plasters (LGP) by incorporating swollen bentonite.

Higher bentonite content reduced dry density, compressive strength, and flexural strength of LGPs while enhancing thermal insulation. LGPs showed dry density (784 - 1196 kg/m<sup>3</sup>), compressive strength (3.9 - 11.7 MPa), flexural strength (-2.1 - 3.9 MPa), and thermal conductivity (0.116 - 0.143 W/m·K). Pores within bentonite's montmorillonite layers improved moisture control, suggesting potential for improved thermal insulation and moisture management in lightweight gypsum plasters.

**Kang et al.** 2018[44] aimed to enhance gypsum's thermal conductivity and moisture traits. They introduced expanded vermiculite, perlite, and three xGnP types with different surface areas to improve the material. Their

focus was on assessing its applicability in construction. They evaluated gypsum boards for thermal behavior and moisture content, with insulation tests yielding promising outcomes. The adjustments made to the gypsum boards yielded improved insulation qualities and enhanced moisture resistance, indicating their potential usefulness for building insulation.

**Braiek et al.** 2017 [45] developed a new composite gypsum material reinforced with palm fibers to improve its thermal properties and reduce weight. The objective was to decrease energy consumption in buildings. This composite material was intended for use in suspended walls or ceilings and had the potential to act as a thermal insulator, possibly replacing traditional gypsum boards. Thermal experiments demonstrated that the palm fiber-reinforced gypsum exhibited low thermal conductivity and excellent thermal insulation properties. These findings suggest that this composite material could effectively enhance energy efficiency in building constructions.

**Mar Barbero-Barrera et al.** 2017 [46] used recycled graphite powder in the manufacture of gypsum boards. A series of samples were prepared and the percentage of graphite ranged from 0% to 25%, by weight substitution, the addition of graphite powder significantly changed the bulk density, thermal conductivity and emissivity of the samples, and also resulted in a half reduction in the outgoing heat flux when melting graphite and gypsum board. The use of plasticizers reduces the bulk density and thermal conductivity of samples.

**Gencel et al.** 2016 [47] developed a gypsum composite with added polypropylene fibers and 20% diatomite, a microscopic plant extract. They conducted physical and thermal tests on the samples. These findings highlight diatomite's potential to enhance gypsum composite's thermal and mechanical traits, presenting promise for diverse applications.

### 2.2.3 Studies that used waste with different binder

**Medina et al.** 2017 [48] created gypsum composites by incorporating polypropylene fibers and isotropic graphite waste. The addition of graphite had a beneficial effect on gypsum's properties. Different levels of graphite altered the composite's characteristics, enhancing mechanical strength (compressive, flexural, Young's modulus), increasing density, improving thermal conductivity, reducing porosity, and minimizing water absorption. These composite materials were employed in construction industry applications, such as panels and design, contributing to heightened material durability and sustainability.

**Benchouia et al.** 2023[49] replaced petroleum-derived polystyrene with Polystyrene/Date Palm Fiber Composite (PS-DPF), made from palm leaf residue.

This new material exhibited superior mechanical and thermal insulation properties compared to virgin polystyrene (VPS) and other insulating materials. The study showed promising results for thermal insulation applications, as it reduced thermal conductivity by up to 50%. The use of composite materials as thermal insulators encourages the utilization of waste in date-producing countries.

**Singh et al.** 2023[50] examined diverse rice straw blends for block production. Sample density ranged from 1070 to 730 kg/m<sup>3</sup>, involving 0-15% rice straw. Blocks' compressive strength varied from 4.6 to 1.4 MPa. Thermal conductivity values ranged from 0.15 to 0.07 W/m·K, implying strong insulation. Blocks displayed notable thermal insulation, moderate acoustics, and strong fire resistance, rendering them appealing and sustainable for various construction projects. These gypsum blocks, with promising attributes and agricultural residues like rice straw, offer practical eco-friendly potential.

**Charai et al.** 2023 [51] explored coal fly ash (CFA) and plant fibers (Alfa fibers - AF) in composites. Varying CFA (0-80%) and short AF (0-6%) ratios, they assessed properties: density, strength, thermal conductivity, and moisture storage. Results highlighted CFA's hygroscopic role and AF's dual action as hygroscopic and strengthening agents. AF compensated for porosity-induced strength loss. The composite holds the potential for passive heat and humidity control in buildings, suitable for practical use.

**Khalaf et al.** 2021[52] explored using miscanthus, recycled textile, and rice husks as reinforcement for a chitosan matrix to create innovative insulating composites for buildings.

These composites, with thermal conductivity of 0.07–0.09 W/(m·K) and density of 350–400 kg/m<sup>3</sup>, were manufactured via thermocompression. Varying particle sizes of miscanthus and rice husks, along with textile inclusion, affected thermal and mechanical properties. Smaller miscanthus particles showed the best mechanical results, suggesting potential for competitive and promising insulation materials.

**Chen et al.** 2021 [53] produced cold-based lightweight aggregates (BCBLWAs) from steel slag converter and slag powder treated with CO<sub>2</sub>. BCBLWAs exhibited varied compressive strengths (0.58 MPa to 5.3 MPa) and bulk densities (550 kg/m<sup>3</sup> to 1300 kg/m<sup>3</sup>). Through analysis of microstructure and CO adsorption, BCBLWAs were incorporated into lightweight concrete, achieving 28.5 MPa compressive strength, 1630 kg/m<sup>3</sup> density, and 0.255 W/(m·K) thermal conductivity. Promising as lightweight concrete aggregate with improved thermal insulation.

**Wang et al.** 2020 [54] created a composite using rice husks, metakaolin, and hydrogen peroxide. This composite displayed densities from 174 to 813 kg/m<sup>3</sup>, thermal conductivity of 0.082 to 0.184 W/(m·K), and

compressive strength from 0.26 to 7.24 MPa. Water absorption ranged from 28.3% to 93.6%, and moisture absorption from 9.7% to 18.6%, showing potential for energy-efficient building applications.

**Marques et al.** 2020 [55] developed polymer-based composite materials using a combination of rice husk and expanded cork. These composites were studied for mechanical, thermal, and acoustic properties, with different ratios and densities examined. Higher rice husk content reduced thermal conductivity and improved mechanical behavior.

The composites show promise for structural applications like walls and floors, offering eco-friendly construction materials with enhanced insulation and strength.

**Platt et al.** 2020[56] conducted a study on using wheat straw bales for building insulation, highlighting their excellent thermal performance. They found that by optimizing the baling process and adjusting bale sizes, these straw bales can be a sustainable and effective choice for insulation in modern construction, offering improved thermal and mechanical properties.

**Guna et al.** 2020 [57] investigated rice husks and peanut shells for sustainable polypropylene composites in building materials. They analyzed the thermal and mechanical traits of these composites. Rice husks' unique wedge shape and low aspect ratio influenced composite properties significantly. Composites showed notable tensile (up to 15.6 MPa) and flexural (up to 37.6 MPa) strengths. Thermal conductivity ranged from 0.156 to 0.270 W/m·K, while water absorption remained below 85%. These composites demonstrated favorable characteristics compared to other insulation materials, holding promise for sustainable building solutions.

**Savic et al.** 2020 [58] created biofiber sandwich panels using *Miscanthus giganteus*, mineral binders, pozzolans, and water. Panels showed good heat



transfer behavior due to essential fibers. Testing included pressure, bending, water absorption, and thermal properties, all showing promising performance and thermal characteristics.

**Muthuraj et al.** 2019 [59] used grain husks and adhesive textile waste mixed with PBAT/PLA bio-resin. The researchers created composites for interior insulation in buildings. Results, with thermal conductivity as low as 0.08 W/m·K.

These eco-friendly composite materials hold promise for effective and sustainable interior insulation applications, combining environmental friendliness with superior thermal performance.


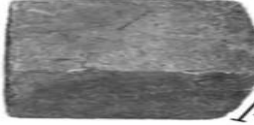

**António et al.** 2018 [60] introduced a composite material incorporating rice husk, expanded cork or recycled rubber, and TDI-based polyurethane binder. Evaluated for strength, thermal properties, sound insulation, and absorption, the study highlighted enhanced building solutions and thermal performance potential. Rice husk, expanded cork, and recycled rubber synergistically created a promising composite for construction applications.


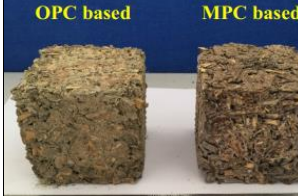
### 2.3 Summary of Literature Review


In previous research studies, there has been a noticeable trend towards exploring the potential of renewable insulation materials derived from agricultural and industrial waste within the construction sector. This exploration often involves incorporating these materials into traditional building elements such as cement, gypsum and plaster. The overarching goal is to take advantage of their properties in order to enhance thermal insulation capabilities and enhance long-term sustainability in building practices. Moreover, these studies entered the realm of agricultural and industrial residues by combining them with different binding agents. This



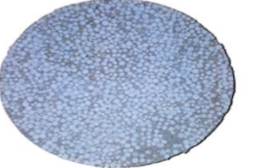
innovative approach has led to the creation of new composite materials that combine the unique properties of each component. In general, this study focuses on the importance of harnessing agricultural and industrial waste as a means for developing thermal insulation materials. In combination with binders, as well as with traditional building materials, they play a critical role in enhancing the thermal efficiency of buildings and contributing to environmentally conscious building practices. Table 1.2 and Table 2.2 provide an overview of research endeavors that incorporated agricultural and industrial waste alongside conventional building materials like cement, gypsum, and plaster. On the other hand, Table 2.3 offers a synopsis of studies that harnessed agricultural waste in combination with various binding agents.

Table 2-1 A summary of studies that dealt with agricultural and industrial waste mixed with traditional building materials (cement)

No.	Authors	The materials used	Results	Model photos
1.	<b>Boumhaut et al. 2017</b> [34]	mortar and Date Palm Fibers mesh (DPF)	The results indicated that with increasing fiber content, the thermal conductivity decreased significantly from 0.795 to 0.243 W/(m K), reducing diffusion by 52%, efficiency by 56%, and density by 39%. Mechanical strength is still acceptable.	
2.	<b>Haba et al. 2017</b> [33]	Cement, Sand, Water, Date palm fibers	The results showed an improvement in the thermal properties, as the bulk density was 954 kg / m <sup>3</sup> and the thermal conductivity was 0.185 W / (m K).	
3.	<b>Alabdulkarem et al. 2018</b> [31]	wood glue, white cement, fibers from date palm, Sodom apple	Hybrid insulating materials with different binders and fibers exhibited thermal conductivity ranging from 0.04234 to 0.05291 W/m·K at temperatures of 10-50 °C.	

4.	<b>Ahmad et al. 2018</b> [30]	Magnesium phosphate cement, fly ash, and corn stalk	This research introduces a corn stalk magnesium phosphate cement concrete (CS-MPC) bio-composite with enhanced thermal conductivity (0.0510 and 0.0986 W.m-1.K-1), mechanical properties ( $f_c' = 6.98\text{MPa}$ and $9.44\text{MPa}$ ).	
5.	<b>Wei et al. 2019</b> [29]	Corn Stalk, Magnesium Phosphate Cement (MPC) or OPC	The composite characteristics encompass an apparent density ranging from 784 to 947 kg/m <sup>3</sup> , compressive strength varying from 0.67 to 3.83 MPa, and a thermal conductivity of 0.159 to 0.22 W/(m·K).	
6.	<b>Dixit et al. 2019</b> [28]	Expanded Polystyrene (EPS) Beads and Ultra-High-Performance Concrete (UHPC)	The result of combining 3-5 mm diameter EPS granules with UHPC base materials in different ratios from 0% to 45% depending on the volume. The resulting composite showed a strength of up to 45 MPa with a density of 1677 kg/m <sup>3</sup> and a thermal conductivity of 0.58 W/m·k.	-

7.	<b>Abbas et al. 2019</b> [27]	Rice Husk, Silica Aerogel, Cement and Sand	The rustle of the aerogel from rice husk, into the cement composites resulted in a reduction in density to 1,133 kg/m <sup>3</sup> (A100) and thermal conductivity to 0.33 W/m <sup>3</sup> .	-
8.	<b>Berger et al. 2020</b> [25]	Wood Waste, Cement, Wood Wool	The outcome demonstrates that wood waste effectively replaces up to 50% of spruce in Wood Wool Cement Board (WWCB), maintaining favorable thermal performance (<0.08 W.m <sup>-1</sup> . K <sup>-1</sup> ).	-
9.	<b>Chen et al. 2020</b> [24]	Miscanthus fibers and concrete	The result of lightweight concrete incorporating miscanthus fiber has low density (554 kg/m <sup>3</sup> ), and effective thermal insulation (0.09 W/(m·K)).	-
10.	<b>Salem et al. 2020</b> [22]	Synthetic vegetable sponge (VSS) mortar	Replacing natural sand with vegetable synthetic sponge waste results in a 63% lower thermal conductivity, densities ranging from 1170 kg/m <sup>3</sup> to 2074 kg/m <sup>3</sup> , and thermal conductivity values of 0.2-1.9 W/(m·K), along with compressive strengths of 23 MPa and 18 MPa.	

11.	<b>Barbieri et al. 2020</b> [21]	Original wheat husk with lime concrete	Wheat hulls as lightweight aggregate in lime concrete yield promising results: 0.09 W/(m·K) thermal conductivity and good compressive strength.	
12.	<b>Asim et al. 2020</b> [23]	natural fibers (jute, coconut, sugar cane, sisal, and basalt) in concrete	Using natural fibers in concrete enhances insulation but reduces compressive strength. The thermal conductivity ranges from 0.26 to 0.3 W/(m·K) with compressive strengths of 2.4 to 5 MPa.	
13.	<b>Maaroufi et al. 2021</b> [20]	Recycled Expanded Polystyrene Mortar	The results of cement compound with polystyrene. They show improved thermal performance (383 mW/m·K to 157 mW/m·K for polystyrene mortar) but low mechanical strength (22.5 MPa to 4 MPa).	
14.	<b>Selvaranj an et al. 2021</b> [19]	Rice husk ash (RHA) and mortar	The result of replacing sand with RHA in the mortar (0-50%). improves thermal conductivity by up to 30% (62% reduction) while maintaining strength. Replacing 30% of sand with OBRHA reduces emissions (13% per kg) and cost (4% per kg).	-


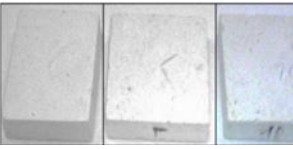
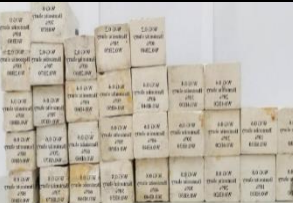

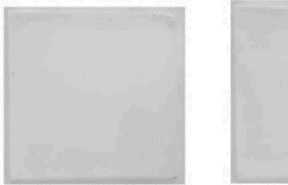

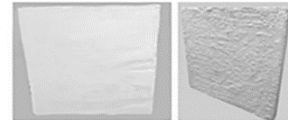
15.	<b>Marques et al. 2021</b> [18]	Cement and rice husk	Rice husk composites excel as insulators, boasting superior environmental sustainability to wood and rubber composites, with values including compressive strength (1.31-9.34 MPa), bulk density (930.7-1311.4 kg/m <sup>3</sup> ), and thermal conductivity (0.2087-0.9302 W/m·K).	
16.	<b>Charai et al. 2022</b> [17]	Alpha fibers and concrete	The study on Alfa fiber concrete composites reveals values for thermal conductivity (W/m·K) ranging from 0.19 to 0.46 and compressive strengths (MPa) from 0.6 to 3.78.	-
17.	<b>Wei et al. 2023</b> [16]	Sawdust, magnesium oxysulfide cement and ordinary Portland cement	Adding sawdust to magnesium oxysulfide cement and ordinary Portland cement led to composites with densities ranging from 542 to 934 kg/m <sup>3</sup> and thermal conductivities from 0.081 to 0.295 W/(m·K).	-

Table 2-2 A summary of studies that dealt with agricultural and industrial waste mixed with traditional building materials (gypsum)

No.	Authors	The materials used	Results	Model photos
1.	<b>Gencil et al. 2016</b> [47]	gypsum, diatomite and polypropylene fibers	Using diatomite in gypsum compounds improves mechanical properties, and reduces thermal conductivity, with values: thermal conductivity 0.384-0.494 W/m·K, unit weight 881.5-999.0 kg/m <sup>3</sup> , water absorption 39.6-52.1 wt.%, and compressive strength 1.1-2.3 MPa.	-
2.	<b>Braiek et al. 2017</b> [45]	Gypsum and Date palm fibers	Gypsum reinforced with date palm fibers showed improved thermal properties, with a density ranging from 736.31 to 1322.18 kg/m <sup>3</sup> and thermal conductivity between 0.174 and 0.452 W/m·k	
3.	<b>Medina et al. (2017)</b> [48]	polypropylene fibers (PPF), isostatic graphite	The study on gypsum composites with 15% IGF and 20% PPF shows improved strength, with compressive strength values ranging from 0.98 MPa to 4.81 MPa, along with enhanced thermal conductivity from 0.167 to 0.33 W/m·K.	-






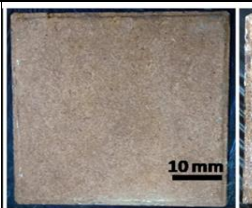
		filler (IGF) and gypsum		
4.	<b>Jiang et al. 2019</b> [43]	Bentonite and gypsum putty	The results of Pre-swelled Bentonite in Gypsum Paste, Density: 784-1196 kg/m <sup>3</sup> , Compressive Strength: 3.9-11.7 MPa, Bending Strength: 2.1-3.9 MPa, Thermal Conductivity: 0.116-0.143 W/m·K due to 40%.	
5.	Sair et al. 2019 [42]	cork, cardboard and gypsum	Cork and cardboard produce a composite with low thermal conductivity (62.30-223.17 mW/m·K) and compressive strength (0.17-0.30 MPa).	
6.	<b>Capasso et al. 2020</b> [41]	Natural foaming agent	The use of vegetable protein foaming agents in gypsum composites to improve insulating properties. Key values include thermal conductivity (0.186-0.477 W/m·K) and density (0.49-1.06 g/cm <sup>3</sup> ).	-





7.	<b>Ouhaibi et al. 2021</b> [39]	Aerosil and plaster	The result of aerosol blending Thermal Insulating Plaster: 15% Aerosil Compound exhibits 83% lower thermal conductivity (0.04 W/m·K), 77% lower diffusion, and 45.8% lighter density. Mechanical strength decreases.	
8.	<b>Boquera et al. 2021</b> [38]	lignin and gypsum	As a result of adding lignin to gypsum mixtures, the basic values include density (0.837-1.030 g/cm <sup>3</sup> ), compressive strength (1.32-10.39 N/mm <sup>2</sup> ), and thermal conductivity 0.19-0.48 W/m·K.	
9.	<b>Bouzit et al. 2021</b> [37]	Moroccan gypsum and polystyrene	As a result of mixing Moroccan gypsum reinforced with polystyrene, it improves thermal conductivity (0.191-0.116 W/m·K), and acoustic absorption. Insulation is maintained at 45 dB.	
10.	<b>Ding et al. in 2022</b> [35]	Chrome leather waste into hydrogel beads, embedded in gypsum	The results of incorporating chrome leather waste into gypsum-embedded hydrogel granules with a density ranging from 0.76 to 1.47 g/cm <sup>3</sup> . The thermal conductivity decreased from 0.383 W/m·K to 0.190 W/m·K.), providing insulation.	-


11.	Singh et al. 2023[50]	Rice straw with gypsum	Composite results: density (730-1070 kg/m <sup>3</sup> ), compressive strength (1.1-4.6 MPa), thermal conductivity (0.07-0.15 W/m·K).	-
-----	-----------------------	------------------------	---	---

Table 2-3 A summary of studies dealing with agricultural and industrial waste mixed with different binders

No.	Authors	The materials used	Results	Model photos
1.	<b>Buratti et al. 2018</b> [61]	Rice husk (RH) and glue	Rice husk (RH) panels show thermal conductivity results at 0.070 W/(m·K), and a density of 170 kg/m <sup>3</sup> .	
2.	<b>António et al. 2018</b> [60]	Rice husk, with different proportions of cork or rubber	The study introduces rice husk composite boards for construction. With varied proportions of cork or rubber, they show promising thermal (60.0-74.3 mW/(m·K)) and acoustic (20-27 dB) properties.	

3.	<b>Muthuraj et al.</b> 2019[59]	Rice husk, wheat husk, wood fiber, textile waste fiber and Poly (lactic acid) (PBAT/PLA) blend binder	Results using agricultural and industrial waste (rice husk, wheat husk, wood fibers, textile waste) with PBAT/PLA binder. The composites showed good mechanical strength and low thermal conductivity (0.08–0.14 W/m·k).	
4.	<b>Savic et al.</b> 2020 [58]	Miscanthus giganteus bio-fiber	Miscanthus giganteus bio-fiber composite thermal insulation evaluated. Properties: thermal conductivity (0.08–0.10 W/(m·K)), density (330–819 kg/m <sup>3</sup> ), compressive (31–1116 kPa) and flexural strength (111–631 kPa).	
5.	<b>Guna et al.</b> 2020 [57]	Rice husk (RH), Groundnut shell (GNS) and Polypropylene (PP)	The results of using cellulosic agricultural waste, rice hulls, and peanut shells with polypropylene. The composite material showed good mechanical strength (tensile strength up to 15.6 MPa), thermal insulation of 0.156-0.270 W/m·K and water absorption of 85%.	

6.	<b>Binici et al. 2020</b> [26]	vermiculite, sunflower stalk, wheat stalk	The results of a new insulating material composed of vermiculite, sunflower stalk, wheat stalk and gypsum have promising properties. Thermal conductivity: 0.063–0.334 W/m·K, compressive strength: ~0.363 MPa, density: 0.166–0.302 g/cm <sup>3</sup> .	
7.	<b>Platt et al. 2020</b> [56]	wheat straw bales	The results of the new wheat straw bale compound used in building insulation ranged from 126 to 129 kg/m <sup>3</sup> and thermal conductivity values from 0.078 to 0.056 W/m·K.	
8.	<b>Marques et al. 2020</b> [55]	rice husk, expanded cork granules and polymer	Composite mixtures combining rice husk and expanded cork for thermal conductivity and mechanics showed potential with density (199-390 kg/m <sup>3</sup> ), compressive stress (68-492 MPa), and thermal conductivity (0.0464-0.0739 W/(m·K)).	
9.	<b>Wang et al. 2020</b> [54]	Rice husk, Metakaolin and Hydrogen peroxide	The results using rice husks, metakaolin, and hydrogen peroxide. Different proportions of components were affected by density (174-813 kg/m <sup>3</sup> ), thermal conductivity (0.082-0.184 W/(m·K)) and compressive strength (0.26-7.24 MPa).	

10.	<b>Benallel et al. 2021</b> [40]	Cardboard waste and plant fibers	The results The incorporation of paperboard waste and vegetable fibers leads to a slight increase in density and thermal conductivity. The optimal insulation ranges from 0.072 to 0.98 W/m <sup>2</sup> .	-
11.	<b>Khalaf et al. 2021</b> [52]	Miscanthus Recycled textile Rice husks and Chitosan	Recycled textiles and rice hulls. It showed thermal conductivity (0.07–0.09 W/(m·K)) and density (350–400 kg/m <sup>3</sup> ).	
12.	<b>Alshahrani et al. 2022</b> [62]	Rice husk ash and Epoxy resin	The results of bio-epoxy coatings with bio-silica for rice husk improves tensile and flexural properties; at 4 vol%, thermal conductivity was enhanced (0.42 W/m·K).	-
13.	<b>Charai et al. 2023</b> [51]	Coal fly ash (CFA), Short plant fibers ,Gypsum plaster	The results of combining building materials with coal fly ash (CFA) and short plant fibers (Alfa Fibers - AF). It improves thermal performance. Composite properties: density (934-1340 kg/m <sup>3</sup> ), compressive strength (1.38-6.98 MPa), thermal conductivity (0.26-0.57 W/m·K).	-

14.	<b>Benchouia et al. 2023</b> [49]	Polystyrene (PS) and Date Palm Leaves Remnants	Palm leaf composite results in polystyrene-based composites (PS-DPF) include tensile strength (14-27 MPa), flexural strength (31-44 MPa), compressive strength (2.9-5.9 MPa), and thermal conductivity (0.118). $-0.141 \text{ W/m}^3$ and density (860–980 $\text{kg/m}^3$ ).	-
-----	-----------------------------------	--	--	---

**CHAPTER THREE**  
**EXPERIMENTAL WORK**



## **CHAPTER THREE**

### **EXPERIMENTAL WORK**

#### **3.1 Introduction**

This chapter elaborates the production of insulation materials aimed at reducing thermal loads in buildings through the utilization of agricultural and industrial waste. It is structured into three main sections:

- Experimental Materials
- Samples' Preparation
- Experimental Tests
- Practical Application

#### **3.2 Experimental Materials**

Eight materials were used in this research work. They were cement, sand, gypsum, water, wood glue, polystyrene beads, rice husk, and wood chips. The following subsection give information about each material.

##### **3.2.1 Cement**

The cement used for the purpose of this study was ordinary Portland cement (OPC), in the first type, which was manufactured by Kufa Cement Factory (KCF). It adheres to the guidelines stipulated in IQS: 5/2010 and also follows ASTM C 150 standards. The chemical analysis of this type of cement is shown in Table 3-1, while the physical properties are shown in Table 3-2.

Table 3-1 Chemical analysis of Ordinary Portland Cement (OPC) \*

Components		Results	Requirements according to Iraqi Specification IQS: 5/2010
			Maximum value
Silicon Dioxide	SiO <sub>2</sub>	20.9%	None
Aluminum Trioxide	Al <sub>2</sub> O <sub>3</sub>	5.81%	None
Ferric Oxide	Fe <sub>2</sub> O <sub>3</sub>	3.56%	None
Calcium Oxide	CaO	61.88%	None
Magnesium oxide	MgO	4.11%	5%
Sulphate	SO <sub>3</sub>	2.29%	2.5% if C <sub>3</sub> A < 5%
Potassium oxide	K <sub>2</sub> O	None	2.5% if C <sub>3</sub> A > 5%
Sodium Oxide	Na <sub>2</sub> O	None	None
Insoluble Residue	Ins.Res.	0.64%	None
Loss on Ignition	LOI	1.49%	1.5%
Free lime	FL	0.51%	4%
Lime Saturation Factor	L.S.F.	0.82	4%
Silicon Ratio	M.S.	11.12	1.02%
Alumina Ratio	M.A.	1.63	None
Tricalcium Silicate Ratio	C <sub>3</sub> S	47.94	None
Dicalcium Silicate Ratio	C <sub>2</sub> S	21.82	None
Tricalcium Aluminates Ratio	C <sub>3</sub> A	20.41	None
Tetra calcium Alumina ferrate Ratio	C <sub>4</sub> AF	9.82	None

\* Data from the laboratory of Kufa Cement Factory.

Table 3-2 Physical characteristics of Ordinary Portland Cement (OPC) \*

Property	Test result	Iraqi Standards No.8/1968
Setting times: -Initial setting time [min] - Final setting time [min]	155 230	More than 45 minutes Less than 600 minutes
Fineness: -Retained on sieve No. 170 (90 $\mu$ m)	6%	Less than 10 minutes
Compressive strength (mortars): 3 days 7 days	23 N/mm <sup>2</sup> 30 N/mm <sup>2</sup>	More than 15 N/mm <sup>2</sup> More than 23 N/mm <sup>2</sup>

\* Data from the laboratory of Kufa Cement Factory

### 3.2.2 Sand

Sand is a naturally occurring granular material composed of finely divided mineral and rock particles. It forms through the weathering and erosion of rocks, with variations in composition depending on its source. Sand grains typically range from 0.0625 to 2 millimeters in diameter [63]. The sand used in this study, which conforms to ASTM C33-16, was produced by AL NAWAFTH Company/ Najaf.

### 3.2.3 Calcined gypsum

Commercial gypsum used for construction purposes and manufactured by Al Mezan Company was used for the purpose of this study. Calcined gypsum (plaster of Paris) constitutes about 95% of gypsum uses, and its purity ranges between 85-95%. It depends mainly on heating gypsum to 130 °C, where water associated with weak bonds is lost, turning into

a semi-aqueous gypsum  $\text{CaSO}_4 \cdot 1/2\text{H}_2\text{O}$ , commercially known as Calcined gypsum, and it is mostly used in construction such as wall adhesives, suspended ceilings, wall lining, partitions, and thermal insulators. The chemical analysis of this type of gypsum is shown in Table 3-3, and the physical characteristics are shown in Table 3-4 according to international standard ISO 17025.

Table 3-3 Chemical composition of Gypsum\*

Components	Requirements	Results	Examination method
The percentage of sulfur trioxide	Not less than (45) %	53.9	Guidance reference ISO17025
Percentage of calcium oxide	Not less than two-thirds of the percentage of sulfur dioxide	36.22	
Percentage of dissolved salts and magnesium salts	Total not more than (0.25) %	0.026	
Combined water ratio	Not less than % (4) and not more than % (9)	5.22	
Impurity percentage	Not more than (5)	3.74	

\* Data from Al-Meezan Company

Table 3-4 Physical characteristics of Gypsum\*

Components	Requirements	Results	Examination method
Degree of fineness	The remainder passes through a 16-inch sieve at 100%.	100%	Guidance reference ISO17025
Cohesion time	Not less than (8) minutes and not more than (25) minutes	10 min	
Compressive strength	Not less than (50) kg/cm <sup>2</sup>	95.65 kg/cm <sup>2</sup>	
Fracture standards	Not less than (15)kg/cm <sup>2</sup>	35.10kg/cm <sup>2</sup>	
Hardness strength	Not more than (5) mm	4.3 mm	

\* Data from Al-Meezan Company

### 3.2.4 Polystyrene Beads (EPS)

Polystyrene beads, also known as EPS (expanded polystyrene) beads, are small rounded shape particles made of expanded polystyrene foam. EPS beads are lightweight plastic material, having about 98% air. Therefore, These beads are commonly used in various applications due to their unique properties, such as low density, high load-bearing capacity at low weight, absolute water and vapor barrier, air tightness for controlled environments, long life, low maintenance, fast, and economic construction and good thermal insulation properties [64]. The size of the EPS beads varies, typically from 3 to 8 mm in diameter,

depending on the specific application and intended use as shown in Figure 3-1. These beads have a very low relative density (0.02) and a density of about  $19.8 \text{ kg/m}^3$ . Due to their lightweight nature and insulating properties, polystyrene beads contribute to reducing the overall weight of materials and improving energy efficiency in various products and systems [64].



Figure 3-1 Polystyrene beads

### 3.2.5 Rice husk

The rice husk is the outer protective layer of a rice grain, which is removed during the processing of rice [65]. It is a byproduct that has gained attention for its potential applications in various industries, including construction. Rice husk has been explored as a sustainable and eco-friendly material due to its abundance and unique properties.

It is composed of cellulose, lignin, and silica, making it suitable for use in various applications such as insulation, composite materials, energy generation, and more. In the context of construction, rice husks can be incorporated into various building materials to enhance their thermal insulation, and sustainability. Iraqi rice husks were collected from the mills of -Najaf Governorate, Al-Mishkhab District rice fields in middle of Iraq. Rice husks and fine rice husks that are used as animal feed were used in this research work, as shown in Figure 3-2. Table 3-5 shows the chemical composition of rice husk (RH).

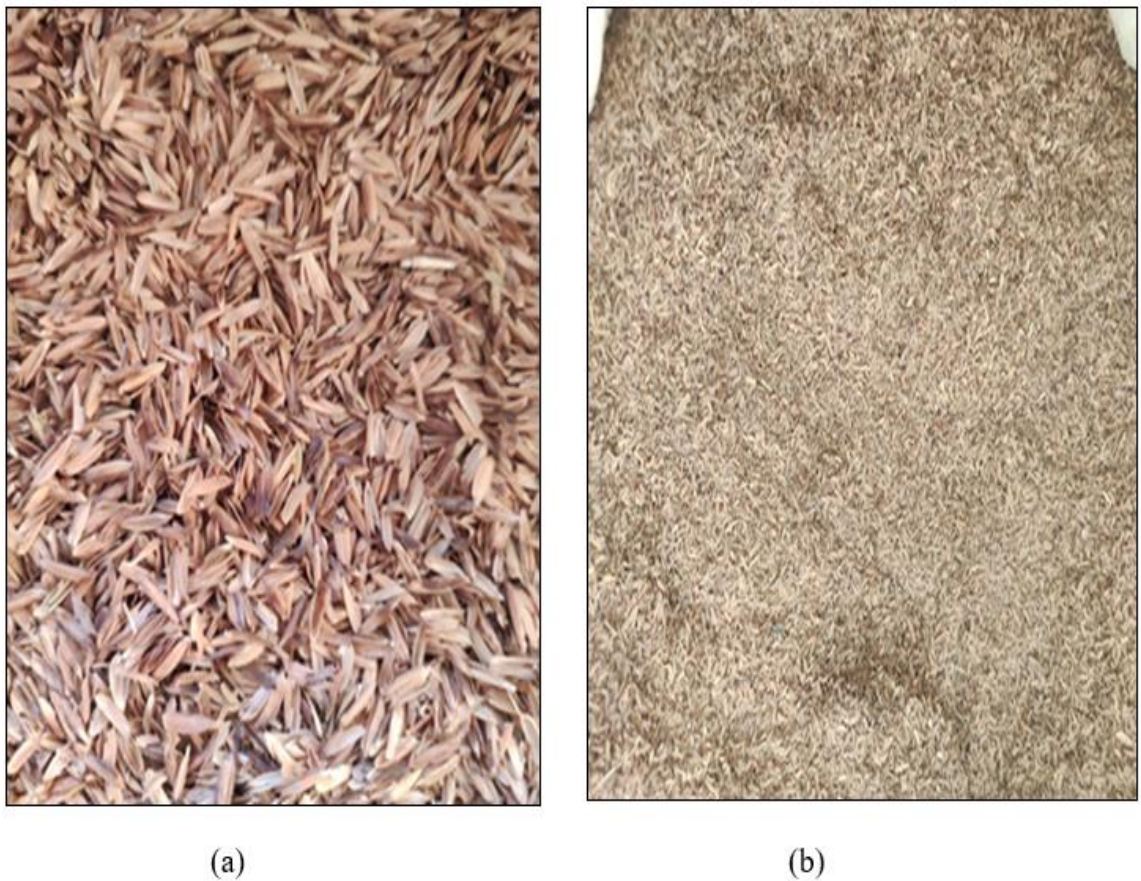


Figure 3 -2 (a) Rice husks (b) Fine rice husks

Table 3-5 Chemical properties of the Iraqi rice husk[66]

Chemical Composition	
Compound	Compound Composition wt %
SiO <sub>2</sub>	89
Al <sub>2</sub> O <sub>3</sub>	4.1
Fe <sub>2</sub> O <sub>3</sub>	0.31
CaO	1.31
MgO	1.7
Na <sub>2</sub> O	1.5
P <sub>2</sub> O <sub>5</sub>	0.56
MnO	0.2
K <sub>2</sub> O	3.77
CL	0.36
LOI	2.64

### 3.2.6 Wood chips

Wood chips are small pieces of wood produced during the process of cutting, milling or planing wood. Wood chips was obtained from the waste of a local factory for manufacturing of household furniture in Najaf, and its dimensions range from 3-10 mm, as shown in Figure 3-3.





Figure 3-3 Wood chips

### 3.2.7 Wood glue

Wood glue is a polymer that is produced from the union of formalin in an acidic medium with urea. Its raw materials are formaldehyde, sodium hydroxide or caustic soda, and cellulose. It is considered one of the important materials in decorations, wood glueing, and the manufacture of foam products.

### 3.2.8 Water

Tap water was used for the purpose of this research. The water used should be clean from oil, acid, alkali, organic matter, and any other matter that affects the mixture. The same condition of mixing water was implemented for curing the samples.

### 3.3 Sampls' preparation

The insulation materials produced from industrial and agricultural waste in this research have been divided into three groups based on the binding material used. These groups are described as follows:

- **First Group - Cementitious Compounds:** Cement serves here as the primary binding material. The insulation materials in this group consist of industrial and agricultural waste combined with cementitious compounds to achieve the desired thermal insulation. The proportions of insulation materials and cement vary within this group.
- **Second Group - Gypsum Compounds:** In this group, the binding material relies on gypsum compounds. Industrial and agricultural wastes are mixed with gypsum compounds to create insulation materials used for thermal insulation.
- **Third Group - Wood Glue:** This group utilizes wood glue as the binding material. Waste materials are blended with wood glue to create insulation materials based on this binding substance.

Table 3-6 shows the nomenclature of the samples used in this research. Each sample is named based on the first letter of the binder, making it easier to identify each sample and monitor results effectively.

Table 3-7 displays the weight percentages of materials used in each sample. This table reflects the exact composition and structure of each

sample by providing the percentage by weight of each material used in its manufacture.

Table 3-6 Samples names and components

<b>Sample code</b>	<b>Components</b>
<b>First Group</b>	
<b>C0</b>	Sand, Cement
<b>C1</b>	Fine Rice Husk, Sand, Cement
<b>C2</b>	Polystyrene, Sand, Cement
<b>C3</b>	Fine Rice Husk, Cement
<b>C4</b>	Sawdust, Sand, Cement
<b>C5</b>	Polystyrene, Sawdust, Rice Husk, Sand, Cement
<b>Second Group</b>	
<b>G0</b>	Gypsum
<b>G1</b>	Fine Rice Husk, Gypsum
<b>G2</b>	Rice Husk, Gypsum
<b>G3</b>	Polystyrene, Gypsum
<b>G4</b>	Sawdust, Gypsum
<b>G5</b>	Polystyrene, Sawdust, Rice Husk, Gypsum
<b>Third Group</b>	
<b>WG1</b>	Rice Husk, Wood glue
<b>WG2</b>	Fine Rice Husk, Rice Husk, Sawdust, Wood glue
<b>WG3</b>	Sawdust, Wood glue
<b>WG4</b>	Fine Rice Husk, Sawdust, Wood glue

Table 3-7 Components of the samples and their proportions

**First Group**

<b>Samples</b>	<b>Cement (%)</b>	<b>Sand (%)</b>	<b>Polystyrene (%)</b>	<b>Rice Huck (%)</b>	<b>Fine Rice Huck (%)</b>	<b>Sawdust (%)</b>	<b>Water (%)</b>
<b>C0</b>	24.78	68.17	-	-	-	-	7.04
<b>C1</b>	41.67	41.67	-	-	8.33	-	8.33
<b>C2</b>	49.18	32.78	1.63	-	-	-	16.41
<b>C3</b>	66.7	-	-	-	11.11	-	22.19
<b>C4</b>	45.45	30.3	-	-	-	9.9	14.35
<b>C5</b>	27.8	37.03	1.85	3.7	-	7.4	22.22
<b>Second Group</b>							
<b>Samples</b>	<b>Gypsum (%)</b>	<b>Polystyrene (%)</b>		<b>Rice Huck (%)</b>	<b>Fine Rice Huck (%)</b>	<b>Sawdust (%)</b>	<b>Water (%)</b>
<b>G0</b>	58	-		-	-	-	42
<b>G1</b>	66.7	-		-	16.7	-	16.6
<b>G2</b>	75.47	-		5.7	-	-	18.83
<b>G3</b>	67.7	3.8		-	-	-	28.5
<b>G4</b>	58.13	-		-	-	13.95	32.92
<b>G5</b>	44.11	2.9		5.88	-	11.76	35.35
<b>Third Group</b>							
<b>Samples</b>	<b>Fine Rice Huck (%)</b>			<b>Rice Huck (%)</b>	<b>Sawdust (%)</b>	<b>Wood glue%</b>	
<b>WG1</b>	-			13.79	-	86.2	
<b>WG2</b>	16.67			16.67	16.67	50	
<b>WG3</b>	-			-	19.35	80.6	
<b>WG4</b>	24.24			-	-	75.76	

### 3.3.1 Samples failure

Significant challenges were faced in achieving optimal bonding for samples containing various materials such as EPS beads, rice husk, wood chips, cement, gypsum, sand and wood glue. Where many samples were made but after drying they did not reach the cohesion stage. The main reasons for the failure of the cohesion of the samples were identified and mixing was enhanced to improve future results. Here are some points that were reasons for failure:

1. Sample mixture ratios

There were a challenge in getting the right proportions of materials, as their balance was not optimal. For example, if the sample contains large quantities of EPS beads or rice husks, this leads to an imbalance in the composition ratios of the sample and thus its incohesion. Table 3-8 shows the failed mixtures that were excluded.

2. Balance between binders and fillers

An ideal balance between binders (cement, gypsum, glue) and fillers (EPS beads, rice husk, wood chips) has not been achieved. An optimal balance is necessary to ensure strong and effective cohesion. Steps were taken to overcome these problems, where the proportions of the sample mixture were readjusted to control the amounts of each component.

3. Ingredients quality

A local-made glue of a non-thick consistency was used, which did not make the samples reach the required consistency; therefore, it was replaced with wood glue of a thick consistency.

4. Drying method

The samples that used wood glue as a binder were left to dry without turning them on over. This led to the glue to drip and pool at the bottom of the samples, causing the failure. This was treated by turning the aforementioned samples on over twice a day.

Table 3-8 Failed mixtures that were excluded.

No. of sample	Samples Details
1.	Fine Rice Huck200g,Gypsum 400g,Water 100g
2.	Rice Huck 60,Gypsum 400g,Water 100g.
3.	Poly Styren15g, Gypsum 100g, Water 100g.
4.	Fine Rice Huck 200g,Cement500g,Sand 500g, Water 100g.
5.	Poly Styren 20g, Cement 300g, Sand 500g, Water 100g.
6.	Sawdust 80g, Gypsum 300g, Water 100g.
7.	Sawdust 70g, Cement 200g, Sand 200g, Water 100g.
8.	Rice Huck 60, Wood glue100g
9.	Rice Huck 60,Wood glue150g
10.	Rice Huck 60,Wood glue200g

### 3.3.2 Mixing Procedure

This process involves mixing the dry materials manually inside plastic bags to prevent them from splattering, especially since the materials are lightweight, such as rice husks, polystyrene beads, and wood chips. No water is added during this step to ensure even distribution. After dry mixing is complete, water or wood glue is introduced. This step turns the dry mix into a cohesive, workable material.

### 3.3.3 Casting and Curing

After completing the mixing process, the following main steps are to be implemented:

- **Pouring mixtures into Molds:** the fresh mixture for each sample was poured into molds designed for each specific test, including

thermal conductivity, compressive strength, and water absorption. These molds are illustrated in Figure 3-4.

- **Drying and Solidification:** The mixture was left in the molds for a designated period until its dryness was achieved.
- **Submerging Cementitious Compounds in Water:** After removing the cement and sand-based compounds from the molds, they were placed inside a water tank, as shown in Figure 3-5. The tank is maintained at a specified temperature of  $23 \pm 2$  °C to ensure a sealed environment.
- **Testing on Day 28:** After 28 days[67], the cementitious samples were retrieved from water and underwent the specified tests, including evaluations of thermal conductivity, compressive strength, and water absorption.
- Figure 3-6 illustrates the samples prepared for testing thermal conductivity and compressive strength after the drying process is finished.



(a)



(b)



Figure 3-4 (a) Thermal conductivity test mold (b) Water absorption test mold (c) Compressive strength test mold

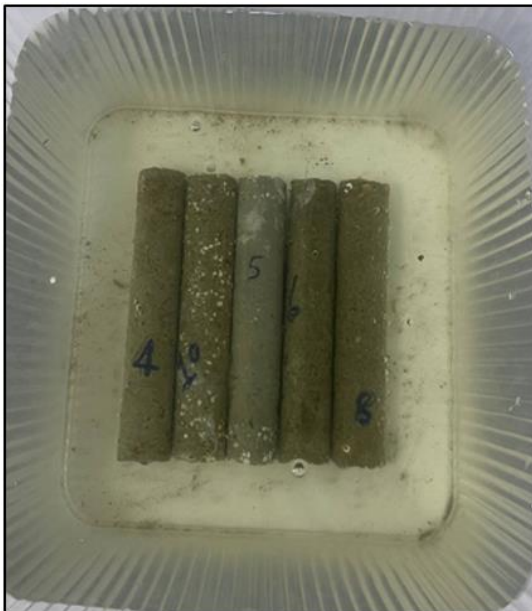


Figure 3-5 Submersion of the cementitious samples in water





Figure 3-6 Samples prepared for testing

### 3.4 Tests procedures

The tests used for investigating the properties of insulating materials were thermal conductivity, compressive strength, density and water content measurements.

#### 3.4.1 Thermal Conductivity Test

Thermal conductivity was measured using a KD2-Pro thermal analyzer shown in Figure 3-7. It is a fully portable thermal properties analyzer. It uses the cross-line heat source method to measure thermal conductivity. It complies with EN61326-1:2013 and EN50581-2012 standards. Thermal conductivity/resistance sensor TR-1 (for solids) corrects temperature drift. TR-1 sensor length is 100mm, diameter is 2.4mm.

The analysis was conducted in the Nanotechnology Laboratory at the University of Kufa, College of Engineering. A thermal conductivity test was performed, where each sample was held vertically on a flat surface and the sensor was inserted into it. Then the thermal conductivity meter was turned on. Waiting until the thermal conductivity reading appeared on the screen, the reading was taken.

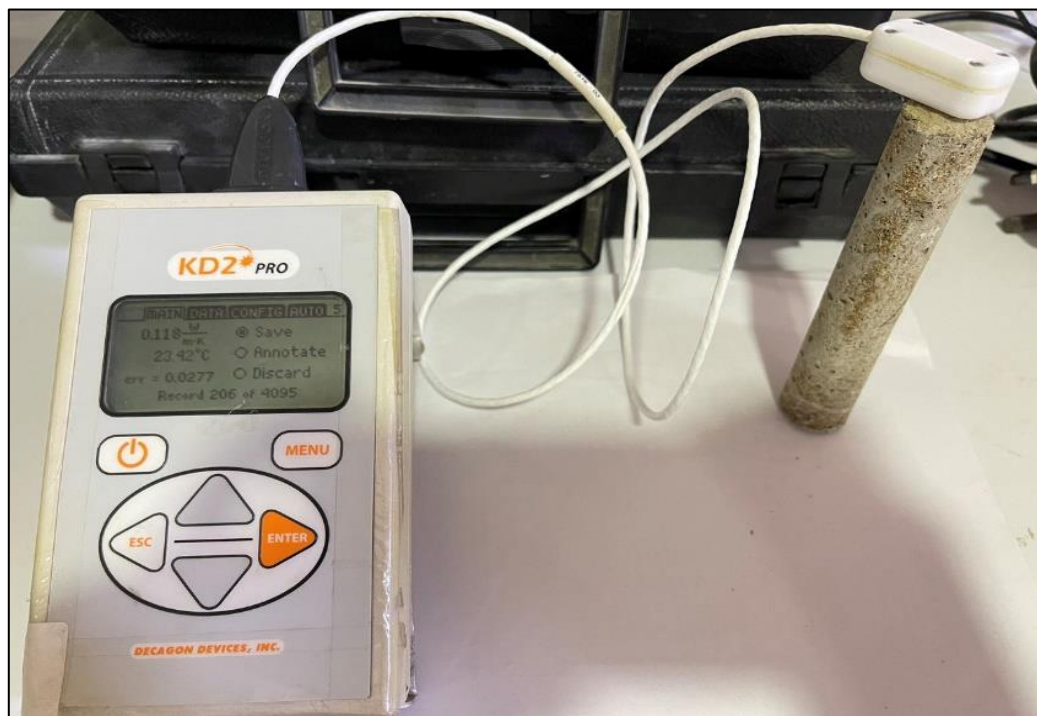


Figure 3-7 Thermal conductivity test device

### 3.4.2 Compressive Strength Test

The compressive strength assessment involved cube-shaped specimens measuring 5 cm \* 5 cm \* 5 cm. Three samples were prepared for testing at three-time points: 7, 14 and 28 days. The testing took place at Al-Furat Al-Awsat University, Al-Najaf Technical Institute, the Department of Civil Technologies, utilizing the ADR 2000 pressure testing device as displayed in Figure 3-8.



Figure 3-8 Compressive strength test device

Test procedures followed relevant specifications such as (4E ASTM 7500-1, ISO EN BS GROB3 / ASTM C 165-07). A laboratory test rig with a maximum capacity of 2,000 (kN) was used to apply the load to the side faces of the cube specimens. The samples were centrally aligned and securely located to ensure proper contact between the top sampling surface and the plunger. The load was gradually applied through continuous and controlled rotation of the moving component, avoiding sudden impacts. This loading continued until the sample failed, as shown in Figure 3-9. The maximum applied load and the corresponding resistance value were recorded.

The evaluation included samples of insulating materials that were classified into three groups, The compressive strength (stress) was determined using the equation (3.1)[68].

$$\sigma = P / A \quad (3.1)$$

where:

$\sigma$  = compressive strength (stress), MPa;  $P$  = maximum applied load (failure load), N; and  $A$  = loaded surface area of the cube, mm<sup>2</sup>

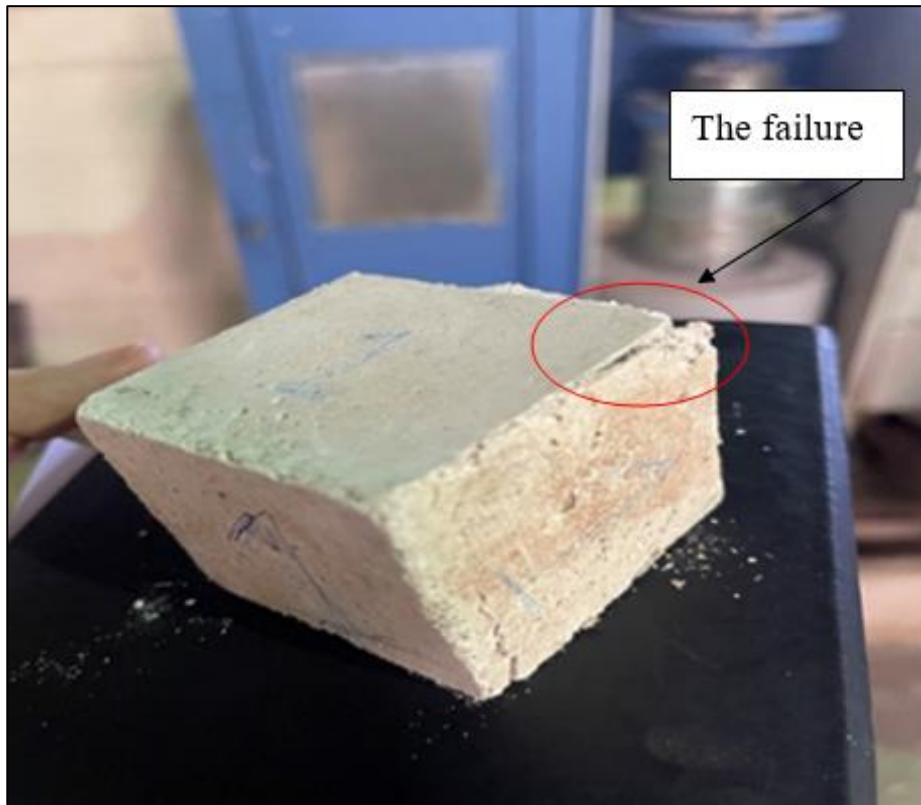


Figure 3-9 Failure of a specimen

### 3.4.3 Water Absorption Test

The water absorption test involves weighing the samples both before and after immersing them in water for a 24-hour duration. Subsequently, the samples are meticulously dried using paper towels to eliminate any excess surface water. Precise measurements of the weights are taken before and after immersion, and the water absorption percentage (%) is calculated using the provided formula. A small electronic scale with 0.01g resolution was used to measure weights. It comes with a digital screen that accurately displays the weight, and contains simple and easy-to-use control buttons. Eq. (3-2) was used to calculate the percentage of the water absorption. The water absorption

test serves a crucial purpose in evaluating insulating materials. Measuring the weight change before and after immersion in water provides insight into the material's susceptibility to moisture. This is particularly valuable as excessive moisture can degrade the performance of insulating materials and compromise their thermal efficiency. Knowing how much water a material can absorb helps in selecting the right insulation for applications where exposure to external moisture is a concern, ensuring the long-term effectiveness of the insulation in various environments.

$$\text{Water absorption (\%)} = \frac{W_f - W_i}{W_i} \times 100 \quad \text{Eq (3-2)}$$

where  $W_f$  represents the final weight of the sample after immersion in water, and  $W_i$  is the initial weight of the dry sample before immersion.

#### 3.4.4 Bulk Dry Density Test

The Bulk Dry Density Test for insulation materials is an important test used to measure the dry mass of the material per unit volume. The bulk dry density is measured by following relationship [69]:

$$\text{Bulk dry density (kg/ m}^3\text{)} = \left[ \frac{A}{C - D} \right] \times \rho \quad (3.2)$$

where  $A$  is the weight of the oven-dried test sample (kg);  $C$  is the weight of surface-dried test sample after immersion (kg);  $D$  is the apparent weight in water (kg); and  $\rho$  is the density of water (kg/m<sup>3</sup>)



### 3.5 Practical application

Two test models were built. Each model consists of a 1 m<sup>3</sup> cubic room. Within this setup, one room remains uninsulated (Room-1) for comparative analysis, while the other (Room-2) includes two types of insulation materials—external and internal—with a thickness of 3 cm, as shown in Figure 3-10. The structural frame of these two rooms was created using iron beams, and the rooms were covered with a layer of gypsum boards of 1.5 cm thickness as shown Figure 3-11, which shows the cross-section of the two rooms. This methodology facilitated a comprehensive assessment of the effect of the produced insulating materials on the thermal properties of the rooms.



Figure 3-10 (a) Test room that is covered with insulating materials  
(b) Test room without insulation

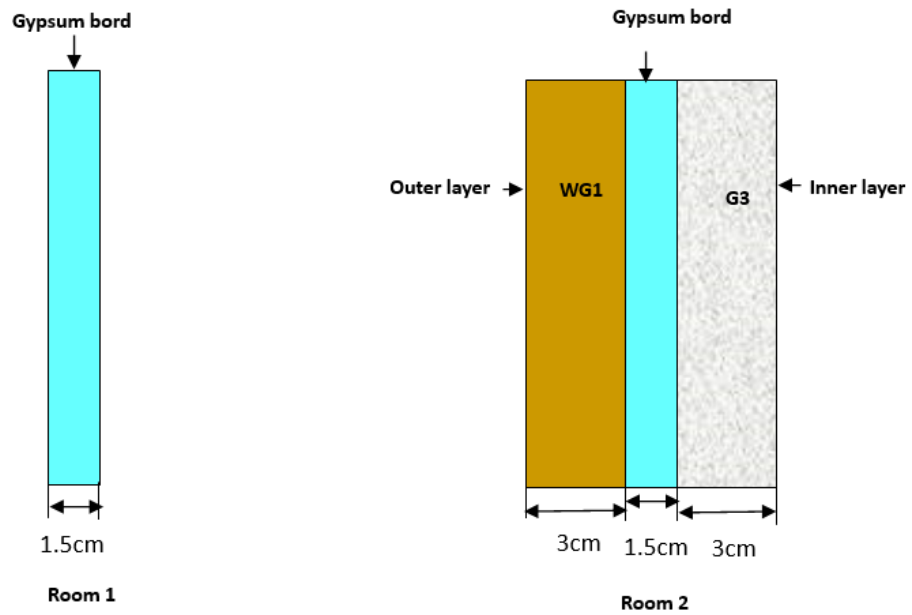


Figure 3-11 Cross-section of the rooms wall

### 3.6 Measurement of Temperature

To measure temperatures in the two constructed rooms and evaluate the impact of insulation materials during daylight hours, spanning a duration of 8 hours from 8:00 AM to 4:00 PM, the following devices and equipments were utilized:

#### 3.6.1 Thermocouples

The K-type thermocouples (3 mm dia, 1.5m length,  $\pm 1.5$  °C error) shown in Figure 3-12 were used to measure the temperature at points on the interior and exterior surfaces of the test rooms, as well as a thermocouple to measure the outside air temperature and a thermocouple to measure the interior air of the test rooms. Figure 3-13 shows the locations where thermocouples were fixed. Duct Tape is used to hold the thermocouples securely in place.

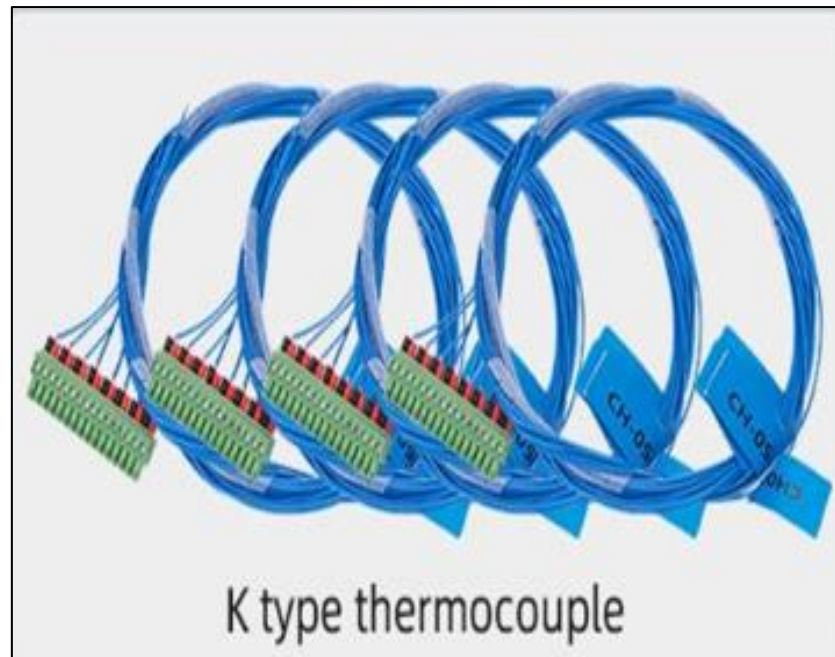


Figure 3-12 Thermocouples

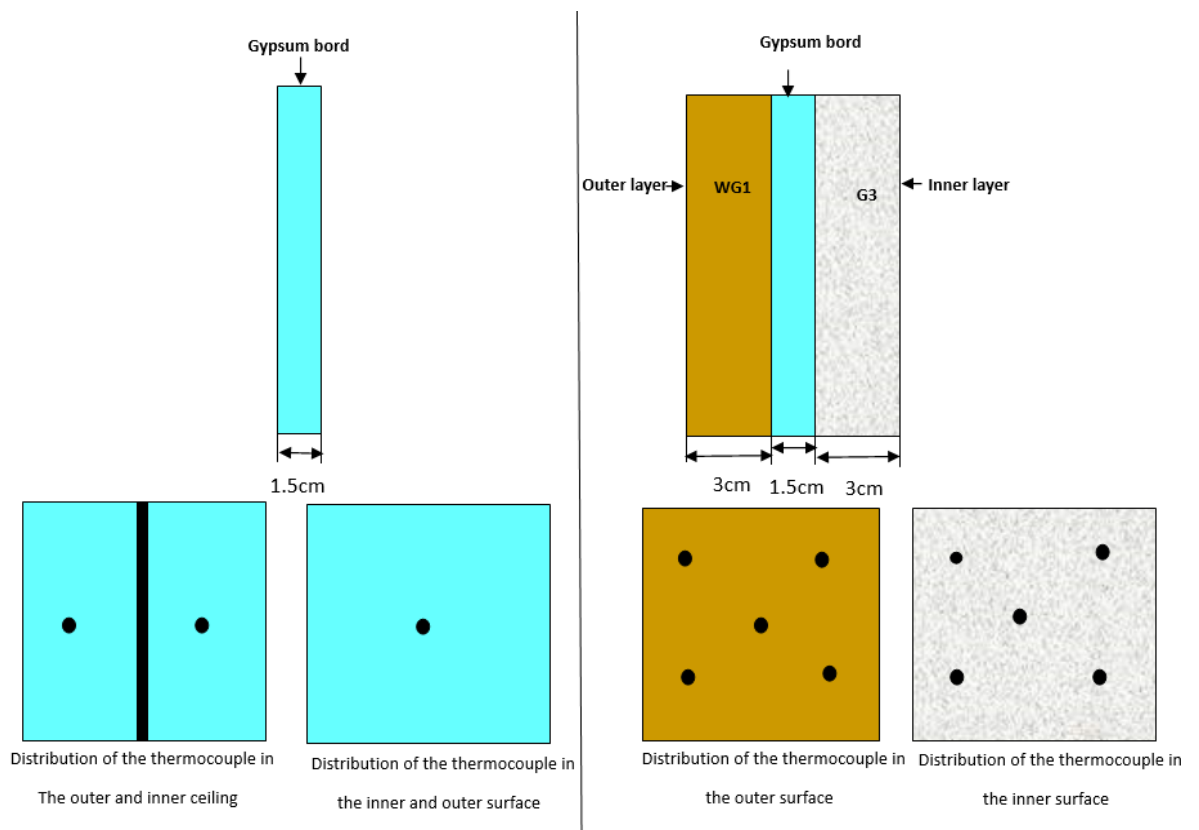


Figure 3 -13 Locations of thermocouples in each direction



### 3.6.2 Data logger

As displayed in Figure 3-14, Three CKT4000+ data loggers (each of 32 channels, 0.2 °C basic accuracy, and 0.1 °C resolution) were used to collect the faces' temperature with time.



Figure 3-14 Data logger

### 3.7 Solar Radiation

The measurement of radiation intensity is achieved through an instrument known as a pyranometer. This instrument measures the global solar irradiance (direct and diffuse radiation) received from the entire hemisphere on a flat surface. While, a solar power meter measures the instantaneous electrical power of a solar system (PV cell built in the instrument), which reflects the solar energy converted to electrical energy. In this research work, a solar power meter (TENMARS TM-207, 1999 W/m<sup>2</sup> max. range, ±10 W/m<sup>2</sup> accuracy, spectrum reaction 400–1100 nm spectrum reaction, and

EN61326(1997) + A1(1998) + A2(2001) compatibility) was used, as shown in Figure 3-15.



Figure 3 -15 Solar power meter

### 3.8 Reflectivity

A surface reflectance test was conducted to evaluate the reflectivity of the insulation material's surface, assessing its ability to reflect light or radiation. This test measures the amount of radiation reflected from the surface in comparison to the incident radiation. The results of this test offer insights into how effectively the surface reflects radiation. Quantifying reflected radiation aids in materials characterization and determining their suitability for various applications, including thermal insulation and energy management. The corresponding device is shown in Figure 3-16. The gloss meter (model YG268 Tri Gloss meter model

from Shenzhen 3nh Technology Co., Ltd) was used in this research work. It conforms to ISO 2813 and China standard GB/T 9754, having a display screen of 2.3 inches, measuring area (mm) of 20°:9x10 60°:9x15 85°:5x38, resolution of  $\pm 0.2$  GU, repeatability of 0-100 GU). The device has an automatic calibration function.



Figure 3-16 Gloss meter

**CHAPTER FOUR**  
**RESULTS AND DISCUSSION**

## CHAPTER FOUR

### RESULTS AND DISCUSSION

#### **4.1 Introduction**

This chapter focuses on analyzing and interpreting the results obtained from the scientific investigations outlined in Chapter Three. The study involves producing insulation materials for buildings, encompassing three groups: cement-base products, gypsum-base products, and wood glue-base products. A variety of mechanical and thermal tests were conducted on the prepared samples, including evaluations of compressive strength, thermal conductivity, water absorption, and apparent bulk density. This chapter also illustrates and discusses the practical application of the best materials obtained on an insulated room model, measuring the amount of transferred heat, and comparing it with another non-insulated room.

#### **4.2 Tests Results**

##### **4.2.1 Thermal conductivity**

Thermal conductivity testing of insulating materials is the process of measuring a material's ability to transfer heat. This is done by determining the material's thermal conductivity coefficient. The measurement is in one unit such as  $W/m \cdot K$  or  $W/m^{\circ}C$ . This test can help evaluate the performance of insulating materials and select the most effective materials in preventing heat transfer between areas of different temperatures.

##### **4.2.1.1 Cement\_base products**

Thermal conductivity testing was conducted on all dried samples in the laboratory using the KD2 Pro device at a temperature of  $24^{\circ}C$ . The device specifications are described in section (3.6.1) of Chapter Three. The outcomes are displayed in Figure 4-1. These outcomes illustrate the

changes in thermal conductivity across various proportions of cement and sand samples with the incorporation of agricultural and industrial waste. Comparing the results shown in the graphical representation in Figure 4-1 indicates that the sample having the lowest thermal conductivity is C1, which consists of a mixture of fine rice husk, sand, cement and water. This particular mixture showed a coefficient of thermal conductivity of 0.118 W/m·K, which corresponding to a reduction of 83.6% compared to the reference product ( $\Delta k\% = \frac{k_{Co} - k_{Ci}}{k_{Co}} * 100$ ). Inclusion of fine rice husks greatly improved the performance of this mixture.

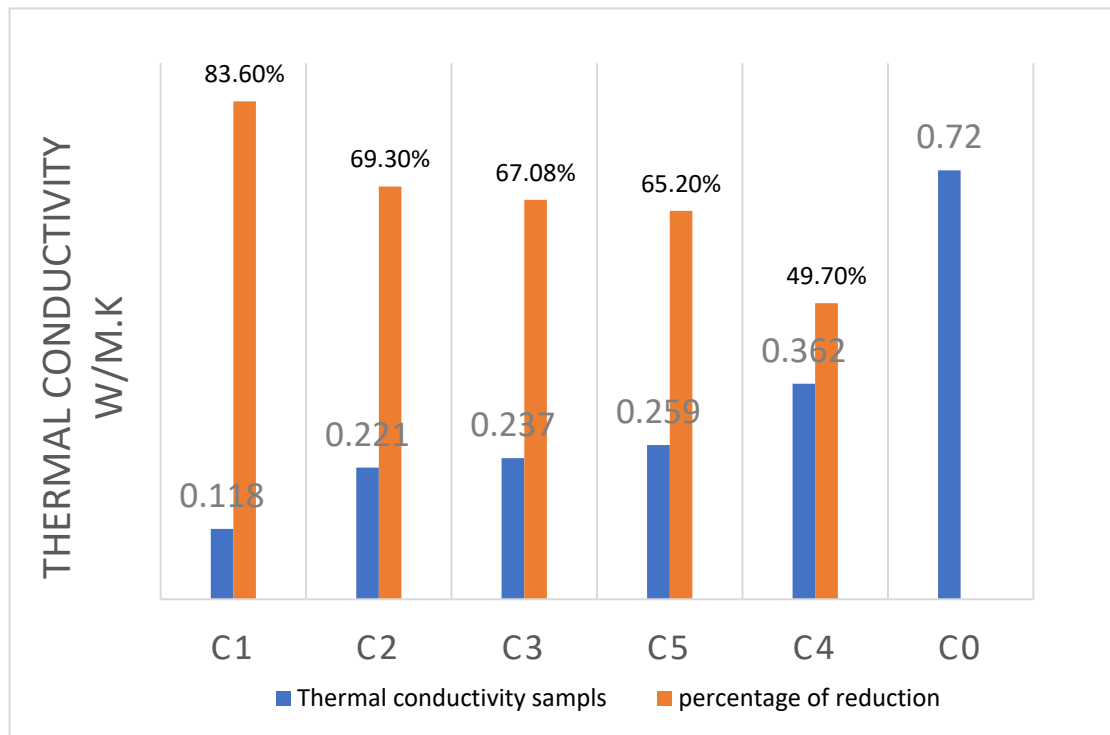


Figure 4-1 Thermal conductivities and percentages of reduction of cement\_base products

#### 4.2.1.2 Gypsum\_base products

The results of the thermal conductivity test performed on gypsum composite samples containing industrial and agricultural wastes have been analyzed and illustrated in Figure 4.2. The recorded thermal conductivity values ranged from 0.116 to 0.291, indicating much lower values compared to those of conventional gypsum admixtures. The sample G3 showed the lowest thermal conductivity of 0.116 and highest reduction of 83.88% compared to the base sample. This result is attributed to the internal structure of the polystyrene beads, which are characterized by small air gaps (porous medium) that impede heat transfer and support insulation. Perhaps, the distribution of beads within the gypsum mixture generated additional voids, which increased thermal insulation and led to a decrease in the thermal conductivity value. In general, the incorporation of industrial and agricultural wastes into gypsum composites has yielded promising results by significantly reducing thermal conductivity and enhancing insulating properties compared to conventional gypsum formulations.

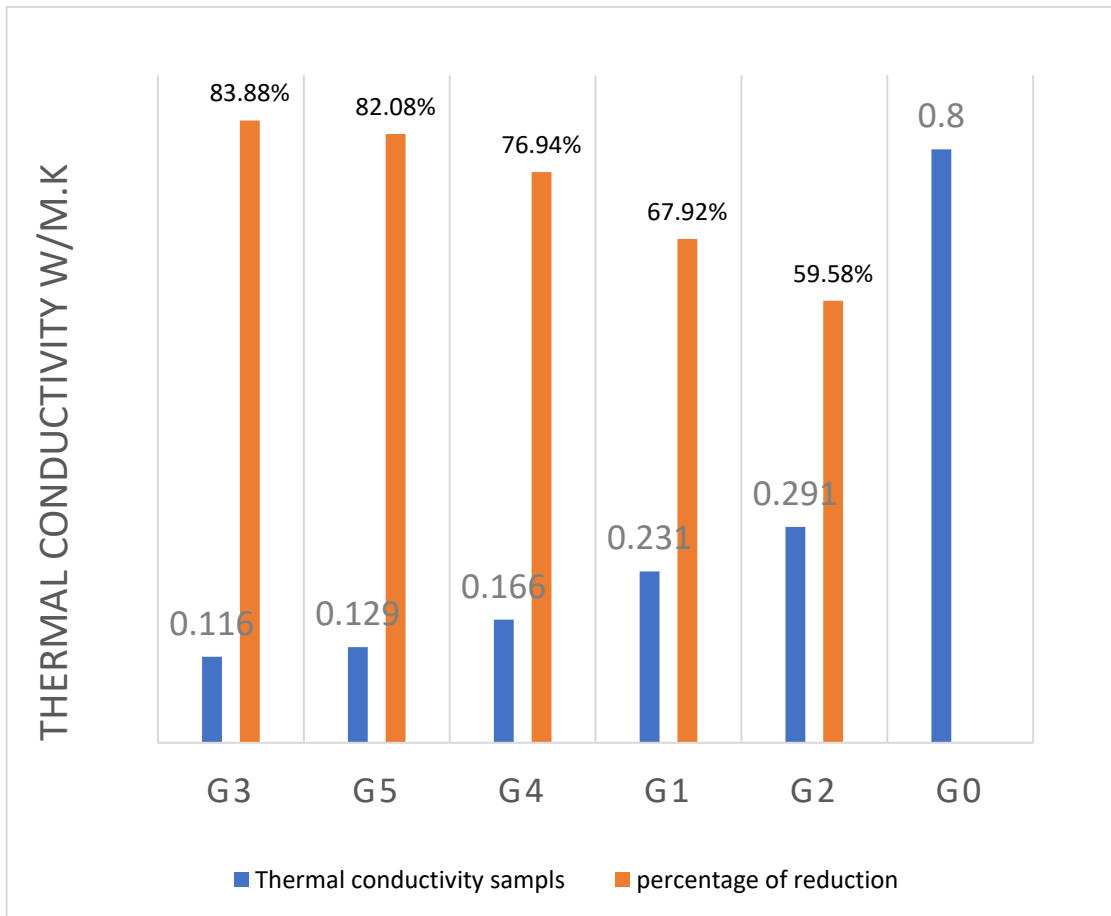


Figure 4-2 Thermal conductivities and percentages of reduction of gypsum\_base products.

#### 4.2.1.3 Wood glue\_base products

The results in Figure 4-3 indicate a significant reduction in the thermal conductivity of composites containing agricultural and industrial waste mixed with wood glue. This reduction is compared with composites containing waste mixed with gypsum and cement.

The findings suggest that the sample containing coarse rice husks with glue WG2 has the lowest thermal conductivity of 0.043 W/mK. This may be due to the air filled tubular shape of the rice husks, which reduces heat transfer. Conversely, the sample containing fine rice husk WG1 with glue



has higher thermal conductivity. The fine particles facilitate smoother heat transfer within the material.

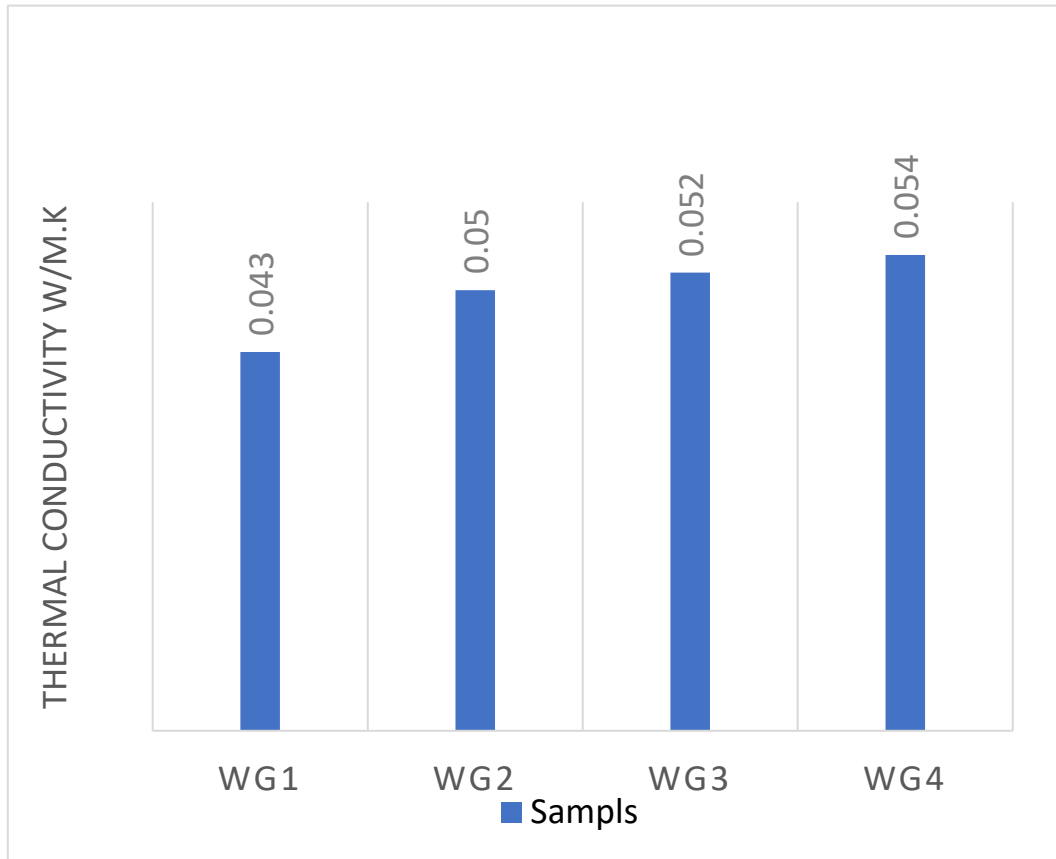


Figure 4-3 Thermal conductivity of Wood glue\_base products

#### 4.2.2 Compressive Strength

Compressive Strength Testing of Materials involves evaluating the ability of these materials to withstand axial loads without significant deformation.

#### 4.2.2.1 Compressive strength of Cement\_base products

The compressive strength test results of cement-base products are shown in Figure 4-4. This figure shows the effects of partial replacement of cement with agricultural and industrial waste. Average compressive strength was measured at 7, 14 and 28 days for each sample [67], with three samples taken each time. Figure 4-4 shows that sample C5 had the lowest compressive strength, while sample C4 had the highest strength. This may be due to the compressible nature of polystyrene beads, and when they are present among the components of the sample, they increase its compressibility.

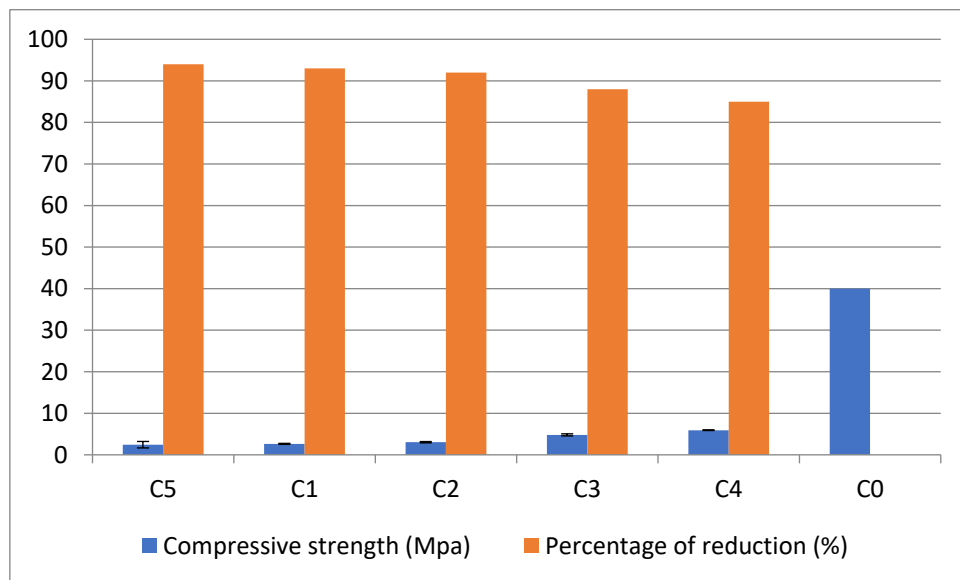


Figure 4-4 Compressive strength of Cement\_base products

#### 4.2.2.2 Compressive strength of gypsum\_base products

Figure 4-5 shows the results of the compressive strength of the materials that were produced, specifically gypsum compounds with the addition of agricultural and industrial waste. The study included replacing part of the gypsum with these wastes. The sample showing the highest compressive strength is the one containing finely ground rice husk mixed with gypsum.

G1. This may be due to the fact that finely ground rice husk has a smooth, uniform and strong structure, which contributes to enhancing the compressive strength of the sample. In addition, gypsum plays a positive role in enhancing cohesion and strength within the sample. Gypsum acts as a binding agent, binding the rice husk particles together, thus improving overall structure and strength. On the contrary, the G3 sample showed the lowest compressive strength due to the light weight and low density of the polystyrene beads. This property reduces the compressive force of the sample. Furthermore, the inherent fragility of polystyrene may make it less able to withstand loading forces.

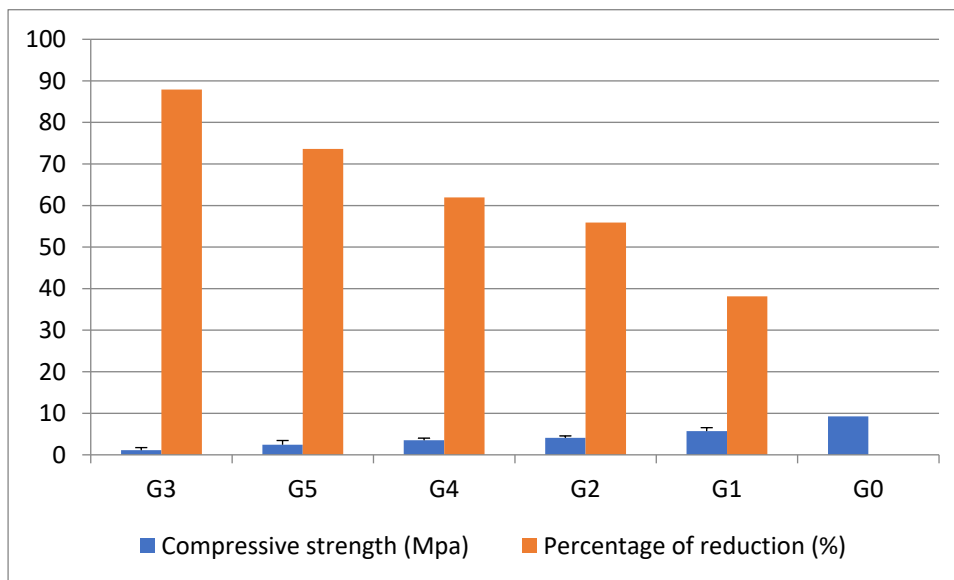


Figure 4-5 Compressive strength of gypsum\_base products

#### 4.2.2.3 Compressive strength of wood glue\_base products

A compressive strength test was conducted on composite insulation materials containing various agricultural residues mixed with wood glue.

Figure 4-6 clearly shows that the sample containing rice husk mixed with WG1 wood glue achieved the highest compressive strength among all the different samples. The structural structure of rice husks is likely to be more resistant to pressure than other wastes that have been added to gypsum. On the other hand, the sample containing wood chips WG3 showed less compressive strength. This can be explained by the lightweight and low density of wood chips, leading to its low resistance to the forces exerted on it during loading. wood chips may also have a brittle structure, which means that it may be less durable in resisting the forces to which it is subjected.

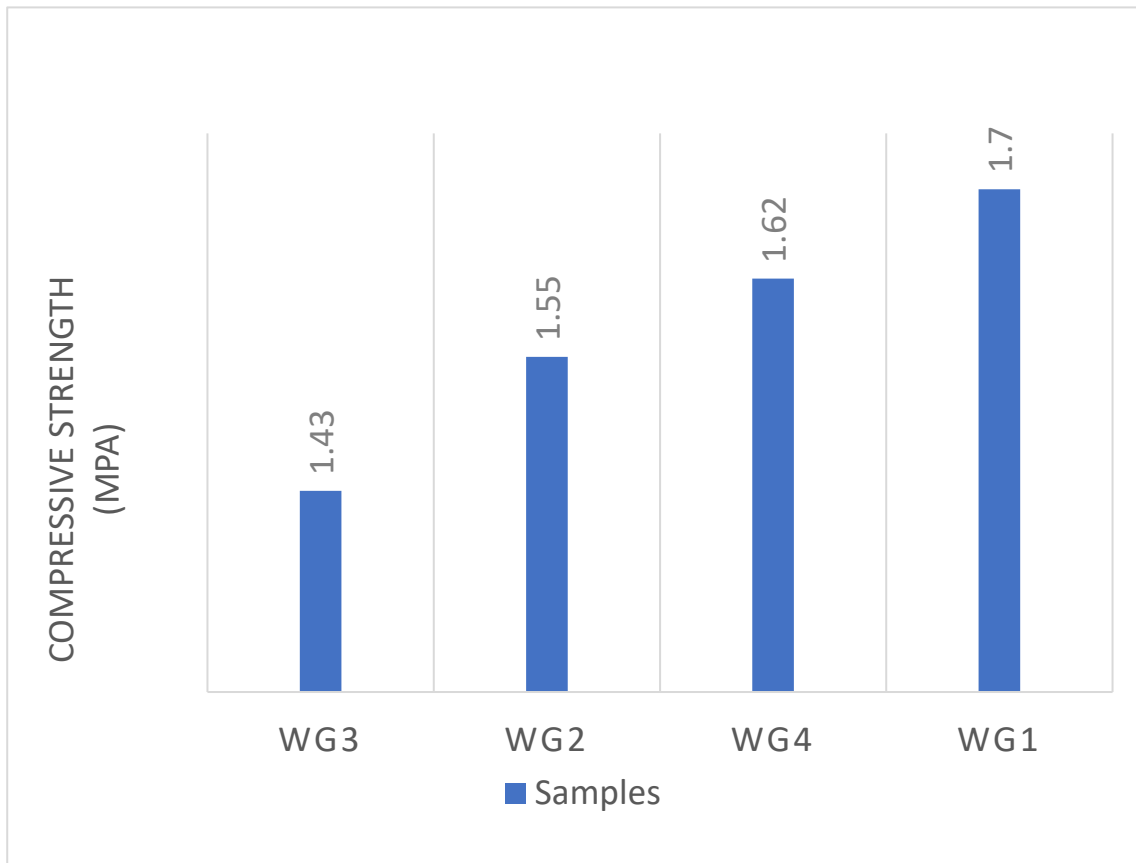


Figure 4-6 Compressive strength of wood glue\_base products

### 4.2.3 Water absorption

Water absorption testing of insulating materials involves assessing the amount of water that a material can absorb when immersed or exposed to

moisture. This test helps determine the material's ability to resist water penetration and its potential for retaining moisture. Water absorption can have implications for the material's durability, dimensional stability, and overall performance in various environmental conditions.

#### 4.2.3.1 Water absorption of cement \_base products

Figure 4-7 shows that the highest water absorption rate was observed in sample C1. It is possible that the sample containing fine rice husks is an organic and natural material with a porous structure that contributes significantly to water absorption. In contrast, the sample containing polystyrene beads, sand and cement C2 exhibited the lowest water absorption. This is due to the nature of polystyrene, which is less prone [64] to absorbing water compared to organic materials.

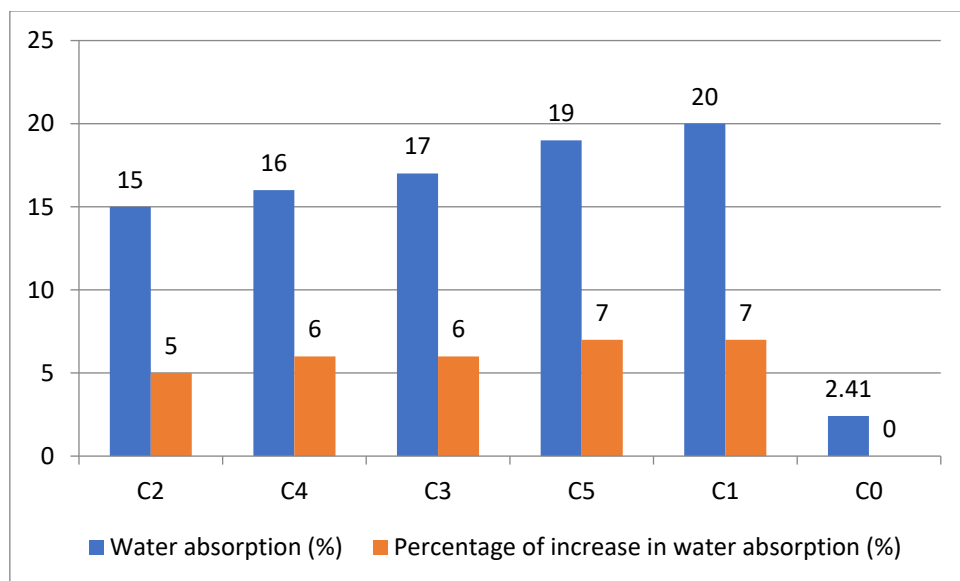


Figure 4-7 Water absorption of cement \_base products

#### 4.2.3.2 Water absorption of gypsum \_base products

Figure 4-8 shows the results of water absorption of gypsum compounds added with agricultural and industrial waste. It is clear that the water absorption values ranged between 19% and 33%, and the highest water

absorption value was observed in the sample containing wood chips and gypsum G4. Conversely, the sample containing EPS beads and gypsum G3 showed the lowest water absorption value. This phenomenon may be attributed to the porous properties and fine structure of wood chips, which enable them to absorb large amounts of water and retain it within the pores and voids.

The G3 sample absorbs less water than the previous sample. This can be attributed to the properties of EPS beads, such as hydrophobicity.

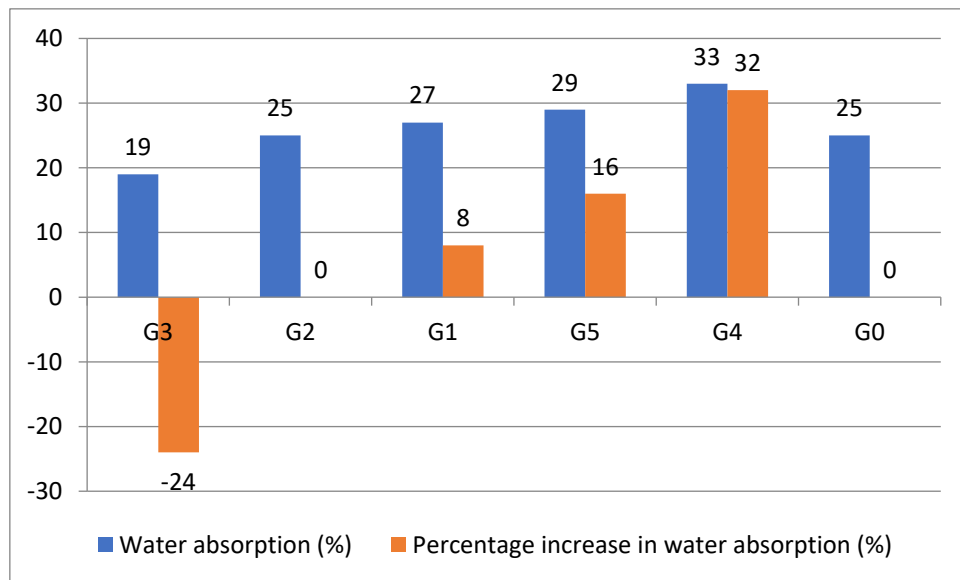


Figure 4-8 Water absorption of gypsum\_base products

#### 4.2.3.3 Water absorption of wood glue\_base products

Samples of agricultural and industrial waste (wood chips, rice husks, fine rice husks) were tested for water absorption, and the results are presented in Figure 4-9. Water absorption values ranged from %31 to 37%. It is evident that the sample containing wood chips exhibited the highest water absorption value. This can be explained by the structural composition and properties of wood chips. Wood chips is porous and contains a network of fine pores and voids. This characteristic enables it to absorb significant

amounts of water and retain it within its pores. Rice husks and fine rice husks may exhibit relatively lower water absorption capacities due to their structure and texture. Therefore, it is apparent that wood chips has the highest water absorption capacity among the different tested samples.

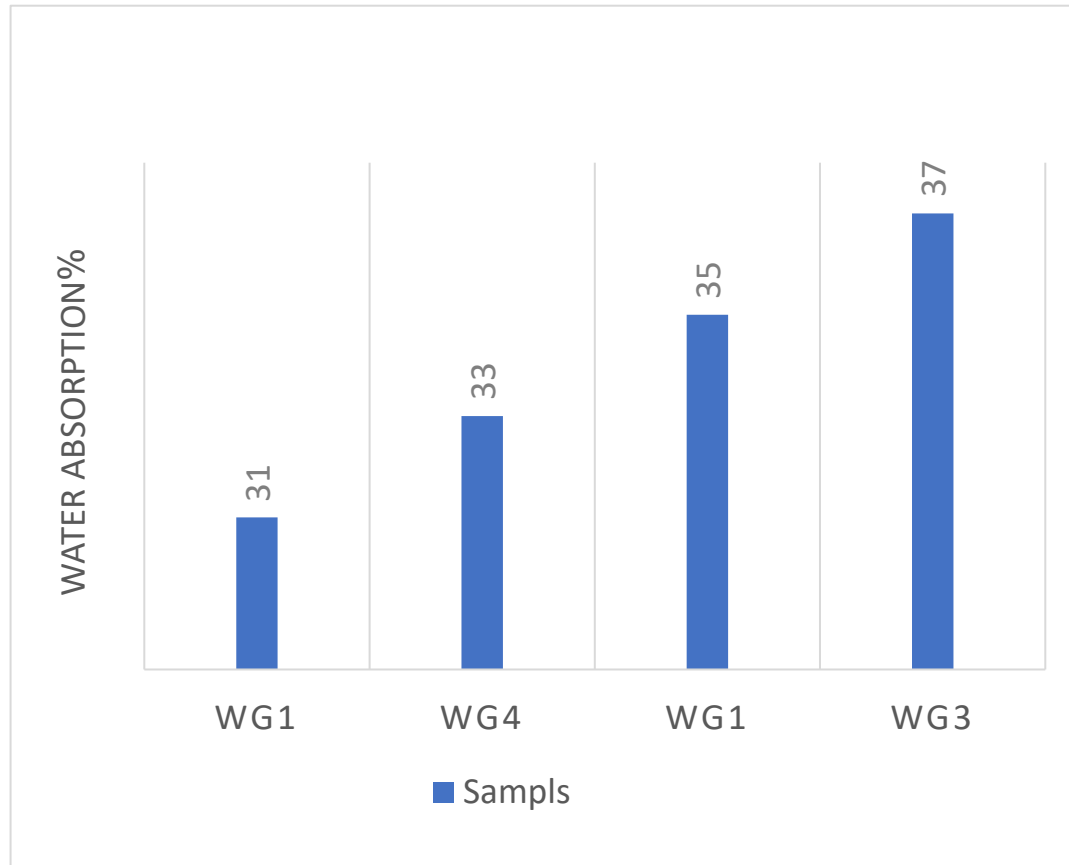


Figure 4-9 Water absorption of wood glue\_base products

#### 4.2.4 Bulk Dry Density

Bulk dry density testing of insulating materials is a method used to determine the mass of a material per unit volume in a dry state.

##### 4.2.4.1 Bulk dry density of cement\_base products

The bulk density test results for the cement and sand compounds ranged from  $967\text{kg/m}^3$  to  $1664\text{ kg/m}^3$  as shown in Figure 4-10 and all samples showed a decrease trend from C0, and the lowest value was for the C3

sample that contained polystyrene beads. The reason is that polystyrene beads are naturally lightweight. Therefore, when a large amount of them is added to the mixture with cement, this leads to a decrease in the apparent dry density. The highest value of density was for the sample containing fine rice husks. Although fine rice husks may naturally be light in weight, their density is higher than that of EPS beads. Therefore, the presence of rice husks in the mixture can increase the bulk density due to their accumulation and compaction in the mixture.

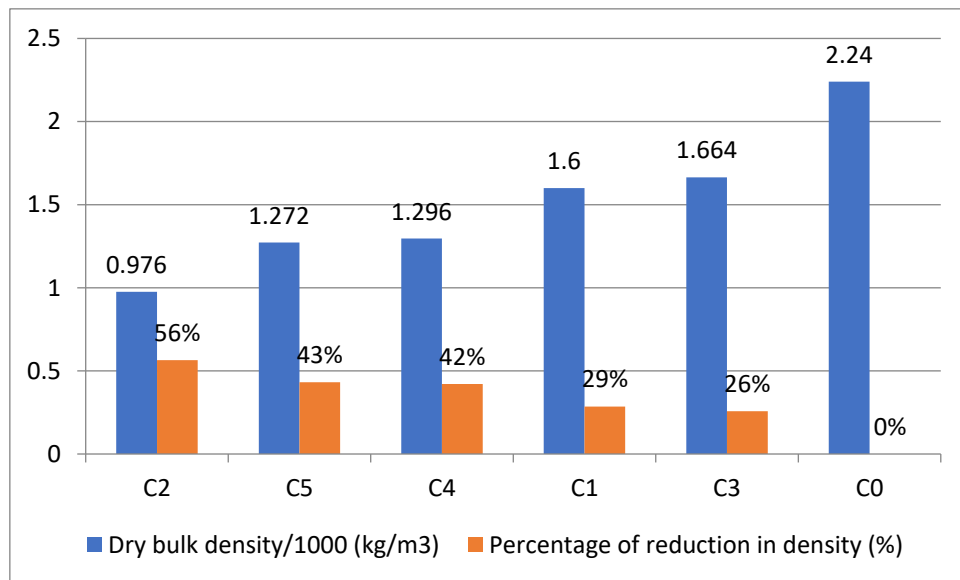


Figure 4-10 Bulk dry density of cement \_base products

#### 4.2.4.2 Bulk density of gypsum \_base products

The results of bulk density for gypsum composite insulation materials presented in figure 4-11 are influenced by the composition and the ratios of the various counterparts within the mixture. This is particularly evident when insulating materials like rice husks or polystyrene beads are introduced to the gypsum mixture, as they can impact the overall bulk density of the composite.

The addition of lightweight components such as polystyrene beads or rice husks to gypsum leads to a reduction in bulk density. This phenomenon



occurs because these components increase the overall volume of the mixture while adding relatively little weight. It is worth noting that density values ranged from 320 to 1224 kg/m<sup>3</sup>, with the highest density value observed in the G2 sample. This is attributed to the incorporation of rice husks, which expand the volume of the sample without significantly increasing its mass.

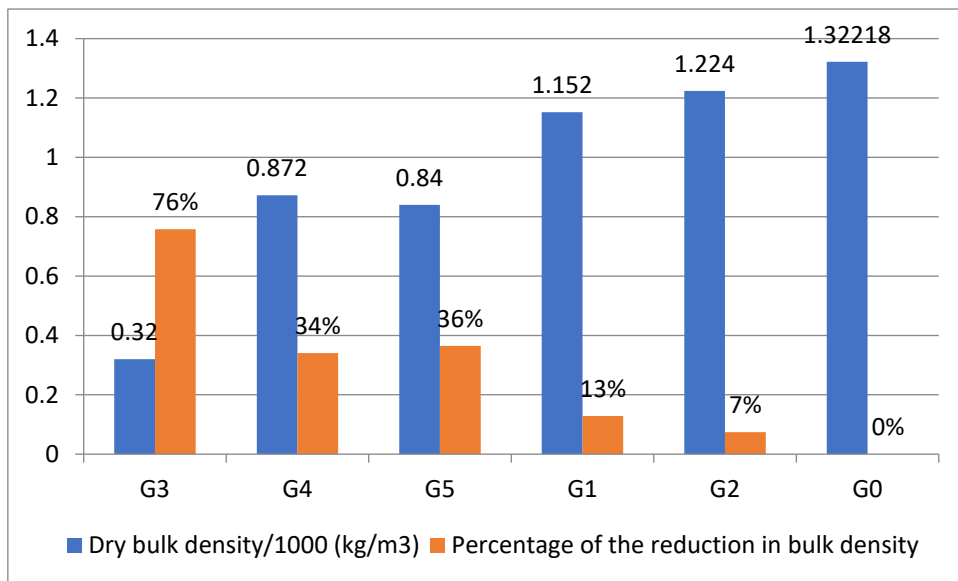


Figure 4-11 Bulk dry density of gypsum\_base products

#### 4.2.4.3 Bulk dry density of wood glue \_base products

The mixture comprising both fine and coarse rice husks, along with wood chips, bonded with wood glue, demonstrated the highest apparent bulk density among the samples derived from agricultural and industrial waste materials, as illustrated in Figure 4-12. This notable density can be primarily attributed to the influence of the structures affecting particle accumulation, the achievement of a more consistent particle distribution due to the combination of different waste types, the promotion of stronger particle bonding facilitated by the wood glue, and the enhancement of compaction during the preparation of the samples, particularly considering the incorporation of materials with diverse particle sizes and shapes.

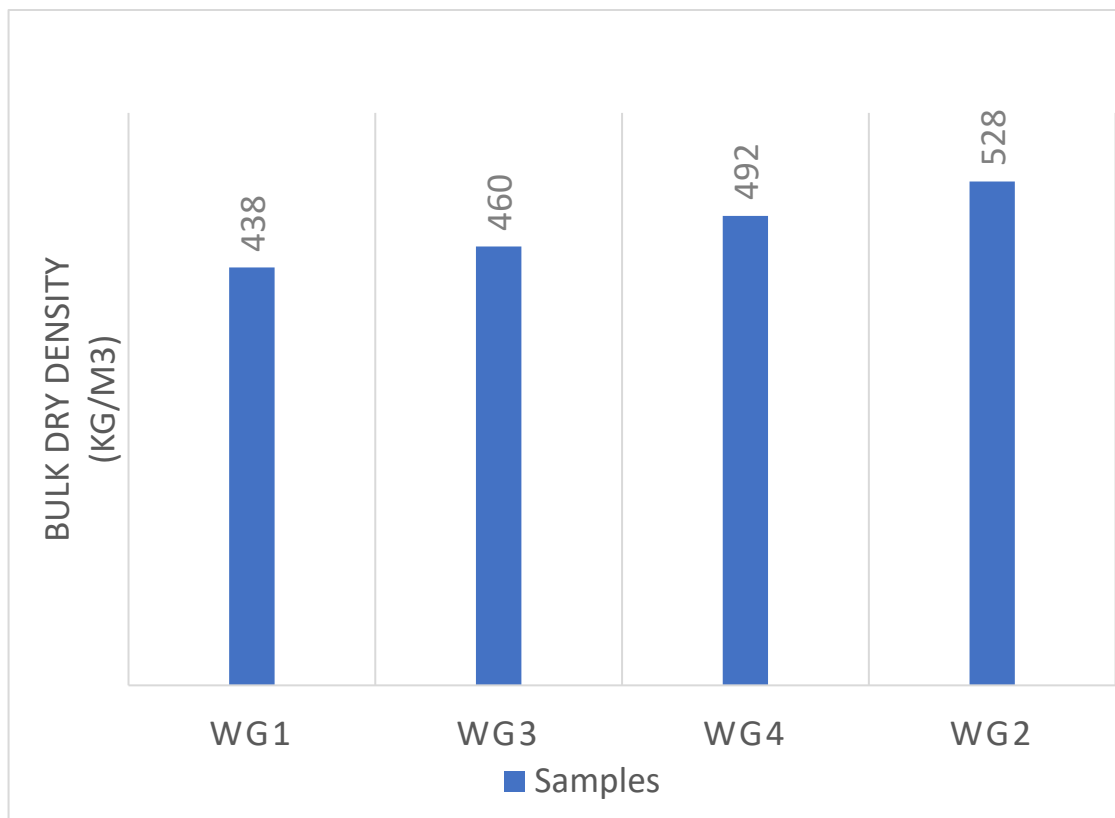


Figure 4-12 Bulk dry density of wood glue \_base products

### **4.3 Practical application of thermal insulation materials**

#### **4.3.1 Material selection**

Thermal conductivity is one of the most important characteristics when choosing insulating materials. If the thermal conductivity is low, the material is more effective in preventing heat transfer between areas with different temperatures. Insulation samples with higher efficiency were selected on the basis of their thermal conductivity values. Specifically, sample WG1 and sample G3 were chosen due to their thermal conductivity values of 0.043 (W/m·K) and 0.116 (W/m·K), respectively. The selected samples were used in experimental tests to evaluate the reduction in heat transfer rate.

#### **4.3.2 Applying thermal insulation materials.**

After conducting the tests and identifying suitable insulation materials, large-scale insulation models were created for further evaluation. For the rice husk waste and wood glue (WG1) samples, molds with dimensions measuring 50 cm in length, 50 cm in width, and 3 cm in thickness were used. Similarly, molds with dimensions of 20 cm in length, 20 cm in width, and 3 cm in thickness, were used to prepare the polystyrene beads and gypsum (G3) samples.

Once the drying phase was successfully completed, these prepared insulation samples were integrated into the room structures. Specifically, the (G3) sample was affixed internally in a compact arrangement, while the (WG1) sample was applied externally. The entire room was then enveloped, as illustrated in Figures 4-13 and 4-14.



Figure 4-13 Casting and installation of the outer insulation layer



Figure 4-14 Casting and installation of the internal insulating layer

#### 4.4 Temperature measurements

Temperature measurements were conducted on the two test rooms to assess the efficiency of the insulation materials. The temperature readings were recorded and saved every one hour from 8:00 AM to 4:00 PM.

14 thermocouples and one data logger were used to record the temperature of the outer and inner faces of the four walls and the ceiling of the base room (Room-1) in addition to the outdoor air and indoor air temperatures. While, for the insulated room (Room-2), the temperature of the faces walls' layers (i.e., the outer face of WG1 ( $T_o$ ), and the inner face of G3 ( $T_i$ )) for five geographical directions (i.e., sky, east, west, north and south) in addition to the outside air temperature and the inside air temperature, were recorded using 52 thermocouples distributed as 5 thermocouples in each geographical direction on the interior and exterior surfaces, and two data loggers.

The solar power meter, described in Chapter 3, was also used to record the energy flux resulting from solar radiation falling on the ceiling of Room-1 and Room-2 every hour. Figure 4-15 indicates the solar radiation on May 17<sup>th</sup>, 2023. The black squares represent the readings of the solar power meter every hour, while the blue straight lines indicate the trend between every two adjacent squares. While, Figures 4-16 to 4-20 show the temperature differences between the outdoor surface and indoor surface of each wall facing the same geographical direction of Room-1 and Room-2.

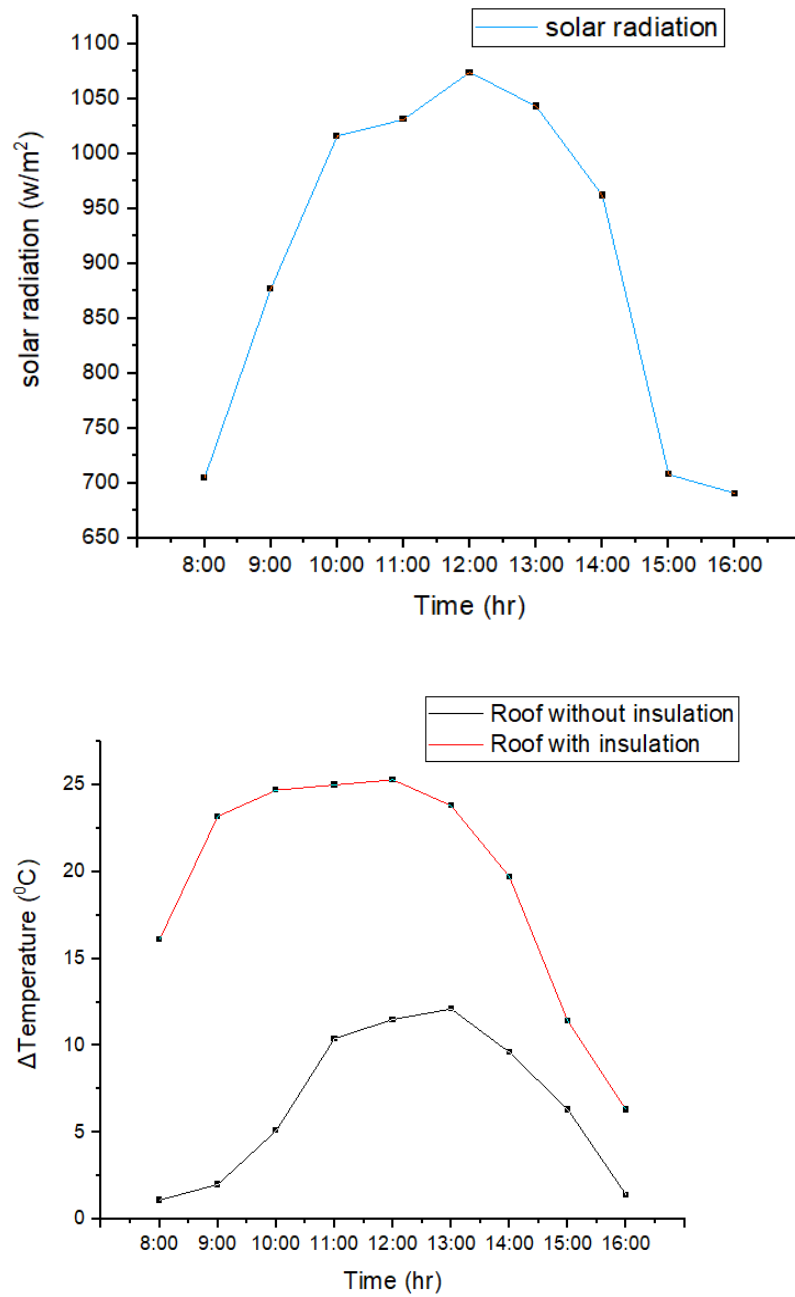


Figure 4-16 Temperature differences between the outdoor and indoor surface temperatures of the ceilings

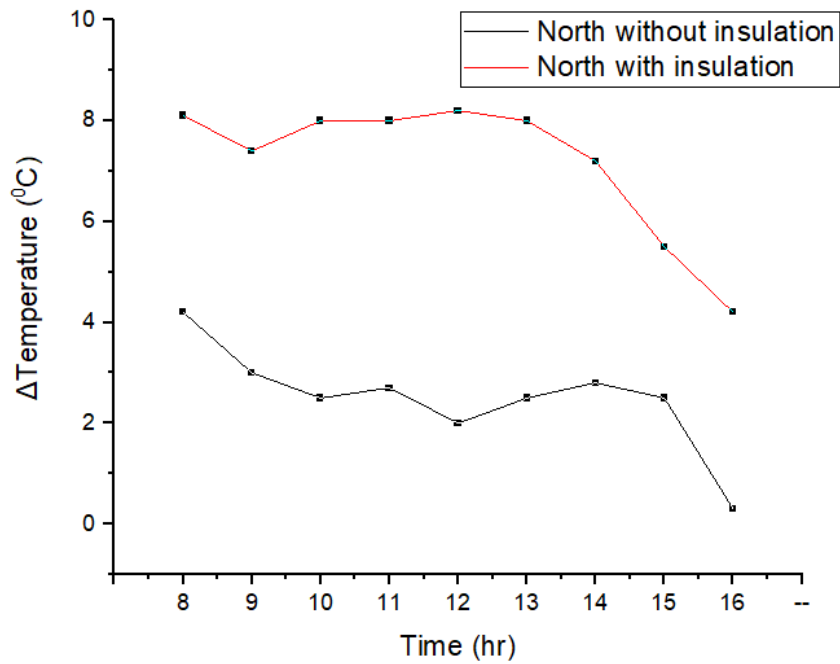


Figure 4-17 Temperature difference between the outdoor and indoor surface temperatures of the northern walls.

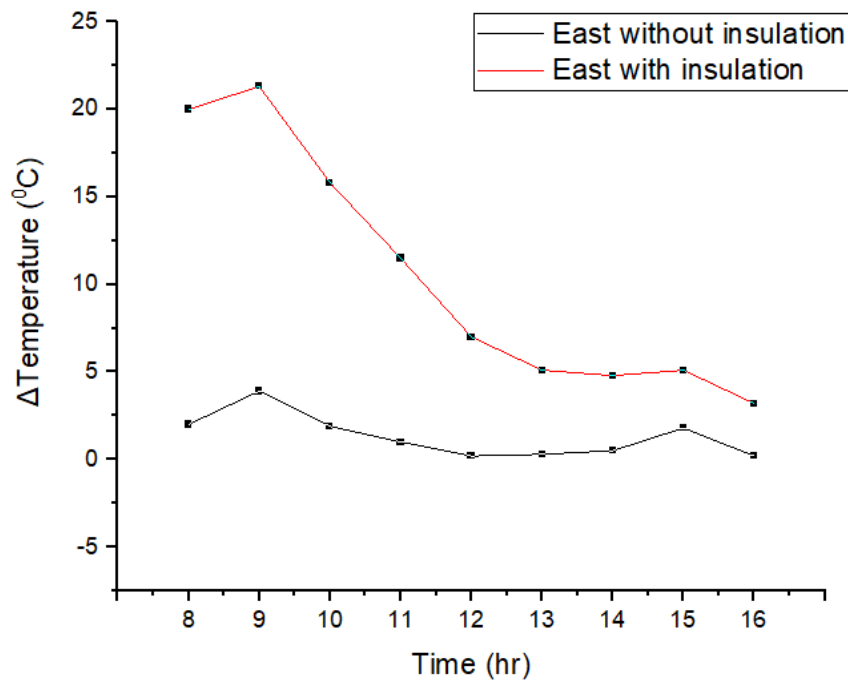


Figure 4-18 Temperature difference between the outdoor and indoor surface temperatures of the eastern walls

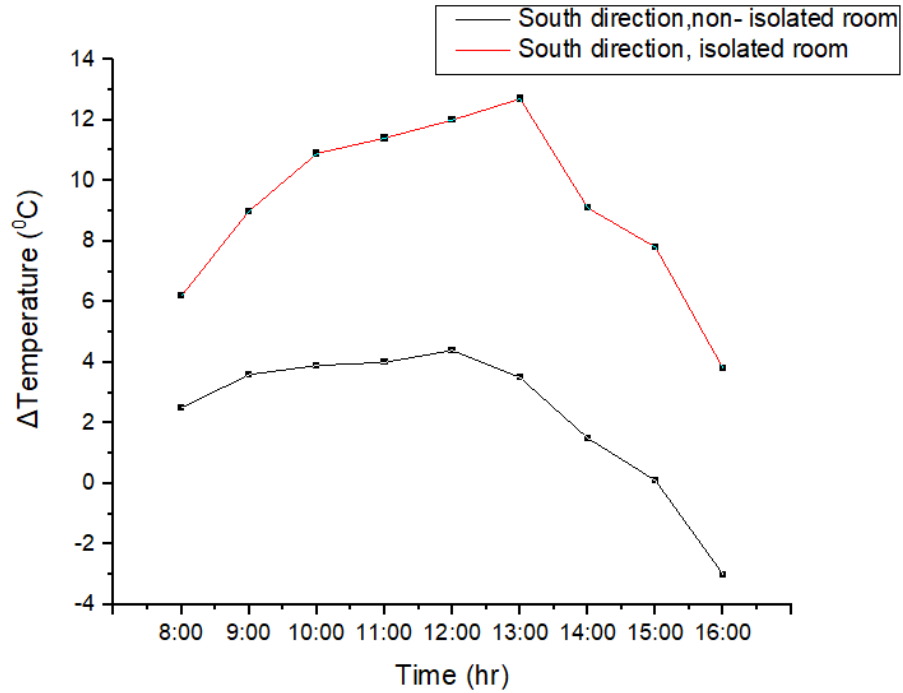


Figure 4-19 Temperature difference between the outdoor and indoor surface temperatures of the southern walls.

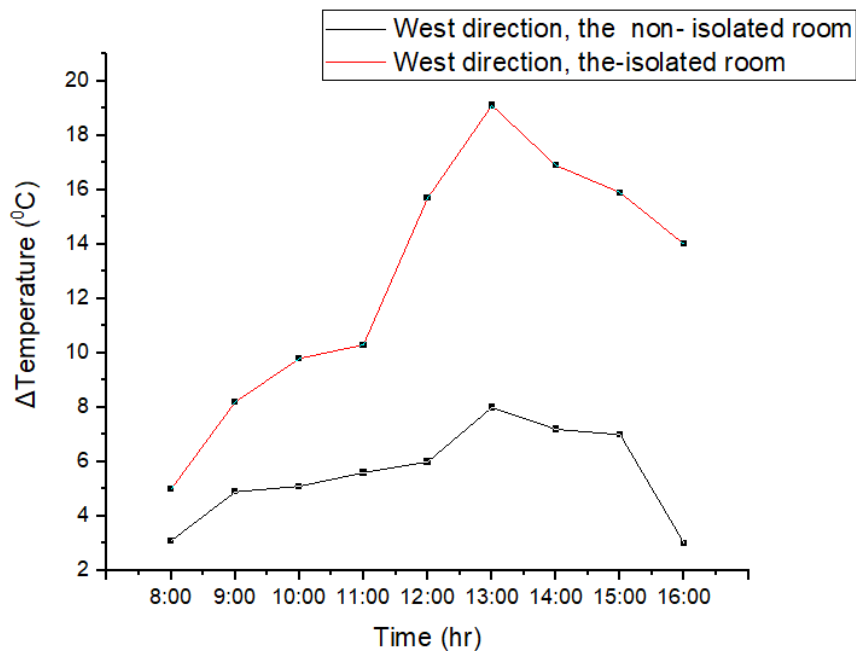


Figure 4-20 Temperature difference between the outdoor and indoor surface temperatures of the western walls.



#### 4.4.1 Data analysis

The analysis of the results revealed that there is a variation in temperatures and the ability of the insulating material (in Room-2) to create a difference in temperature between the external and internal environments, as well as its role in impeding heat transfer. This was compared to the uninsulated chamber (Room-1). It was also noted that the surface temperature of Room-2 showed an increase compared to Room-1. This temperature rise can be attributed to the specific properties of the insulation material (G3) used and its ability to absorb solar radiation. In this case, the outer insulation material consists of rice husks, making rough surface with dark colour, which facilitates absorption of the incident solar radiation, and convert it into thermal energy (heat).

In response to the rise in the surface temperature of the insulation material, measures have been taken to address this concern. The surface of the insulation material, specifically the rice husks, has been coated with white paint to enhance its reflectivity. In addition, the other test rooms were also painted, as shown in Figure 4-21. The application of white paint is intended to improve the reflection of the sun's rays, especially in comparison to dark-color surfaces. This reflective property of white surfaces reduces radiation absorption and helps maintain low surface temperatures for the insulation material. These improvements intend to mitigate thermal effects and enhance the efficiency of the insulation material in maintaining stable temperatures within the insulated room. This approach denotes a pragmatic approach and continuous commitment to the development of thermal insulation technologies, with the aim of improving performance and increasing thermal efficiency.

#### 4.4.2 Glossiness measurement

After implementing the improvements and painting the test rooms (Figure 4-21), the reflectivity of the surfaces was estimated from the results of the Gloss meter instrument under daylight conditions. It was concluded that the non-insulated room (Room-1) showed higher reflectivity compared to the insulated room (Room-2). Figure 4-21 shows the Glossiness values (GU) for the outer ceiling surfaces of both rooms. It is worth noting, in most of the cases, the surface reflectance depends on the wavelength and incident/viewing angle according to the optical properties and structures of the surface[70].



Figure 4-21 Models of the testing rooms after being painted with white color

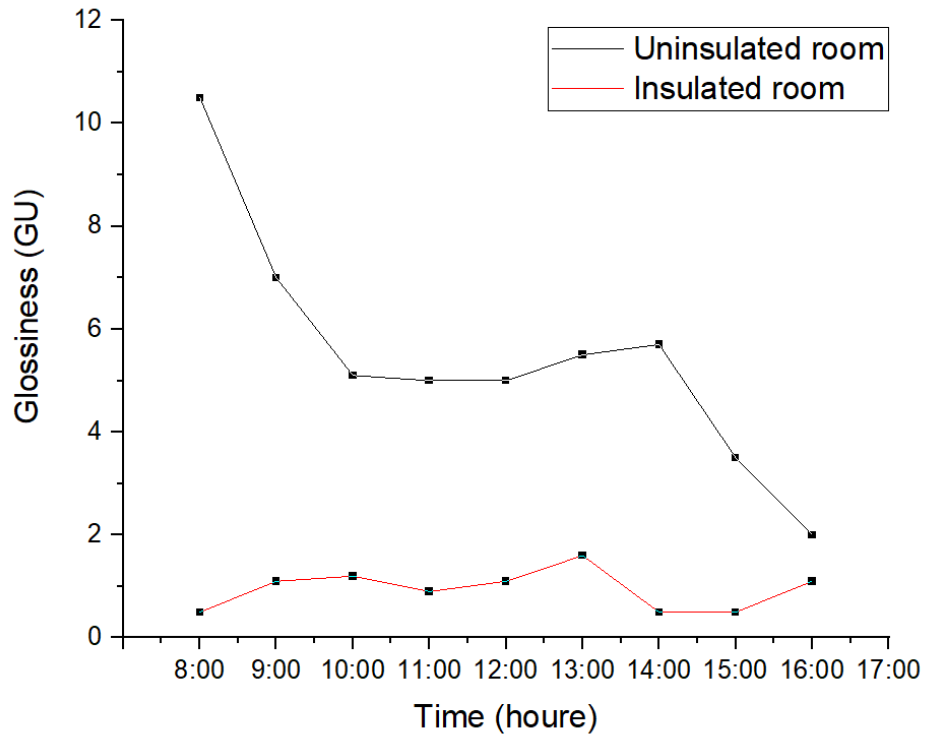


Figure 4-22 Glossiness of insulated and non-insulated rooms

#### 4.5 Heat transfer rate calculations

a- Direct method

Relying on Fourier's law of heat transfer by conduction, i.e.,  $Q = kA \frac{\Delta T}{\Delta x} =$

$A \frac{\Delta T}{\Delta x/k}$ , the heat transfer rate for each wall and ceiling of both rooms

(Room-1 and Room-2) was calculated at each time, as presented in Appedix A. The results are tabulated in table 4-1.

Table 4-1 Heat transfer rates of Room-1 and Room-2 based on Fourier's law

Non-insulated wall (Room-1)						
Time	Northern Wall	Southern Wall	Eastern Wall	Western Wall	Ceiling	Total Heat Transfer
	$Q_1$ (W)	$Q_2$ (W)	$Q_3$ (W)	$Q_4$ (W)	$Q_5$ (W)	$\sum_{i=1}^5 Q_i$ (W)
8:00	224.5989	133.6898	106.9519	165.7754	58.82353	689.8396
9:00	160.4278	192.5134	208.5561	262.0321	106.9519	930.4813
10:00	133.6898	208.5561	101.6043	272.7273	272.7273	989.3048
11:00	144.385	213.9037	53.47594	299.4652	556.1497	1267.38
12:00	133.6898	235.2941	10.69519	320.8556	614.9733	1315.508
13:00	133.6898	187.1658	16.04278	427.8075	647.0588	1411.765
14:00	149.7326	80.2139	26.73797	385.0267	513.369	1155.08
15:00	133.6898	5.347594	96.25668	374.3316	336.8984	946.5241
16:00	16.04278	-160.428	10.69519	160.4278	74.86631	101.6043
Insulated wall (Room-2)						
Time	Northern Wall	Southern Wall	Eastern Wall	Western Wall	Ceiling	Total Heat Transfer
	$Q_1$ (W)	$Q_2$ (W)	$Q_3$ (W)	$Q_4$ (W)	$Q_5$ (W)	$\sum_{i=1}^5 Q_i$ (W)
8:00	8.205128	6.358974	20.51282	5.128205	16.51282	56.71795
9:00	7.589744	9.230769	21.84615	8.410256	23.79487	70.87179

10:00	8.205128	11.17949	16.20513	10.05128	25.33333	70.97436
11:00	8.205128	11.69231	11.79487	10.5641	25.64103	67.89744
12:00	8.410256	12.30769	7.179487	16.10256	25.94872	69.94872
13:00	8.205128	13.02564	5.230769	19.58974	24.41026	70.46154
14:00	7.384615	9.333333	4.923077	17.33333	20.20513	59.17949
15:00	5.641026	8	5.230769	16.30769	11.69231	46.87179
16:00	4.307692	3.897436	3.282051	14.35897	6.461538	32.30769

A comparison between the maximum total heat transfer of the insulated and non-insulated room can be seen in the Figure 4-22. Obvious difference can be noticed due to the presence of the insulating materials. However, the effect of the waste addition can not be quantified because the thickness of walls of Room-2 is bigger than that of Room-1. Therefore, the thermal resistances are different of both rooms. To eliminate this issue, an indirect method was used.

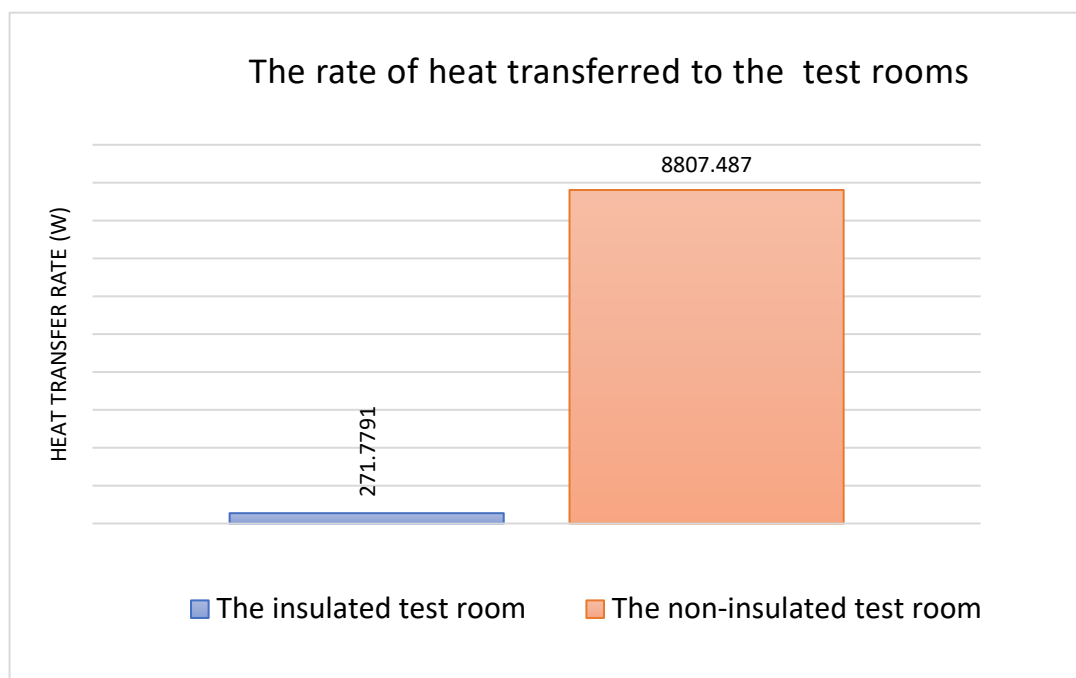


Figure 4-23 Maximim heat transfer rates through the two test rooms based on Fourier's law.

b- Indirect method

Cooling Load Temperature Difference (CLTD) method, a methodology outlined by the American Society of Heating, Refrigerating, and Air-Conditioning Engineers (ASHRAE) was used. This method estimates the cooling loads of different building constructions having comparable properties with those in the study conducted by a research group from ASHRE. This method is based on the CLTD and the solar-air temperature. The study results as usable tables and certain equations were published and became familiar in many textbooks [71]. The procedure of calculating cooling loads (which can be assumed to be equal to the heat transfer rates through the rooms' walls) is presented in Appendix A. Figure 4-23 shows the estimated heat transfer rates of each wall and ceiling of Room-1, and Room-2 on May 17<sup>th</sup>, 2023. In this method, the thickness of each wall and ceiling of Room-1 was assumed to be equal to that of Room-2. This measure is to eliminate the thickness parameter effect on the heat transfer rate value. Details of this method and the calculations can be seen in Appendix A. The results are shown in Figures 4-23, and 4-24. The results shows a reduction in heat transfer rate of 82.22% on May 17<sup>th</sup> and 83.2% on June 20<sup>th</sup>. This percentage was calculated as follows

$$R\% = \frac{Q_{Room-1} - Q_{Room-2}}{Q_{Room-1}} 100 \quad (4-2)$$

In figures 4-23 and 2-24, the heat transfer rates in each geographical direction and the overall heat transfer rate were measured on May 17 when the outside air temperature was 42 degrees Celsius. On June 20, the outside air temperature was measured and recorded at 49 degrees Celsius. However, despite the higher outside temperature on June 20, the overall heat transfer rate was lower. This reduction can be attributed to the improved insulation achieved by applying white paint to the exterior layers of the rooms.

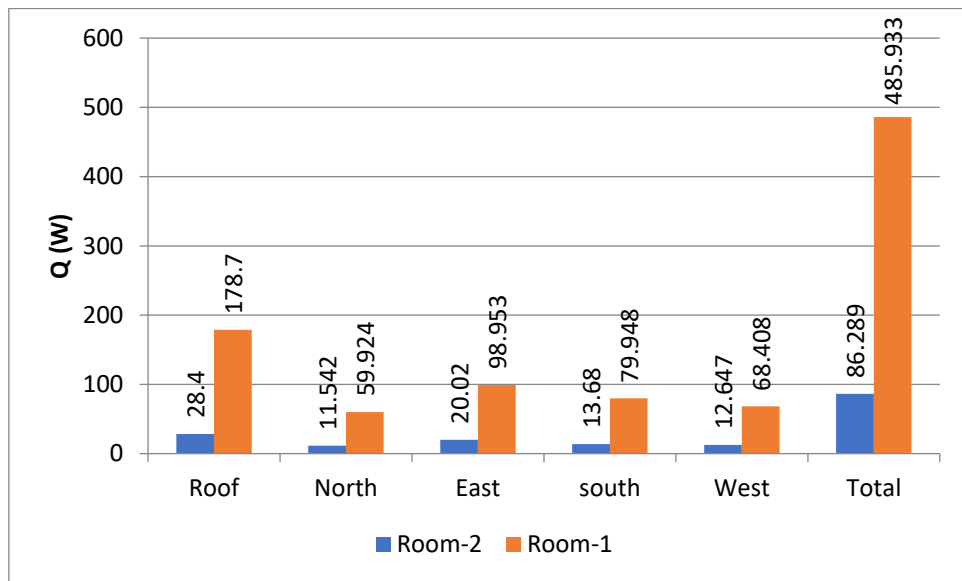


Figure 4-23 Heat transfer rates through the two testing rooms on May 17<sup>th</sup>, 2023, based on CLTD method (before improving the reflectivity of the surfaces)

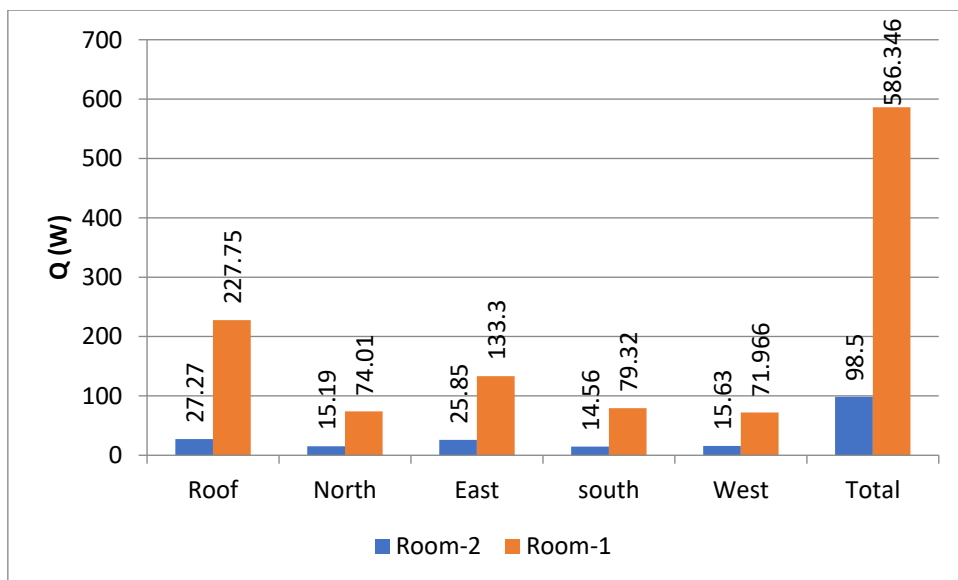


Figure 4-24 Heat transfer rates through the two testing rooms on June 20<sup>th</sup>, 2023, based on CLTD method (after improving the reflectivity of the surfaces)

**CHAPTER FIVE**  
**CONCLUSIONS AND RECOMMENDATIONS**



## CHAPTER FIVE

### CONCLUSIONS AND RECOMMENDATIONS

#### 5.1 Conclusions

This study aims to create sustainable insulation materials by incorporating agricultural and industrial wastes, such as rice husks, sawdust, and polystyrene particles, into traditional building materials. The research had two main goals: improving the insulation of buildings and addressing environmental concerns through the reuse of waste materials. The study dealt with three classes of insulation: cement and sand-based composites, gypsum-based composites, and waste with wood adhesive. The evaluations showed that the materials are compatible with traditional options in thermal performance, making them competitive alternatives. Practical tests in the designated rooms confirmed their effectiveness in reducing heat transfer. In conclusion, reusing waste with traditional ingredients leads to effective isolation for sustainability.

1. Composite materials made from waste and adhesive can be considered as lightweight materials. This means they generally have a low density. The apparent density of these composite materials ranges from  $438 \text{ kg/m}^3$  to  $528 \text{ kg/m}^3$ . In contrast, when using gypsum with waste or cement with waste, the resulting composite materials might have a higher density. For instance, cement and sand-based composites containing waste could reach an apparent density of up to  $1664 \text{ kg/m}^3$ . This can be beneficial in certain cases that require materials with higher density and hardness.

2. It was found that the compressive strength varied significantly between cement and sand or gypsum-based composites, ranging from 1.12 to 5.92 megapascals (MPa). This makes them capable of withstanding structural loads. On the other hand, composites based on waste and wood adhesive exhibited lower compressive strength, ranging from 1.7 MPa to 1.34 MPa. This makes them suitable for non-structural loads, except for the WG1 sample, which exceeded the threshold of 1.7 MPa.
3. The waste and wood glue-based composites are all considered thermal insulators due to their low thermal conductivity, which ranged from 0.043 to 0.054 W/m·K. On the other hand, cement and sand-based composites or gypsum-based composites exhibited a thermal conductivity ranging from 0.116 to 0.362 W/m·K. This makes them heat-resistant materials with significantly lower thermal conductivity compared to other building materials.
4. The practical application of the insulation materials known as WG1 and G3 resulted in a substantial reduction in the rate of heat transfer within the insulated room. This reduction in heat transfer rate reached an impressive 83%. This means that the insulation provided by the WG1 and G3 materials was highly effective in preventing the transfer of heat from one side of the insulated space to the other. This level of heat reduction is indicative of the insulation materials' ability to create a thermal barrier, helping to maintain a more stable and comfortable temperature within the insulated room.

Such findings underscore the effectiveness of these insulation materials in enhancing energy efficiency and contributing to a more comfortable indoor environment.

## **5.2 Recommendations**

1. It is suggested to place the outer layer of rice husks and glue between the building layers, due to its high ability to absorb heat and retain it on the surface. This property is one of the advantages of rice husks that can be used to achieve better control of heat transfer and to maintain comfortable temperatures inside the building.
2. It is suggested to continue studying and developing vital insulating materials and achieving a thermal conductivity coefficient lower than current levels. Through continuous experiments and research, the composition of materials can be improved and various effects on their thermal properties tested.
3. It is suggested to produce bricks made of clay and rice husks in different proportions each time. The thermal conductivity coefficient and pressure strength are measured and used in building sections for concrete structures.
4. The use of rice husks in the production of Thurstone (insulating bricks) instead of aluminum atoms can be an interesting option to improve heat insulation and reduce the impact of construction on the environment.

## References

- [1] “World Energy Outlook 2022.” [Online]. Available: [www.iea.org/t&c/](http://www.iea.org/t&c/)
- [2] L. Yang, H. Yan, and J. C. Lam, “Thermal comfort and building energy consumption implications—a review,” *Appl Energy*, vol. 115, pp. 164–173, 2014.
- [3] Y. H. Yau and S. Hasbi, “A review of climate change impacts on commercial buildings and their technical services in the tropics,” *Renewable and Sustainable Energy Reviews*, vol. 18, pp. 430–441, 2013.
- [4] G. Dixon, T. Abdel-Salam, and P. Kauffmann, “Evaluation of the effectiveness of an energy efficiency program for new home construction in eastern North Carolina,” *Energy*, vol. 35, no. 3, pp. 1491–1496, 2010.
- [5] Energy Dubai. (2020), “How to save on Energy Consumption,” <https://www.energydubai.com/energy-consumers/save-energyconsumption/>.
- [6] L. Aditya *et al.*, “A review on insulation materials for energy conservation in buildings,” *Renewable and sustainable energy reviews*, vol. 73, pp. 1352–1365, 2017.
- [7] A. F. Handbook, “American society of heating, refrigerating and air-conditioning engineers,” *Inc.: Atlanta, GA, USA*, 2009.
- [8] M. S. Al-Homoud, “Performance characteristics and practical applications of common building thermal insulation materials,” *Build Environ*, vol. 40, no. 3, pp. 353–366, 2005.
- [9] B. Abu-Jdayil, A.-H. Mourad, W. Hittini, M. Hassan, and S. Hameedi, “Traditional, state-of-the-art and renewable thermal building insulation materials: An overview,” *Constr Build Mater*, vol. 214, pp. 709–735, 2019.
- [10] Close PD., *Building Insulation*. Building Insulation, 1952.
- [11] C. Craven and R. Garber-Slaght, *Reflective insulation in cold climates*. Cold Climate Housing Research Center Fairbanks, AK, USA, 2011.
- [12] K. Olathe, “Reflective Insulation Manufacturers Association International (RIMA-I),” *Reflective insulation, radiant barriers and radiation control coatings, RIMA-I*, 2002.
- [13] A. M. Papadopoulos, “State of the art in thermal insulation materials and aims for future developments,” *Energy Build*, vol. 37, no. 1, pp. 77–86, 2005.

- [14] M. S. Al-Homoud, "Performance characteristics and practical applications of common building thermal insulation materials," *Build Environ*, vol. 40, no. 3, pp. 353–366, 2005.
- [15] F. Domínguez-Muñoz, B. Anderson, J. M. Cejudo-López, and A. Carrillo-Andrés, "Uncertainty in the thermal conductivity of insulation materials," *Energy Build*, vol. 42, no. 11, pp. 2159–2168, 2010.
- [16] Z. Wei, K. Gu, B. Chen, and C. Wang, "Comparison of sawdust bio-composites based on magnesium oxysulfate cement and ordinary Portland cement," *Journal of Building Engineering*, vol. 63, p. 105514, 2023.
- [17] M. Charai, A. Mezrhab, L. Moga, and M. Karkri, "Hygrothermal, mechanical and durability assessment of vegetable concrete mixes made with Alfa fibers for structural and thermal insulating applications," *Constr Build Mater*, vol. 335, p. 127518, 2022.
- [18] B. Marques *et al.*, "Rice husk cement-based composites for acoustic barriers and thermal insulating layers," *Journal of Building Engineering*, vol. 39, p. 102297, 2021.
- [19] K. Selvaranjan *et al.*, "Thermal and environmental impact analysis of rice husk ash-based mortar as insulating wall plaster," *Constr Build Mater*, vol. 283, p. 122744, 2021.
- [20] M. Maaroufi, R. Belarbi, K. Abahri, and F. Benmahiddine, "Full characterization of hygrothermal, mechanical and morphological properties of a recycled expanded polystyrene-based mortar," *Constr Build Mater*, vol. 301, p. 124310, 2021.
- [21] V. Barbieri, M. L. Gualtieri, and C. Siligardi, "Wheat husk: A renewable resource for bio-based building materials," *Constr Build Mater*, vol. 251, p. 118909, 2020.
- [22] T. Salem, M. Fois, O. Omikrine-Metalssi, R. Manuel, and T. Fen-Chong, "Thermal and mechanical performances of cement-based mortars reinforced with vegetable synthetic sponge wastes and silica fume," *Constr Build Mater*, vol. 264, p. 120213, 2020.
- [23] M. Asim *et al.*, "Comparative experimental investigation of natural fibers reinforced light weight concrete as thermally efficient building materials," *Journal of Building Engineering*, vol. 31, p. 101411, 2020.

- [24] Y. X. Chen, F. Wu, Q. Yu, and H. J. H. Brouwers, "Bio-based ultra-lightweight concrete applying miscanthus fibers: Acoustic absorption and thermal insulation," *Cem Concr Compos*, vol. 114, p. 103829, 2020.
- [25] F. Berger, F. Gauvin, and H. J. H. Brouwers, "The recycling potential of wood waste into wood-wool/cement composite," *Constr Build Mater*, vol. 260, p. 119786, 2020.
- [26] H. Binici, O. Aksogan, A. Dincer, E. Luga, M. Eken, and O. Isikaltun, "The possibility of vermiculite, sunflower stalk and wheat stalk using for thermal insulation material production," *Thermal Science and Engineering Progress*, vol. 18, p. 100567, 2020.
- [27] N. Abbas, H. R. Khalid, G. Ban, H. T. Kim, and H.-K. Lee, "Silica aerogel derived from rice husk: An aggregate replacer for lightweight and thermally insulating cement-based composites," *Constr Build Mater*, vol. 195, pp. 312–322, 2019.
- [28] A. Dixit, S. D. Pang, S. H. Kang, and J. Moon, "Lightweight structural cement composites with expanded polystyrene (EPS) for enhanced thermal insulation," *Cem Concr Compos*, vol. 102, pp. 185–197, Sep. 2019, doi: 10.1016/j.cemconcomp.2019.04.023.
- [29] Y. Wei, C. Song, B. Chen, and M. R. Ahmad, "Experimental investigation on two new corn stalk biocomposites based on magnesium phosphate cement and ordinary Portland cement," *Constr Build Mater*, vol. 224, pp. 700–710, 2019.
- [30] M. R. Ahmad, B. Chen, S. Y. Oderji, and M. Mohsan, "Development of a new bio-composite for building insulation and structural purpose using corn stalk and magnesium phosphate cement," *Energy Build*, vol. 173, pp. 719–733, 2018.
- [31] A. Alabdulkarem, M. Ali, G. Iannace, S. Sadek, and R. Almuzaiqer, "Thermal analysis, microstructure and acoustic characteristics of some hybrid natural insulating materials," *Constr Build Mater*, vol. 187, pp. 185–196, 2018.
- [32] C. Zhou, S. Q. Shi, Z. Chen, L. Cai, and L. Smith, "Comparative environmental life cycle assessment of fiber reinforced cement panel between kenaf and glass fibers," *J Clean Prod*, vol. 200, pp. 196–204, 2018.
- [33] B. Haba, B. Agoudjil, A. Boudenne, and K. Benzarti, "Hygric properties and thermal conductivity of a new insulation material for building based on date palm concrete," *Constr Build Mater*, vol. 154, pp. 963–971, 2017.

- [34] M. Boumhaout, L. Boukhattem, H. Hamdi, B. Benhamou, and F. A. Nouh, “Thermomechanical characterization of a bio-composite building material: Mortar reinforced with date palm fibers mesh,” *Constr Build Mater*, vol. 135, pp. 241–250, 2017.
- [35] X. Ding, S. Wang, R. Dai, H. Chen, and Z. Shan, “Hydrogel beads derived from chrome leather scraps for the preparation of lightweight gypsum,” *Environ Technol Innov*, vol. 25, p. 102224, 2022.
- [36] I. Mehrez, H. Hachem, and A. Jemni, “Thermal insulation potential of wood-cereal straws/plaster composite,” *Case Studies in Construction Materials*, vol. 17, p. e01353, 2022.
- [37] S. Bouzit, F. Merli, M. Sonebi, C. Buratti, and M. Taha, “Gypsum-plasters mixed with polystyrene balls for building insulation: Experimental characterization and energy performance,” *Constr Build Mater*, vol. 283, p. 122625, 2021.
- [38] L. Boquera *et al.*, “Thermo-acoustic and mechanical characterization of novel bio-based plasters: The valorisation of lignin as by-product from biomass extraction for green building applications,” *Constr Build Mater*, vol. 278, p. 122373, 2021.
- [39] S. Ouhaibi *et al.*, “Thermally insulating gypsum composites incorporating aerosil for sustainable energy-saving buildings,” *Journal of Building Engineering*, vol. 43, p. 102848, 2021.
- [40] A. Benallel, A. Tilioua, M. Ettakni, M. Ouakarrouch, M. Garoum, and M. A. A. Hamdi, “Design and thermophysical characterization of new thermal insulation panels based on cardboard waste and vegetable fibers,” *Sustainable Energy Technologies and Assessments*, vol. 48, p. 101639, 2021.
- [41] I. Capasso and F. Iucolano, “Production of lightweight gypsum using a vegetal protein as foaming agent,” *Mater Struct*, vol. 53, pp. 1–13, 2020.
- [42] S. Sair, B. Mandili, M. Taqi, and A. El Bouari, “Development of a new eco-friendly composite material based on gypsum reinforced with a mixture of cork fibre and cardboard waste for building thermal insulation,” *Composites Communications*, vol. 16, pp. 20–24, 2019.

- [43] J. Jiang, Z. Lu, J. Li, Y. Fan, and Y. Niu, "Preparation and hardened properties of lightweight gypsum plaster based on pre-swelled bentonite," *Constr Build Mater*, vol. 215, pp. 360–370, 2019.
- [44] Y. Kang, S. J. Chang, and S. Kim, "Hygrothermal behavior evaluation of walls improving heat and moisture performance on gypsum boards by adding porous materials," *Energy Build*, vol. 165, pp. 431–439, 2018.
- [45] A. Braiek, M. Karkri, A. Adili, L. Ibos, and S. Ben Nasrallah, "Estimation of the thermophysical properties of date palm fibers/gypsum composite for use as insulating materials in building," *Energy Build*, vol. 140, pp. 268–279, 2017.
- [46] M. del Mar Barbero-Barrera, N. Flores-Medina, and V. Pérez-Villar, "Assessment of thermal performance of gypsum-based composites with revalorized graphite filler," *Constr Build Mater*, vol. 142, pp. 83–91, 2017.
- [47] O. Gencil, J. J. del Coz Diaz, M. Sutcu, F. Koksall, F. P. Á. Rabanal, and G. Martínez-Barrera, "A novel lightweight gypsum composite with diatomite and polypropylene fibers," *Constr Build Mater*, vol. 113, pp. 732–740, 2016.
- [48] N. F. Medina and M. M. Barbero-Barrera, "Mechanical and physical enhancement of gypsum composites through a synergic work of polypropylene fiber and recycled isostatic graphite filler," *Constr Build Mater*, vol. 131, pp. 165–177, 2017.
- [49] H. E. Benchouia, B. Guerira, M. Chikhi, H. Boussehel, and C. Tedeschi, "An experimental evaluation of a new eco-friendly insulating material based on date palm fibers and polystyrene," *Journal of Building Engineering*, vol. 65, p. 105751, 2023.
- [50] S. Singh *and.*, B. Guerira, M. "Elevated temperature and performance behaviour of rice straw as waste bio-mass based foamed gypsum hollow blocks," *Journal of Building Engineering*, vol. 69, p. 106220, 2023.
- [51] M. Charai, M. O. Mghazli, S. Channouf, P. Jagadesh, L. Moga, and A. Mezrhab, "Lightweight waste-based gypsum composites for building temperature and moisture control using coal fly ash and plant fibers," *Constr Build Mater*, vol. 393, p. 132092, 2023.
- [52] Y. Khalaf, P. El Hage, J. D. Mihajlova, A. Bergeret, P. Lacroix, and R. El Hage, "Influence of agricultural fibers size on mechanical and insulating properties of



- innovative chitosan-based insulators,” *Constr Build Mater*, vol. 287, p. 123071, 2021.
- [53] Y. X. Chen, G. Liu, K. Schollbach, and H. J. H. Brouwers, “Development of cement-free bio-based cold-bonded lightweight aggregates (BCBLWAs) using steel slag and miscanthus powder via CO<sub>2</sub> curing,” *J Clean Prod*, vol. 322, p. 129105, 2021.
- [54] S. Wang, H. Li, S. Zou, and G. Zhang, “Experimental research on a feasible rice husk/geopolymer foam building insulation material,” *Energy Build*, vol. 226, p. 110358, 2020.
- [55] B. Marques, A. Tadeu, J. António, J. Almeida, and J. de Brito, “Mechanical, thermal and acoustic behaviour of polymer-based composite materials produced with rice husk and expanded cork by-products,” *Constr Build Mater*, vol. 239, p. 117851, 2020.
- [56] S. Platt, D. Maskell, P. Walker, and A. Laborel-Préneron, “Manufacture and characterisation of prototype straw bale insulation products,” *Constr Build Mater*, vol. 262, p. 120035, 2020.
- [57] V. Guna., and A. F. Shubbar “Groundnut shell/rice husk agro-waste reinforced polypropylene hybrid biocomposites,” *Journal of Building engineering*, vol. 27, p. 100991, 2020.
- [58] A. Savic, D. Antonijevic, I. Jelic, and D. Zakic, “Thermomechanical behavior of bio-fiber composite thermal insulation panels,” *Energy Build*, vol. 229, p. 110511, 2020.
- [59] R. Muthuraj, C. Lacoste, P. Lacroix, and A. Bergeret, “Sustainable thermal insulation biocomposites from rice husk, wheat husk, wood fibers and textile waste fibers: Elaboration and performances evaluation,” *Ind Crops Prod*, vol. 135, pp. 238–245, 2019.
- [60] J. António, A. Tadeu, B. Marques, J. A. S. Almeida, and V. Pinto, “Application of rice husk in the development of new composite boards,” *Constr Build Mater*, vol. 176, pp. 432–439, 2018.
- [61] C. Buratti, E. Belloni, E. Lascaro, F. Merli, and P. Ricciardi, “Rice husk panels for building applications: Thermal, acoustic and environmental characterization and

- comparison with other innovative recycled waste materials,” *Constr Build Mater*, vol. 171, pp. 338–349, 2018.
- [62] H. Alshahrani and V. R. A. Prakash, “Thermal, mechanical and barrier properties of rice husk ash biosilica toughened epoxy biocomposite coating for structural application,” *Prog Org Coat*, vol. 172, p. 107080, 2022.
- [63] F. J. Pettijohn, P. E. Potter, and R. Siever, *Sand and sandstone*. Springer Science & Business Media, 2012.
- [64] N. H. Ramli Sulong, S. A. S. Mustapa, and M. K. Abdul Rashid, “Application of expanded polystyrene (EPS) in buildings and constructions: A review,” *J Appl Polym Sci*, vol. 136, no. 20, p. 47529, 2019.
- [65] M. Y. Fattah, F. H. Rahil, and K. Y. H. Al-Soudany, “Improvement of clayey soil characteristics using rice husk ash,” *Journal of Civil Engineering and Urbanism*, vol. 3, no. 1, pp. 12–18, 2013.
- [66] H. M. Al-Baghdadi, A. A. F. Shubbar, and Z. S. Al-Khafaji, “The Impact of Rice Husks Ash on Some Mechanical Features of Reactive Powder Concrete with High Sulfate Content in Fine Aggregate,” *International Review of Civil Engineering (IRECE)*, vol. 12, no. 4, pp. 248–254, 2021.
- [67] K. Svinning, A. Høskuldsson, and H. Justnes, “Prediction of compressive strength up to 28 days from microstructure of Portland cement,” *Cem Concr Compos*, vol. 30, no. 2, pp. 138–151, 2008.
- [68] M. Carrabbaet., and Al-Judi “Translucent zirconia in the ceramic scenario for monolithic restorations: A flexural strength and translucency comparison test,” *J Dent*, vol. 60, pp. 70–76, 2017.
- [69] M. Mohit and Y. Sharifi, “Thermal and microstructure properties of cement mortar containing ceramic waste powder as alternative cementitious materials,” *Constr Build Mater*, vol. 223, pp. 643–656, 2019.
- [70] Y. Qu, “5.07 - Sea Surface Albedo,” in *Comprehensive Remote Sensing*, S. Liang, Ed., Oxford: Elsevier, 2018, pp. 163–185. doi: <https://doi.org/10.1016/B978-0-12-409548-9.10371-9>.
- [71] Khaled Al-Judi, *Air conditioning and refrigeration engineering*. 1991.

## الملخص

يتجه قطاع البناء نحو بناء المباني الموفرة للطاقة، ويساهم تطوير مواد العزل الحراري المستدامة في هذا الاتجاه. واستخدام هذه المواد يقلل بشكل كبير من استهلاك الطاقة، مما يقلل الحاجة إلى المواد غير المتجددة ويقلل النفايات. تم في هذه الدراسة إنتاج ثلاث مجموعات من مواد البناء العازلة، المجموعة الأولى التي تعتمد على الأسمنت والرمل مع المخلفات تم إنتاج خمس عينات مختلفة. كما أنتجت المجموعة الثانية المعتمدة على الجبس مع المخلفات خمس عينات، والمجموعة الثالثة المعتمدة على المخلفات مع غراء الخشب أنتجت أربع عينات مختلفة. تم تحضير العينات بنسب تدريجية حتى الوصول إلى عينات ذات قوام متماسك. تم إجراء الاختبارات الحرارية والفيزيائية على العينات، حيث تم إجراء فحص (الموصلية الحرارية، قوة الضغط، الكثافة الجافة، امتصاص الماء)، ولوحظت النتائج أن القيم المجموعة الأولى كانت التوصيل الحراري، قوة الضغط، الكثافة الجافة، وامتصاص الماء، على التوالي. تتراوح من (0.118 وات/م.ك إلى 0.362 وات/م.ك) (2.64 ميغا باسكال إلى 5.92 ميغا باسكال) (1272 كجم/م<sup>3</sup> إلى 1664 كجم/م<sup>3</sup>) (15% إلى 20%)، وقيم المجموعة الثانية هي التوصيل الحراري و مقاومة الانضغاط والكثافة الجافة وامتصاص الماء على التوالي من (0.116 وات/م.ك إلى 0.291 وات/م.ك) (1.12 ميغا باسكال إلى 4.08 ميغا باسكال) (320 كجم/م<sup>3</sup> إلى 1224 كجم/م<sup>3</sup>) (19% إلى 33%)، و أما قيم المجموعة الثالثة فهي التوصيل الحراري وقوة الانضغاط والكثافة الجافة وامتصاص الماء على التوالي وتتراوح من (0.043 وات/م.ك إلى 0.054 وات/م.ك) (1.43 ميغا باسكال إلى 1.7 ميغا باسكال) (438 كجم/م<sup>3</sup> إلى 528 كجم/م<sup>3</sup>) (31% إلى 37%). بعد ذلك تم اختيار عيتين للتطبيق العملي وحساب معدل انتقال الحرارة من خلالهما وقدرتهما على تقليل انتقال الحرارة في الغرفة المخصصة للاختبار، حيث تم تطبيق في الجدار الداخلي لغرفة الاختبار المعزولة عينة (G3)، وتطبيق على الجدار الخارجي لغرفة الاختبار المعزولة عينة (WG1). أظهرت الغرفة المعزولة انخفاضاً في معدل انتقال الحرارة بنسبة 83 عن الغرفة الغير معزولة.

## Appendix-A

### Heat transfer reduction calculations

a- Direct method

Relying on Fourier's law of heat transfer by conduction

$$Q = kA \frac{\Delta T}{\Delta x} = A \frac{\Delta T}{\Delta x/k}$$

Where:

Q: is the amount of heat transfer across the conductor (measured in watts).

K: is the thermal conductivity of the material (measured in watts per meter per degree Celsius).

$\Delta T$ : is the temperature difference between the ends,

A: is the cross-sectional surface area,

$\Delta X$ : is the distance between the ends.

#### For Room1

North direction at 8:00 PM

$$Q = A * \frac{\Delta T}{\frac{\Delta X_{wall}}{K_{wall}}} = 1 * \frac{4.2}{\frac{0.015}{0.8}} = 224.5989 \text{ W}$$

#### For Room2

North direction at 8:00 PM

$$Q = 1 * \frac{\Delta T}{\frac{\Delta X_{WGx}}{K(WG1)} + \frac{\Delta X_{wall}}{K_{wall}} + \frac{\Delta X(G3)}{K(G3)}} = \frac{8}{\frac{0.03}{0.043} + \frac{0.015}{0.8} + \frac{0.03}{0.116}} = 8.205128 \text{ W}$$

Table A-1 Heat transfer rates of Room-1 and Room-2 based on Fourier's law

Room1 (Non-insulated wall)				
Direction	Time	Q(w)	$\Delta T(^{\circ}C)$	$\Delta X$
Ceiling	8:00	58.82353	1.1	0.015
	9:00	106.9519	2	0.015

	10:00	272.7273	5.1	0.015
	11:00	556.1497	10.4	0.015
	12:00	614.9733	11.5	0.015
	13:00	647.0588	12.1	0.015
	14:00	513.369	9.6	0.015
	15:00	336.8984	6.3	0.015
	16:00	74.86631	1.4	0.015
Northern Wall	8:00	224.5989	4.2	0.015
	9:00	160.4278	3	0.015
	10:00	133.6898	2.5	0.015
	11:00	144.385	2.7	0.015
	12:00	133.6898	2.5	0.015
	13:00	133.6898	2.5	0.015
	14:00	149.7326	2.8	0.015
	15:00	133.6898	2.5	0.015
	16:00	16.04278	0.3	0.015
Eastern Wall	8:00	106.9519	2	0.015
	9:00	208.5561	3.9	0.015
	10:00	101.6043	1.9	0.015
	11:00	53.47594	1	0.015
	12:00	10.69519	0.2	0.015
	13:00	16.04278	0.3	0.015
	14:00	26.73797	0.5	0.015
	15:00	96.25668	1.8	0.015
	16:00	10.69519	0.2	0.015
Southern Wall	8:00	133.6898	2.5	0.015
	9:00	192.5134	3.6	0.015
	10:00	208.5561	3.9	0.015
	11:00	213.9037	4	0.015
	12:00	235.2941	4.4	0.015
	13:00	187.1658	3.5	0.015

	14:00	80.2139	1.5	0.015
	15:00	5.347594	0.1	0.015
	16:00	-160.428	-3	0.015
Western Wall	8:00	165.7754	3.1	0.015
	9:00	262.0321	4.9	0.015
	10:00	272.7273	5.1	0.015
	11:00	299.4652	5.6	0.015
	12:00	320.8556	6	0.015
	13:00	427.8075	8	0.015
	14:00	385.0267	7.2	0.015
	15:00	374.3316	7	0.015
	16:00	160.4278	3	0.015

Room2 (Insulated wall)				
Direction	Time	Q(w)	$\Delta T(^{\circ}C)$	$\Delta X$
Ceiling	8:00	16.51282	16.1	0.075
	9:00	23.79487	23.2	0.075
	10:00	25.33333	24.7	0.075
	11:00	25.64103	25	0.075
	12:00	25.94872	25.3	0.075
	13:00	24.41026	23.8	0.075
	14:00	20.20513	19.7	0.075
	15:00	11.69231	11.4	0.075
	16:00	6.461538	6.3	0.075
Northern Wall	8:00	8.205128	8	0.075
	9:00	7.589744	7.4	0.075
	10:00	8.205128	8	0.075
	11:00	8.205128	8	0.075
	12:00	8.410256	8.2	0.075
	13:00	8.205128	8	0.075
	14:00	7.384615	7.2	0.075
	15:00	5.641026	5.5	0.075

	16:00	4.307692	4.2	0.075
Eastern Wall	8:00	20.51282	20	0.075
	9:00	21.84615	21.3	0.075
	10:00	16.20513	15.8	0.075
	11:00	11.79487	11.5	0.075
	12:00	7.179487	7	0.075
	13:00	5.230769	5.1	0.075
	14:00	4.923077	4.8	0.075
	15;00	5.230769	5.1	0.075
	16:00	3.282051	3.2	0.075
Southern Wall	8:00	6.358974	6.2	0.075
	9:00	9.230769	9	0.075
	10:00	11.17949	10.9	0.075
	11:00	11.69231	11.4	0.075
	12:00	12.30769	12	0.075
	13:00	13.02564	12.7	0.075
	14:00	9.333333	9.1	0.075
	15;00	8	7.8	0.075
	16:00	3.897436	3.8	0.075
Western Wall	8:00	5.128205	5	0.075
	9:00	8.410256	8.2	0.075
	10:00	10.05128	9.8	0.075
	11:00	10.5641	10.3	0.075
	12:00	16.10256	15.7	0.075
	13:00	19.58974	19.1	0.075
	14:00	17.33333	16.9	0.075
	15;00	16.30769	15.9	0.075
	16:00	14.35897	14	0.075
Q Total room1 (W)			8807.487	
Q Total room2 (W)			545.23	

Reduction in heat transfer rate

$$R\% = \frac{Q_{Room-1} - Q_{Room-2}}{Q_{Room-1}} 100$$

$$R\% = \frac{8807.487 - 545.23}{8807.487} 100 = 93\%$$

b- Indirect method

Calculations by CLTD (Cooling Load Temperature Difference)

Note: All the following calculations are based on the method described in (Air conditioning and refrigeration engineering book) [71]

$$q = A.U. CLTD_c \quad (A-2)$$

$$U = \frac{1}{\frac{1}{h_o} + \sum \frac{\Delta x}{K} + \frac{1}{h_i}} \quad (A-3)$$

**For roof**

$$CLTD_c = [(CLTD + LM) K + (25.5 - T_r) + (T_o - 29.4)] * f. \quad (A-4)$$

**For wall**

$$CLTD_c = [(CLTD) + LM] K + (25.5 - T_r) + (T_o - 29.4). \quad (A-5)$$

CLTD<sub>c</sub>: Correction factor for latitude and month.

CLTD: Cooling Load Temperature Difference.

LM: Load Modifier, an additional correction related to walls and roof.

Correction for Indoor Air Temperature:  $(25.5 - T_r) = 0.5 \text{ } ^\circ\text{C}$

$$(25.5 - T_r) = 0.5 \text{ } ^\circ\text{C} \quad \text{Where } T_r = 25^\circ\text{C}$$

$T_o$  = Correction for Outdoor Air Temperature

Where  $T_o = (t_o - DR)$

$t_o$ : External ambient temperature

$$DR: \text{ daily rang} = \frac{\text{Number of daylight}}{2}$$

f: Correction factor for the presence of ventilation between the secondary roof and the inclined roof = 1, when there is no ventilation.

K: Wall color correction factor

1.0 = for dark or light walls in industrial areas.

0.83 = for permanent medium walls.

0.65 = for permanent light-colored walls.

K: Ceiling color correction factor

1.0 = for dark or light ceilings in industrial areas.



0.5 =for permanent light roof.

Dark colors: dark blue, dark red, and dark green.

Medium colors: light blue, light green, light red, coffee, and concrete color.

Light colors: white, light yellow, and light brown.

### Test on May 17, 2023, before paintin rooms

At 3:00 PM, with an outside temperature of 45 °C degrees Celsius.

#### Room2

For north direction

$$q = A.U. CLTD_c$$

$$U = \frac{1}{\frac{1}{h_o} + \frac{\Delta x_{WG1}}{K(WG1)} + \frac{\Delta x_{wall}}{K_{wall}} + \frac{\Delta x(G3)}{K(G3)} + \frac{1}{h_i}}$$

$$U = \frac{1}{\frac{1}{22.7} + \frac{0.03}{0.043} + \frac{0.015}{0.8} + \frac{0.03}{0.116} + \frac{1}{9.37}} = 0.8882 \text{ W/m}^2 \cdot ^\circ\text{C}$$

$$CLTD_c = [(CLTD + LM) K + (25.5 - T_r) + (T_o - 29.4)] * f.$$

$$CLTD = 6$$

$$CLTD_c = [(6 + 0.5) 0.83 + (25.5 - 25) + (36.5 - 29.4)] * 1$$

$$CLTD_c = 12.995$$

$$Q = 1 * 0.8882 * 12.995 = 11.542 \text{ W}$$

Table A1 CLTD<sub>c</sub> values calculations for room2 on May 17

Component	Direction	CLTD	LM	CLTD <sub>c</sub>	A(m <sup>2</sup> )	Q (W)	Q <sub>Total</sub> (W)
Walls	North	6	0.5	12.995	1	11.542	86.388
	East	18	0.0	22.54	1	20.020	
	South	11	-1.6	15.402	1	13.680	
	West	8	0.0	14.24	1	12.647	
Roof		29	0.5	32.085	1	28.4	

\*CLTD for walls from Table (6.3) wall No (3) and Table (6.4) Groupe D[71].

\*CLTD for roof from Table (6.2) Without Suspended Ceiling[71].

\*LM from Table (6.5)· May, Latitude 32 North [71].

## Room 1

$$U = \frac{1}{\frac{1}{22.7} + \frac{0.03+0.015+0.03}{0.8} + \frac{1}{9.37}} = 4.089 \text{ W/m}^2 \cdot ^\circ\text{C}$$

Table A2 CLTD<sub>C</sub> values calculations for room 1 on May 17

Component	Direction	CLTD	LM	CLTD <sub>C</sub>	A(m <sup>2</sup> )	Q (W)	Q <sub>Total</sub> (W)
Walls	North	8	0.5	17.6	1	59.924	485.944
	East	20	0.0	29.1	1	98.953	
	South	16	-1.6	23.5	1	79.948	
	West	11	0.0	20.1	1	68.408	
Roof		43	0.5	52.1	1	178.7	

\*CLTD for walls from Table (6.3), (6.4) wall No. (5) Groupe E [71].

\*CLTD for roof from Table (6.2) Without Suspended roof No. (1)[71].

\*LM from Table (6.5), May, Latitude 32 North[71].

## The test on June 20<sup>th</sup>, 2023, after white painting

At 1:00 PM, with an outside temperature of 49<sup>o</sup>C.

$$(T_o - 29.4) = 12 \text{ } ^\circ\text{C}$$

## Room2

Table A3 CLTD<sub>C</sub> values calculations for room2 on June 20<sup>th</sup>

Component	Direction	CLTD	LM	CLTD <sub>C</sub>	A(m <sup>2</sup> )	Q (W)	Q <sub>Total</sub> (W)
Walls	North	5	0.5	17.1	1	15.19	98.5
	East	17	0.0	28.6	1	25.85	
	South	7	-2.2	16.4	1	14.56	
	West	6	0.0	17.6	1	15.63	
Roof		18	1.1	30.7	1	27.27	

\*CLTD for walls from Table (6.3) wall No (3) and Table (6.4) Groupe D[71].

\*CLTD for roof from Table (6.2) Without Suspended Ceiling[71].

\*LM from Table (6.5), June, Latitude 32 North [71].

# Room1

Table A4 CLTD<sub>C</sub> values calculations for room on June 20<sup>th</sup>

Component	Direction	CLTD	LM	CLTD <sub>C</sub>	A(m <sup>2</sup> )	Q (W)	Q <sub>Total</sub> (W)
Walls	North	6	0.5	18.1	1	74.01	586.362
	East	21	0.0	32.6	1	133.3	
	South	10	-2.2	19.4	1	79.32	
	West	6	0.0	17.6	1	71.966	
Roof		43	1.1	53.5	1	227.75	

\*CLTD for walls from Table (6.3), (6.4) wall No. (1) Groupe E [71].

\*CLTD for roof from Table (6.2) Without Suspended roof No. (3)[71].

\*LM from Table (6.5), May, Latitude 32 North[71].

Figures A1 Tables of CLTD<sub>C</sub> and LM values

**تابع جدول 2-6 فرق درجات حمل التبريد CLTD للسقف بدون سقف تانوي**

Roof No	Description of Construction	Weighty kg m <sup>-2</sup>	U-value, m <sup>2</sup> .°C	Solar Time, h																								24CLTD	CLTD	Maxi-Differ- num	Mini-Differ- num	Maxi-Differ- num	Differ- num
				1	2	3	4	5	6	7	8	9	10	11	12	13	14	15	16	17	18	19	20	21	22	23							
Without Suspended Ceiling																																	
1	Steel sheet with 25.4-mm (or 50.8-mm) insulation	34 (39)	1.209 (0.704)	0	-1	-2	-2	-3	-2	3	11	19	27	34	40	43	44	43	39	33	25	17	10	7	5	3	1	14	-3	44	47		
2	25.4-mm wood with 25.4-mm insulation	39	0.965	3	2	0	-1	-2	-2	-1	2	8	15	22	29	35	39	41	41	39	35	29	21	15	11	8	5	16	-2	41	43		
3	101.6-mm l.w. concrete	88	1.209	5	3	1	0	-1	-2	-2	1	5	11	18	25	31	36	39	40	40	37	32	25	19	14	10	7	16	-2	40	42		
4	50.8-mm h.w. concrete with 25.4-mm (or 50.8-mm) insulation	142	1.170 (0.693)	5	3	2	0	-1	0	2	6	11	17	23	28	33	36	37	37	34	30	25	20	16	12	10	16	-1	37	38			
5	25.4-mm wood with 50.8-mm insulation	44	0.619	2	0	-2	-3	-4	-4	-4	-2	3	9	15	22	27	32	35	36	35	32	27	20	14	10	6	3	16	-4	36	40		
6	152.4-mm l.w. concrete	117	0.897	12	10	7	5	3	2	1	0	2	4	8	13	18	24	29	33	35	36	35	32	28	24	19	16	18	0	36	36		
7	63.5-mm wood with 25.4-mm insulation	63	0.738	16	13	11	9	7	6	4	3	4	5	8	11	15	19	23	27	29	31	31	30	27	25	22	19	19	3	31	28		
8	203.2-mm l.w. concrete	151	0.715	20	17	14	12	10	8	6	5	4	4	5	7	11	14	18	22	25	28	30	30	29	27	25	22	20	4	30	26		
9	101.6-mm h.w. concrete with 25.4-mm (or 50.8-mm) insulation	254	1.136 (0.681)	14	12	10	8	7	5	4	4	6	8	11	15	18	22	25	28	29	30	29	27	24	21	19	16	18	4	30	26		
10	63.5-mm wood with 50.8-mm insulation	63	0.528	18	15	13	11	9	8	6	5	5	5	7	10	13	17	21	24	27	28	29	29	27	25	23	20	19	5	29	24		
11	Roof terrace system	366	0.602	19	17	15	14	12	11	9	8	7	8	8	10	12	15	18	20	22	24	25	26	25	24	22	21	20	7	26	19		
12	152.4-mm h.w. concrete with 25.4-mm (or 50.8-mm) insulation	366	1.190 (0.664)	18	16	14	12	11	10	9	8	8	9	10	12	15	17	20	22	24	25	25	25	24	22	20	19	19	8	25	17		
13	101.6-mm wood with 25.4-mm (or 50.8-mm) insulation	83	0.602 (0.443)	21	20	18	17	15	14	13	11	10	9	9	10	12	14	16	18	20	22	23	24	24	23	22	22	9	24	15			

جدول 6-4 فرق درجات حرارة حمل التبريد CLTD للجدران

	Solar Time, h																								H of Max-imum CLTD	Min-imum CLTD	Max-imum CLTD	Differ-ence CLTD	
	1	2	3	4	5	6	7	8	9	10	11	12	13	14	15	16	17	18	19	20	21	22	23	24					
Group A Walls																													
N	8	7	7	6	5	4	3	3	3	3	3	4	4	5	6	6	7	8	9	10	11	11	10	10	9	21	3	11	8
NE	9	8	7	6	5	5	4	4	6	8	10	11	12	13	13	13	14	14	14	14	13	13	12	11	10	19	4	14	10
E	11	10	8	7	6	5	5	5	7	10	13	15	17	18	18	18	18	18	18	17	17	16	15	13	12	16	5	18	13
SE	11	10	9	7	6	5	5	5	5	7	10	12	14	16	17	18	18	18	18	17	17	16	15	14	12	17	5	18	13
S	11	10	8	7	6	5	4	4	3	3	4	5	7	9	11	13	15	16	16	16	15	14	13	12	19	3	16	13	
SW	15	14	12	10	9	8	6	5	5	4	4	5	5	7	9	12	15	18	20	21	21	20	19	17	21	4	21	17	
W	17	15	13	12	10	9	7	6	5	5	5	5	6	6	8	10	13	17	20	22	23	22	21	19	21	5	23	18	
NW	14	12	11	9	8	7	6	5	4	4	4	4	5	6	7	8	10	12	15	17	18	17	16	15	22	4	18	14	
Group E Walls																													
N	7	6	5	4	3	2	2	2	3	3	4	5	6	7	8	10	10	11	12	12	11	10	9	8	20	2	12	10	
NE	7	6	5	4	3	2	3	5	8	11	13	14	14	14	14	14	15	14	14	13	12	11	9	8	16	2	15	13	
E	8	7	6	5	4	3	3	6	10	15	18	20	21	21	20	19	18	18	17	15	14	12	11	9	13	3	21	18	
SE	8	7	6	5	4	3	3	4	7	10	14	17	19	20	20	19	18	17	16	14	13	11	10	15	3	20	17		
S	8	7	6	5	4	3	2	2	3	3	5	7	10	14	16	18	19	18	17	16	14	13	11	10	17	2	19	17	
SW	12	10	8	7	6	4	4	3	3	3	4	5	7	10	14	16	18	21	24	25	24	22	19	17	14	3	25	22	
W	14	12	10	8	6	5	4	3	3	4	4	5	6	8	11	15	20	24	27	27	25	22	19	16	20	3	27	24	
NW	11	9	8	6	5	4	3	3	3	3	4	5	6	7	9	11	14	18	21	21	20	18	15	13	20	3	21	18	
Group F Walls																													
N	5	4	3	2	1	1	1	2	3	4	5	6	8	9	11	12	12	13	13	13	11	9	7	6	19	1	13	12	
NE	5	4	3	2	1	1	3	8	13	16	17	16	16	15	15	15	15	14	13	12	10	9	7	6	11	1	17	16	
E	5	4	3	2	2	1	4	9	16	21	24	25	24	22	20	19	18	17	15	13	11	10	8	7	12	1	25	24	
SE	5	4	3	2	2	1	2	6	10	15	20	23	24	23	22	20	19	17	16	14	12	10	8	7	16	1	22	21	
S	5	4	3	2	2	1	1	1	2	4	7	11	15	19	21	22	21	19	17	15	12	10	8	7	16	1	30	29	
SW	8	6	5	4	3	2	1	1	2	3	4	6	10	14	16	20	24	28	30	29	25	20	16	13	19	1	33	31	
W	9	7	5	4	3	2	2	2	3	4	6	8	11	16	22	27	32	33	30	24	19	15	12	19	1	33	31		
NW	8	6	4	3	2	2	1	1	2	3	4	6	7	9	12	15	19	24	26	24	20	16	12	10	19	1	26	25	
Group G Walls																													
N	2	1	0	0	0	1	4	5	5	7	8	10	12	13	13	14	14	15	12	8	6	5	4	3	18	0	15	15	
NE	2	1	1	0	0	0	5	15	20	22	20	16	15	15	15	15	14	12	10	8	6	5	4	3	9	0	22	22	
E	2	1	1	0	0	0	6	17	26	30	31	28	22	19	17	17	16	15	13	11	8	7	5	4	3	10	0	31	31
SE	2	1	1	0	0	0	3	10	18	24	27	28	27	23	20	18	16	15	13	11	8	7	6	4	3	11	0	28	28
S	2	1	1	0	0	0	1	3	7	12	17	22	25	26	24	21	17	14	11	8	7	5	4	3	14	0	26	26	
SW	3	2	2	1	1	1	3	5	6	8	10	15	23	31	37	40	37	27	16	11	8	6	5	4	16	0	35	35	
W	3	2	2	1	1	1	3	4	6	9	14	21	28	33	35	34	29	20	13	10	7	6	4	16	0	40	39		
NW	3	2	2	1	1	0	0	1	3	4	6	8	10	12	15	20	26	31	31	29	14	10	7	5	4	18	0	31	31

تابع جدول 6-5 تصحيح CLTD لخط العرض والشهر (LM) للسقف والجدران (يستخدم مع الجدولين 6-2 و 6-4 بموجب الملاحظات في ذيلهما)

Lat.	Month	N	NNE NNW	NE NW	ENE WNW	E W	ESE WSW	SE SW	SSE SSW	S	HOR
40	Dec	-3.3	-4.4	-5.5	-7.2	-5.5	-3.8	0.0	3.8	5.5	-11.6
	Jan/Nov	-2.7	-3.8	-5.5	-6.6	-5.0	-3.3	0.5	4.4	6.1	-10.5
	Feb/Oct	-2.7	-3.8	-4.4	-5.0	-3.3	-1.6	1.6	4.4	6.6	-7.7
	Mar/Sept	-2.2	-2.7	-2.7	-3.3	-1.6	0.5	2.2	3.8	5.5	-4.4
	Apr/Aug	-1.1	-1.6	-1.1	-1.1	0.0	0.0	1.1	1.6	2.2	1.6
	May/Jul	0.0	0.0	0.0	0.0	0.0	0.0	0.0	0.0	0.5	0.5
Jun	0.5	0.5	0.5	0.0	0.5	0.0	0.0	-0.5	-0.5	1.1	
48	Dec	-3.3	-4.4	-6.1	-7.7	-7.2	-5.5	-1.6	1.1	3.3	-13.8
	Jan/Nov	-3.3	-4.4	-6.1	-7.2	-6.1	-4.4	-0.5	2.7	4.4	-13.3
	Feb/Oct	-2.7	-3.8	-5.5	-6.1	-4.4	-2.7	0.5	4.4	6.1	-10.0
	Mar/Sept	-2.2	-3.3	-3.3	-3.8	-2.2	-0.5	2.2	4.4	6.1	-6.1
	Apr/Aug	-1.6	-1.6	-1.6	-1.6	-0.5	0.0	2.2	3.3	3.8	-2.7
	May/Jul	0.0	-0.5	0.0	0.0	0.5	0.5	1.6	1.6	2.2	0.0
Jun	0.5	0.5	1.1	0.5	1.1	0.5	1.1	1.1	1.6	1.1	
56	Dec	-3.8	-5.0	-6.6	-8.8	-8.8	-7.7	-5.0	-2.7	-1.6	-15.5
	Jan/Nov	-3.3	-4.4	-6.1	-8.3	7.7	-6.6	-3.3	-0.5	1.1	-15.0
	Feb/Oct	-3.3	-4.4	-5.5	-6.6	5.5	-3.8	0.0	3.3	5.0	-12.2
	Mar/Sept	-2.7	-3.3	-3.8	-4.4	-2.7	-1.1	2.2	4.4	6.6	-8.3
	Apr/Aug	-1.6	-2.2	-2.2	-2.2	-0.5	0.5	2.7	3.8	5.0	-4.4
	May/Jul	0.0	0.0	0.0	0.0	1.1	1.1	2.7	3.3	3.8	-1.1
Jun	1.1	0.5	1.1	0.5	1.6	1.6	2.2	2.7	3.3	0.5	
64	Dec	-3.8	-5.0	-6.6	-8.8	-9.4	-10.0	-8.8	-7.7	-6.6	-16.6
	Jan/Nov	-3.8	-5.0	-6.6	-8.8	-8.8	-8.8	-7.2	-5.5	-4.4	-16.1
	Feb/Oct	-3.3	-4.4	-6.1	-7.7	-7.2	-5.5	-2.2	0.5	2.2	-14.4
	Mar/Sept	-2.7	-3.8	-5.0	-5.5	-3.8	-2.2	1.1	3.8	6.1	-11.1
	Apr/Aug	-1.6	-2.2	-2.2	-2.2	-0.5	0.5	2.7	5.0	6.1	-6.1
	May/Jul	-0.5	0.0	0.5	0.0	1.6	2.2	3.3	4.4	5.5	-1.6
Jun	1.1	1.1	1.1	1.1	2.2	2.2	3.3	3.8	5.0	0.0	

جدول 6-5 تصحيح CLTD لخط العرض والشهر ( LM ) للسقوف والجدران  
( يستعمل مع الجدولين 6-2 و 6-4 بموجب الملاحظات في ذيلهما )

Lat.	Month	N	NNE NNW	NE NW	ENE WNW	E W	ESE WSW	SE SW	SSE SSW	S	HOR
16	Dec	-2.2	-3.3	-4.4	-4.4	-2.2	-0.5	2.2	5.0	7.2	-5.0
	Jan/Nov	-2.2	-3.3	-3.8	-3.8	-2.2	-0.5	2.2	4.4	6.6	-3.8
	Feb/Oct	-1.6	-2.7	-2.7	-2.2	-1.1	0.0	1.1	2.7	3.8	-2.2
	Mar/Sept	-1.6	-1.6	-1.1	-1.1	-0.5	-0.5	0.0	0.0	0.0	-0.5
	Apr/Aug	-0.5	0.0	-0.5	-0.5	-0.5	-1.6	-1.6	-2.7	-3.3	0.0
	May/Jul	2.2	1.6	1.6	0.0	-0.5	-2.2	-2.7	-3.8	-3.8	0.0
	Jun	3.3	2.2	2.2	0.5	-0.5	-2.2	-3.3	-4.4	-3.8	0.0
24	Dec	-2.7	-3.8	-5.0	-5.5	-3.8	-1.6	1.6	5.0	7.2	7.2
	Jan/Nov	-2.2	-3.3	-4.4	-5.0	-3.3	-1.6	1.6	5.0	7.2	6.1
	Feb/Oct	-2.2	-2.7	-3.3	-3.3	-1.6	-0.5	1.6	3.8	5.5	3.8
	Mar/Sept	-1.6	-2.2	-1.6	-1.6	-0.5	-0.5	0.5	1.1	2.2	1.6
	Apr/Aug	-1.1	-0.5	0.0	-0.5	-0.5	-1.1	0.5	1.1	1.6	0.0
	May/Jul	0.5	1.1	1.1	0.0	0.0	1.6	-1.6	2.7	3.3	0.5
	Jun	1.6	1.6	1.6	0.5	0.0	-1.6	-2.2	-3.3	3.3	0.5
32	Dec	-2.7	-3.8	-5.5	-6.1	-4.4	-2.7	1.1	5.0	6.6	-9.4
	Jan/Nov	-2.7	-3.8	-5.0	-6.1	-4.4	-2.2	1.1	5.0	6.6	8.3
	Feb/Oct	-2.2	-3.3	-3.8	-4.4	-2.2	-1.1	2.2	4.4	6.1	5.5
	Mar/Sept	-1.6	-2.2	-2.2	-2.2	-1.1	-0.5	1.6	2.7	3.8	2.7
	Apr/Aug	-1.1	-1.1	-0.5	-1.1	0.0	-0.5	0.0	0.5	0.5	0.5
	May/Jul	0.5	0.5	0.5	0.0	0.0	-0.5	-0.5	-1.6	-1.6	0.5
	Jun	0.5	1.1	1.1	0.5	0.0	-1.1	-1.1	-2.2	-2.2	1.1
40	Dec	-3.3	-4.4	-5.5	-7.2	-5.5	-3.8	0.0	3.8	5.5	-1.6
	Jan/Nov	-2.7	-3.8	-5.5	-6.6	-5.0	-3.3	0.5	4.4	6.1	-3.3
	Feb/Oct	-2.7	-3.8	-4.4	-5.0	-3.3	-1.6	1.6	4.4	6.6	-2.7



جمهورية العراق  
وزارة التعليم العالي والبحث العلمي  
جامعة الفرات الاوسط التقنية  
الكلية التقنية الهندسية – نجف  
تقليل الأحمال الحرارية للمباني عن طريق إضافة المخلفات إلى مواد البناء  
رسالة مقدمة الى  
قسم هندسة تقنيات ميكانيك القوى  
كجزء من متطلبات نيل درجة الماجستير تقني في هندسة الميكانيكية (حراريات)  
تقدمت بها الطالبة  
شهد حسن حميد

اشراف  
الأستاذ المساعد كريم جعفر علوان

أيلول 2023